ISSN: 2227-6912
E-ISSN: 2790-0479
https://doi.org/10.61413/DUYR2105

Azerbaijan Technical University

MACHINE SCIENCE

1
2026

International scientific-technical journal

MACHINE SCIENCE

MAŞINŞÜNASLIQ МАШИНОВЕДЕНИЕ

International scientific-technical journal
Beynəlxalq elmi-texniki jurnal
Международный научно-технический журнал

Number 1
2026

Founder: The Ministry of Education of Azerbaijan Republic
Təsisçi: *Azərbaycan Respublikasi Təhsil Nazirliyi*
Учредитель: *Министерство образования Азербайджанской Республики*

The journal is included into the list confirmed by Higher Attestation Commission of the Azerbaijan Republic of editions for the publication of works of competitors for scientific degrees

Jurnal Azərbaycan Respublikasi Ali Atestasiya Komissiyasinin təsdiq etdiyi elmi dərəcə iddiaçilarinin əsərlərinin çap edildiyi dövri elmi nəşrlərin siyahisina daxil edilmişdir.

Журнал входит в перечень, утвержденных ВАК Азербайджанской Республики, изданий для публикации трудов соискателей ученых степеней

Journal was founded according the order No1861 Ministry of Education of Azerbaijan Republic on the date 25.11.2011. Registration No 3521. Journal is published at least twice a year.

Jurnal Azərbaycan Respublikasi Təhsil Nazirliyinin 25.11.2011-ci il tarixli 1861 sayli əmri əsasinda təsis edilmişdir. Qeydiyyat No 3521. İldə ən azi iki nömrə nəşr edilir.

Учреждено приказом за №1861 от 25.11.2011 года Министерства образования Азербайджанской Республики. Регистрация № 3521. Ежегодно публикуется два номера.

It has been published since 2001. Published in 2001 - 2011 with a name "Mechanics-machine building"
2001-ci ildən nəşr edilir. 2001 – 2011-ci illərdə "Mexanika-maşinqayirma" adi ilə çap edilmişdir.
Издается с 2001 года. В 2001 – 2011 годах издано под называнием «Механика-машиностроение»

The "MACHINE SCIENCE" journal is supported by Azerbaijan Technical University, which means there are no publication fees for authors.
"MAŞINŞÜNASLIQ" jurnali Azərbaycan Texniki universiteti tərəfindən dəstəklənir və məqalələrin nəşri üçün müəlliflərdən hər hansi ödəniş tələb olunmur.
Журнал «МАШИНОВЕДЕНИЕ» поддерживается Азербайджанским Техническим Университетом, что означает, что с авторов не взимается плата за публикацию статей.

Editorial address:	Baku, AZ1073, H.Javid ave., 25. AzTU	© Machine Science, 2026
Redaksiyanin ünvani:	Tel: (+994 12) 539 12 25	**ISSN:** 2227-6912
Адрес редакции:	E-mail: msj@aztu.edu.az	**E-ISSN:** 2790-0479

Contents

MACHINE SCIENCE

ISSN: 2227-6912
E-ISSN: 2790-0479

2026, № 1 Pages 4-12

STAGGERED BIPLANE BLADE CONCEPT FOR ENHANCED AERODYNAMIC PERFORMANCE IN VERTICAL-AXIS WIND TURBINES

Zohour Safia OULHACI[1], Omar LADJEDEL[2,a*], Omar IMINE[1,b], Tayeb YAHIAOUI[1,c], Anar HAJIYEV[3,d]

[1]Laboratoire de Mécanique Appliquée, USTO-MB, PO 1505, El Mnaouer, Oran, Algeria
[2]Laboratoire d'Aérohydrodynamique Navale, USTO-MB, PO 1505, El Mnaouer, Oran, Algeria

*E-Mail: [a]*omar.ladjedel@univ-usto.dz, [b]omar.imine@univ-usto.dz, [c]tayeb.yahiaoui@univ-usto.dz, [e]anar.hajiyev@aztu.edu.az*

https://doi.org/10.61413/SORJ4351

Abstract: The accelerating global demand for clean electricity, combined with the progressive depletion of fossil fuel reserves, has placed renewable energy technologies at the forefront of engineering research. According to the International Energy Agency (IEA), wind power generated over 2,330 TWh in 2023-representing a 10% year-on-year increase-and global wind capacity is projected to nearly double to over 2,000 GW by 2030. Among wind energy converters, vertical-axis wind turbines (VAWTs) of the Darrieus type have attracted renewed interest owing to their omnidirectional operation, mechanical simplicity, and suitability for urban and offshore environments. Nevertheless, their aerodynamic efficiency remains a limiting factor compared to horizontal-axis machines. This study proposes a novel VAWT configuration based on the tandem biplane blade concept, combining geometric modifications aimed at improving aerodynamic performance. Two-dimensional steady-state Reynolds-Averaged Navier–Stokes (RANS) simulations were performed using the Spalart–Allmaras turbulence model in ANSYS Fluent, applied to a NACA 0018 airfoil at a chord Reynolds number of $\mathrm{Re}\,c = 7.4\times10^4$ and a tip-speed ratio of $\lambda = 2$. Four blade arrangements were evaluated: a single-blade baseline, two blades without offset, two blades with a $0.5C$ upstream stagger, and two blades with a $0.5C$ downstream stagger. The results demonstrate that tandem-staggered configurations yield significant improvements in lift and tangential force coefficients relative to the single-blade reference, with the upstream-offset arrangement exhibiting the most favorable aerodynamic characteristics. These findings validate the biplane concept as a promising pathway for enhancing VAWT power output and operational stability.

Keywords: *wind energy; vertical-axis turbine; Darrieus; geometric optimization; aerodynamic performance; numerical simulation.*

INTRODUCTION

The transition toward low-carbon electricity systems has made wind energy one of the fastest-growing power generation technologies worldwide. The IEA reported record renewable capacity additions of 507 GW in 2023, with wind power accounting for a major share, and projects that global wind capacity will approach 2,000 GW by 2030 [1]. Within the landscape of wind energy converters, vertical-axis wind turbines (VAWTs) of the Darrieus type have regained significant attention over the past decade for distributed and urban applications, primarily owing to their insensitivity to wind direction, low acoustic signature, and structural simplicity [2]. However, their aerodynamic efficiency-typically characterized by a maximum power coefficient Cp in the range $0.35-0.45$ for optimized H-Darrieus configurations [3] remains lower than that of horizontal-axis wind turbines (HAWTs), motivating sustained research into performance enhancement strategies.

Parametric studies have examined the influence of blade airfoil geometry [4], rotor solidity, tip-speed ratio [5-7], number of blades [7], and pitch angle on VAWT efficiency. Geometric modifications at the blade level-including leading-edge alterations, camber variations, and multi-element configurations-have also demonstrated potential for improving both lift generation and dynamic stall resistance [2]. The present paper addresses the latter approach by introducing a novel biplane tandem blade concept for Darrieus VAWTs.

The aerodynamic behavior of four isolated blade arrangements was investigated numerically using steady-state RANS simulations in ANSYS Fluent. The study first establishes a single-blade baseline and then evaluates the effect of inter-blade stagger distance and direction on the lift, drag, and tangential force coefficients across incidence angles from 0° to 30°, corresponding to a tip-speed ratio of $\lambda = 2$. The results confirm that the biplane concept significantly enhances the aerodynamic potential of VAWTs compared to classical single-blade Darrieus configurations.

MATHEMATICAL FORMULATION

The aerodynamic flow field around Darrieus VAWT blades is governed by the incompressible Reynolds-Averaged Navier–Stokes (RANS) equations. In the two-dimensional steady-state formulation employed here, conservation of mass and momentum are expressed as:

$$\nabla \cdot \bar{U} = 0$$

$$\rho\left(\bar{U} \cdot \nabla\right)\bar{U} = -\nabla\bar{p} + \nabla \cdot \left[\mu\left(\nabla\bar{U} + \left(\nabla\bar{U}\right)^{T}\right) - \rho u'^{-}\right]$$

where Ū and p̄ denote the Reynolds-averaged velocity and pressure fields, respectively, and −ρu'u'ᵀ is the Reynolds stress tensor requiring a turbulence closure. The commercial CFD solver ANSYS Fluent was employed to discretize and solve these equations using the finite volume method (FVM).

Fluent supports a broad range of turbulence closures, including Spalart–Allmaras, k–ε (standard, RNG, and Realizable), k–ω (Standard and SST), the seven-equation RSM, DES, and LES with Smagorinsky subgrid-scale models. In this study, the one-equation Spalart–Allmaras (S–A) turbulence model was selected. This closure solves a single transport equation for a modified eddy viscosity ṽ, making it computationally efficient for attached and mildly separated boundary-layer flows. Although higher-fidelity approaches such as k–ω SST or URANS methods may be preferred for capturing dynamic stall at higher tip-speed ratios [8], the S–A model has been shown to provide acceptable predictions for steady-state blade aerodynamics at moderate angles of attack and low-to-moderate Reynolds numbers, as used in the present preliminary investigation [9, 10]. The model incorporates wall damping functions, logarithmic-layer corrections, and provisions for laminar-to-turbulent transition. The turbulent eddy viscosity μt is recovered from ṽ via the relation:

$$\frac{D\nu}{Dt} = \frac{1}{\sigma\nu}\left[\frac{\partial}{\partial x_j}\left\{(\mu + \rho\nu)\frac{\partial\nu}{\partial x_j}\right\} + C_{b2}\rho\left(\frac{\partial\nu}{\partial x_j}\right)\right] + G_\nu - Y_\nu + S_\nu \tag{1}$$

The turbulent viscosity is evaluated using the following relations:

$$\mu_t = \rho\nu f_{\nu 1}, \qquad f_{\nu 1} \equiv \frac{(\nu/\nu)}{(\nu/\nu)^3 + C_{\nu 1}{}^{\beta}}$$

METHODOLOGY

The blade geometry is based on the symmetric NACA 0018 airfoil, which has been extensively validated for Darrieus VAWT applications across a wide range of tip-speed ratios [10]. The NACA 0018 profile was generated from its tabulated Cartesian coordinates and imported into GAMBIT, the pre-processing environment used for domain construction and mesh generation. The resulting mesh was exported as a .msh file for use in ANSYS Fluent.

The computational domain was decomposed into two sub-regions: a stationary outer domain representing the far-field, and an inner rotating domain enclosing the blade(s). This sliding-mesh-compatible layout enables straightforward extension to transient rotor simulations. Simulations were carried out under the following reference conditions: chord length $c = 6cm$; freestream velocity $U\infty = 18\,m/s$; chord Reynolds number $\mathrm{Re}\,c = 7.4\times10^4$. This Reynolds number falls in the low-Re regime relevant to small-scale urban VAWTs, where laminar-turbulent transition effects on the suction surface are known to influence aerodynamic loads [10].

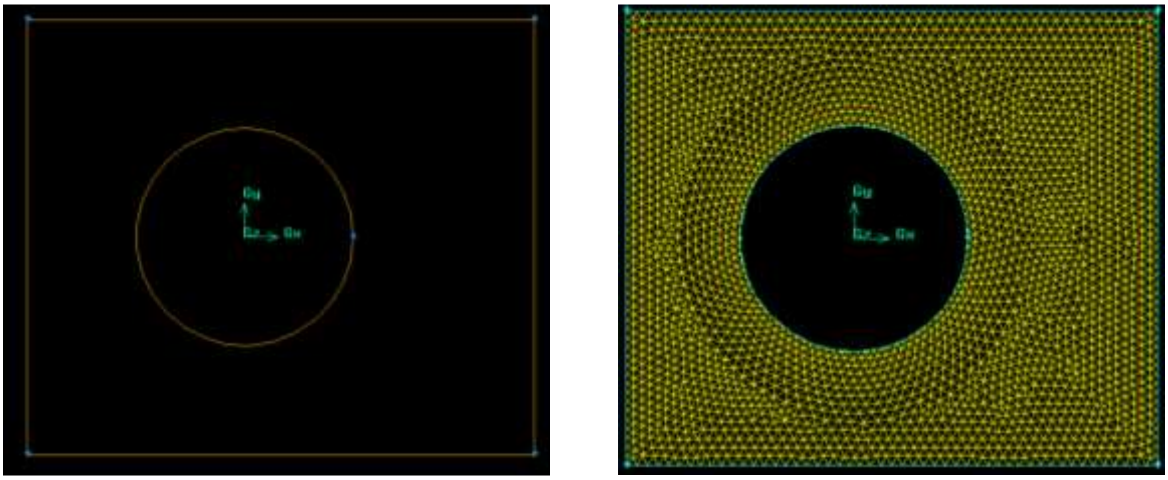

(a) *(b)*

Fig.1. External domain: (a) geometry and (b) mesh.

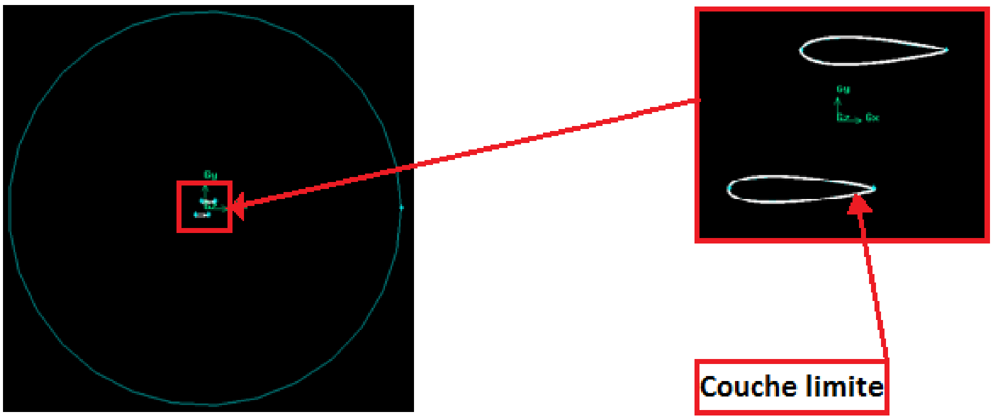

Fig.2. Internal domain with a zoom on the blades.

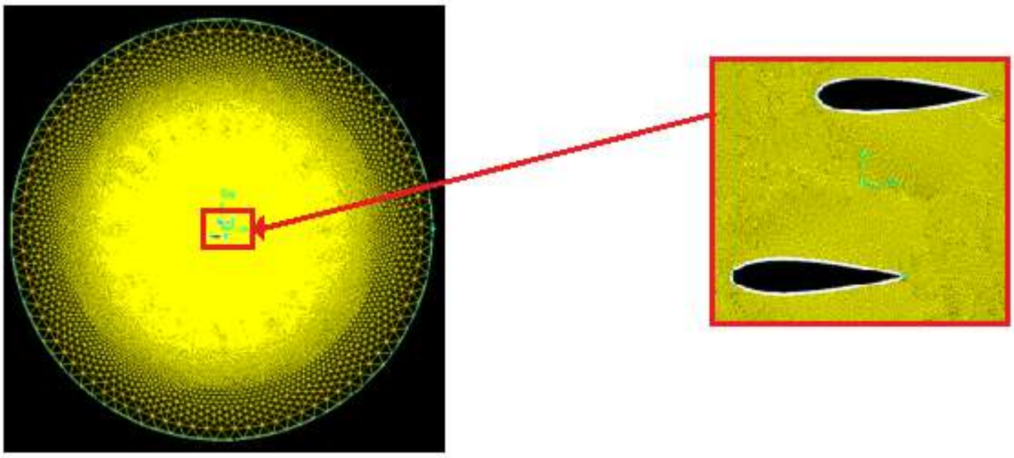

Fig.3. Mesh of the internal domain.

To assess the aerodynamic benefit of the biplane concept, four isolated-blade configurations were analyzed (Figure 4): (a) a single-blade baseline; (b) two blades in tandem without chordwise offset; (c) two blades with an upstream stagger of $0.5C$; and (d) two blades with a downstream stagger of $0.5C$. This systematic variation of inter-blade stagger distance is motivated by classical multi-element airfoil theory, in which the position of a secondary element relative to the primary element governs the extent of boundary-layer energization and flow reattachment [10].

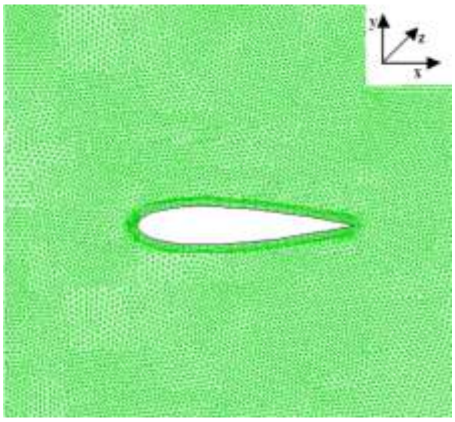

(a) One Blade.

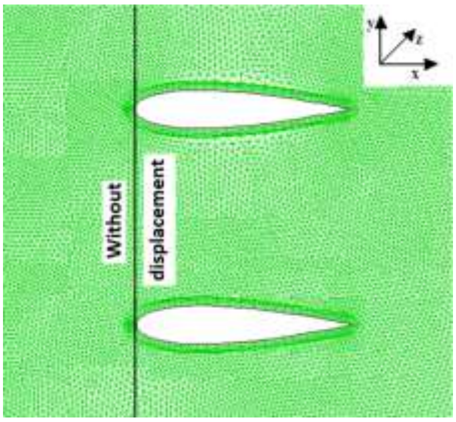

(b) Two blades without offset.

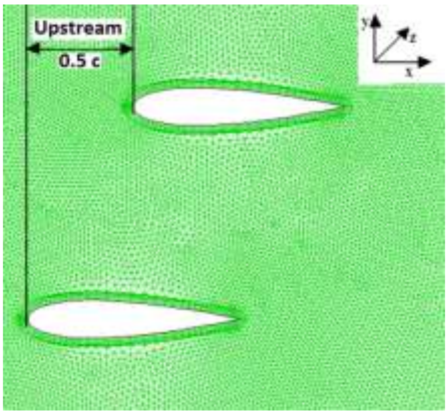

(c) Two blades with a 0.5C upstream offset.

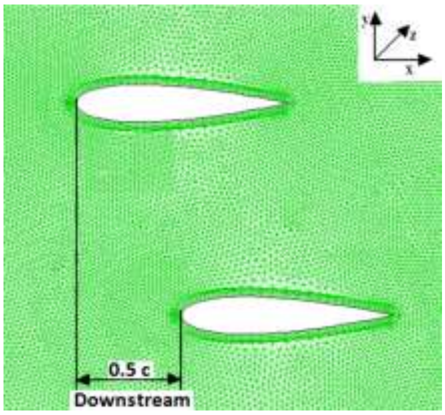

Two blades with a 0.5C downstream stagger.

Fig.4. Tested cases of isolated blades.

Steady-state RANS computations were performed for geometric angles of attack ranging from 0° to 30°, encompassing both attached and separated flow regimes. The tip-speed ratio $\lambda = 2$ was selected as a representative operating condition for small urban Darrieus rotors [11, 12]. Boundary conditions were assigned as follows: velocity inlet ($U\infty = 18\,m/s$) at the upstream face; pressure outlet at the downstream face; no-slip wall conditions on all blade surfaces; and symmetry conditions on the lateral boundaries.

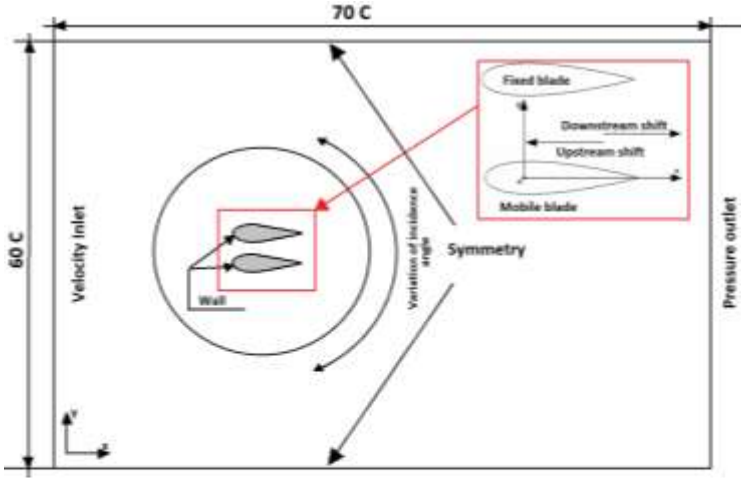

Fig.5. Geometry of the two-dimensional domain.

RESULTS AND DISCUSSION

The aerodynamic coefficients obtained from the four tested configurations are presented and compared in Figures 6–8. All force coefficients were non-dimensionalized using the same reference dynamic pressure (½ ρ U∞² c), enabling a consistent performance comparison across configurations.

The lift coefficient CL (Figure 6) increases monotonically with incidence angle up to approximately 15°–20° for most configurations, beyond which flow separation induces a progressive stall. Notably, the upstream-staggered biplane arrangement sustains higher CL values across the mid-range angles (10°–25°), indicating delayed stall and enhanced boundary-layer momentum compared to the single-blade reference.

The drag coefficient CD (Figure 7) exhibits the expected quadratic growth with incidence, with the downstream-staggered configuration showing the most pronounced increase beyond 20°, consistent with earlier wake blockage from the upstream blade.

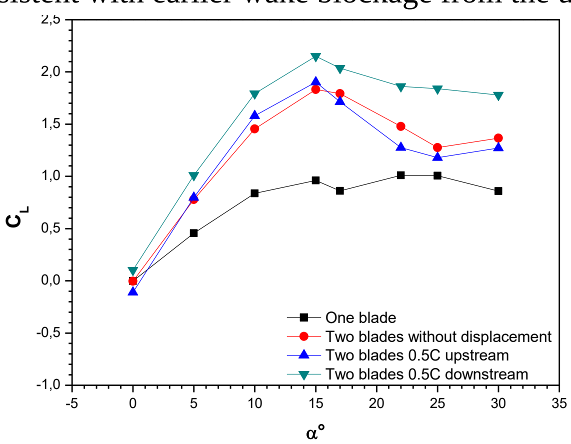

Fig.6. Variation of the lift coefficient as a function of the attack angle .

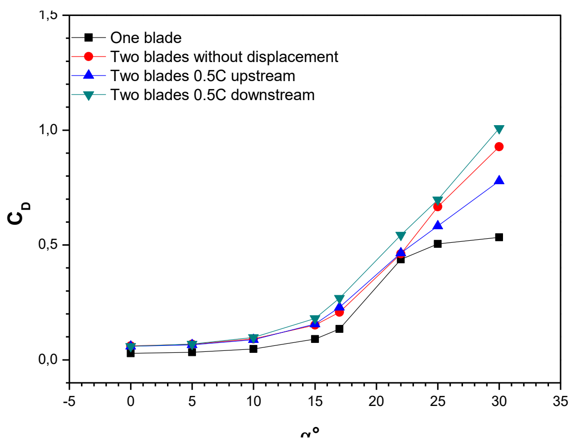

Fig.7. Variation of the drag coefficient as a function of the attack angle.

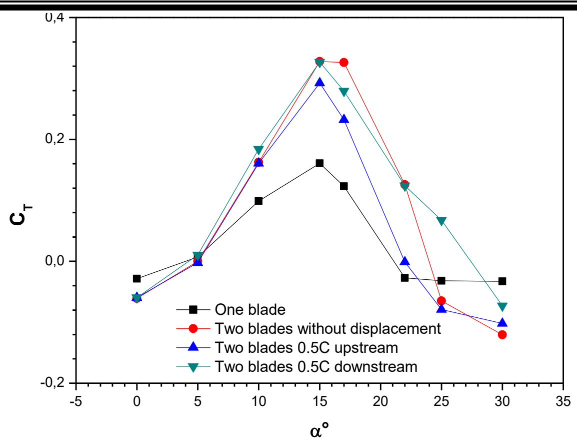

Fig.8. Variation of the tangential coefficient as a function of the attack angle.

Of particular significance for VAWT performance is the tangential force coefficient Ct (Figure 8), which directly governs the driving torque of the rotor. The upstream-staggered biplane configuration exhibits the highest Ct over the 10°–25° range, corresponding to the high-incidence phase of the upwind blade passage in a VAWT rotor at $\lambda = 2$. This result is consistent with multi-element airfoil studies showing that an upstream secondary element can energize the suction-surface boundary layer of the main blade, increasing effective circulation and delaying separation [6, 13]. The biplane configurations show overall promising mechanical energy potential in the field of VAWTs, in agreement with prior numerical investigations of tandem blade arrangements [6, 14-18].

Figures 9–11 present the velocity streamline distributions for the three tandem configurations at angular positions of 0°, 15°, and 30°. At 0° incidence, all configurations exhibit fully attached flow with smooth streamlines over both blade surfaces. At 15°, the onset of a recirculation zone is visible on the suction side of the downstream blade in the standard (no-offset) arrangement, whereas the upstream-staggered configuration maintains largely attached flow owing to the momentum transfer from the upstream element [19-25]. At 30°, all configurations display significant vortex shedding and separated flow, though the intensity and spatial extent of the wake differ markedly [26-30].

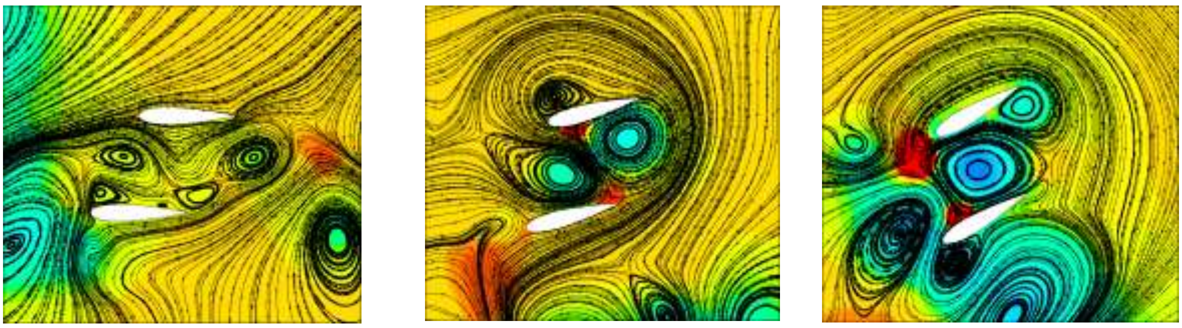

2 Offset blades 0.5C upstream 0° | 2 Offset blades 0.5C upstream 15° | 2 Offset blades 0.5C upstream 30°

Fig.9. Distribution of streamlines for the two blades with a 0.5C upstream offset at different positions.

The upstream-staggered arrangement produces the most organized vortex pattern, which is associated with reduced form drag and a more coherent pressure recovery on the downstream blade pressure side. The inter-blade vortex interactions identified here corroborate findings reported by Castelli et al. [6] and Sabaeifard et al. [14], who documented analogous wake-interaction mechanisms in multi-eleme^{2}nt VAWT configurations. These flow visualizations reinforce the quantitative trends observed in the force coefficient data and confirm that blade stagger geometry is a critical design variable for biplane VAWT optimization [30-34].

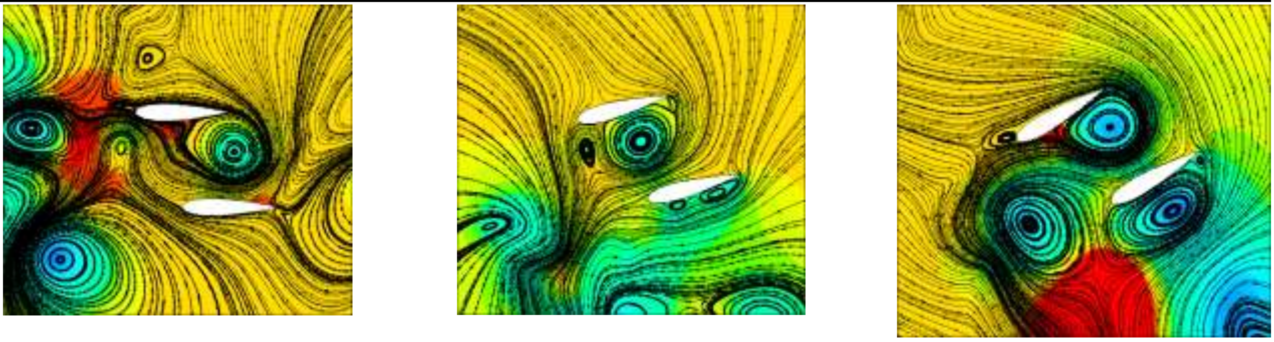

2 Offset blades 0.5C Downstream 0°   2 Offset blades 0.5C Downstream 15°   2 Offset blades 0.5C Downstream 30°

Fig.10. Distribution of streamlines for the two blades with a 0.5C downstream offset at different positions

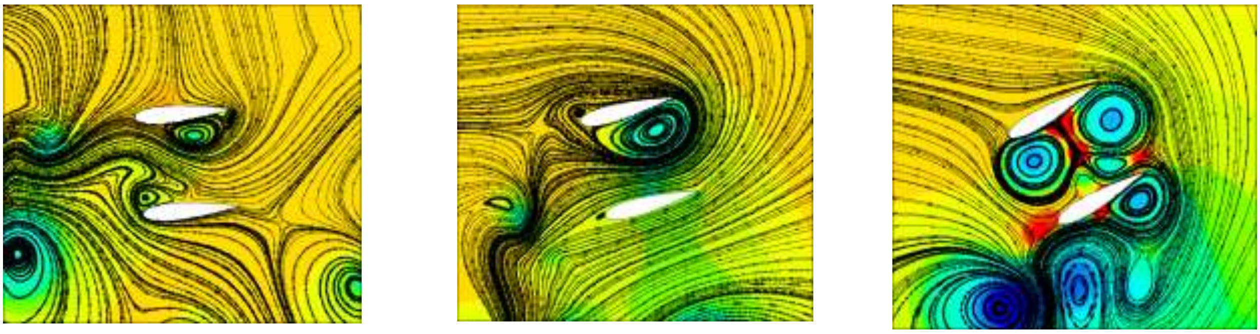

2 Blades standard à 0°   2 Blades standard à15°   2 Blades standard à 30°

Fig.11. Distribution of streamlines for the two standard blades (without offset) at different positions.

CONCLUSION

This study presented a two-dimensional steady-state CFD investigation of a novel biplane tandem blade concept applied to a Darrieus vertical-axis wind turbine. Four isolated-blade configurations using the NACA 0018 airfoil were evaluated at a chord Reynolds number of Rec = 7.4 $\times 10^4$ and a tip-speed ratio of $\lambda = 2$ using the Spalart–Allmaras RANS turbulence model in ANSYS Fluent. The following conclusions can be drawn from the results:

(i) The biplane configurations consistently outperform the single-blade baseline in terms of tangential force coefficient across the mid-range incidence angles (10°–25°), which are aerodynamically dominant in Darrieus operation at $\lambda = 2$.

(ii) Among the tested arrangements, the upstream-staggered configuration (0.5C offset) demonstrates the highest aerodynamic potential, attributed to the beneficial momentum transfer from the secondary blade to the primary blade boundary layer, which delays flow separation and sustains higher lift.

(iii) Streamline visualizations confirm that inter-blade vortex interactions are governed by the stagger direction, with the upstream configuration producing more organized wake structures and reduced drag penalties.

These findings establish the biplane concept as a viable and promising geometric strategy for enhancing VAWT performance. Future work should address unsteady (URANS or LES) simulations to capture dynamic stall effects during full rotor rotation, three-dimensional tip-vortex losses, and experimental wind-tunnel validation of the optimal biplane configuration to substantiate the numerical predictions and guide prototype development.

REFERENCES

[1]. IEA. Renewables 2024: Analysis and Forecast to 2030. IEA, Paris, 2024. https://www.iea.org/reports/renewables-2024

[2]. Ismail M. F., Vijayaraghavan K. The effects of aerofoil profile modification on a vertical axis wind turbine performance. Energy, 80 (2015).

[3]. Taher G., Ali A. M., Al-Ajmi M., Hassan I. M. Effect of number of blades and blade chord length on the performance of Darrieus wind turbine. American Journal of Mechanical Engineering and Automation, 2015, pp. 16–25.

[4]. Tirkey A., Sarthi Y., Patel K., Sharma R., Sen P. K. Study on the effect of blade profile, number of blades, Reynolds number, and aspect ratio on the performance of vertical axis wind turbine. IJSETR, 3(12), December 2014.

[5]. Jamati F. Etude Numérique D'une Eolienne Hybride Asynchrone. Université de Montréal, 2011.

[6]. Castelli M. R., Englaro A., Benini E. The Darrieus wind turbine: proposal for a new performance prediction model based on CFD. Energy, 36 (2011).

[7]. Castelli M. R., De Betta S., Benini E. Effect of Blade Number on a Straight-Bladed Vertical-Axis Darrieus Wind Turbine. World Academy of Science, Engineering and Technology, 61 (2012).

[8]. Rezaeiha A., Kalkman I., Montazeri H., Blocken B. Effect of the shaft on the aerodynamic performance of urban vertical axis wind turbines. Energy Conversion and Management, 149 (2017), 616–630.

[9]. Nasr S., Nazih M. Étude comparative entre éolienne à axe horizontal et éolienne à axe vertical. Buletinul Institutului Politehnic din Iasi, Université Libanaise, Tripoli, 2011.

[10]. Leconte P., Rapin M., Szechenyi E. Eoliennes. Techniques de l'Ingénieur, BM 4 640, 2001.

[11]. Hansen M. O. L. Aerodynamics of Wind Turbines. 2nd ed. Earthscan, UK and USA, 2008.

[12]. Rezaeiha A., Montazeri H., Blocken B. Characterization of aerodynamic performance of vertical axis wind turbines: Impact of operational parameters. Energy Conversion and Management, 169 (2018), 45–77. https://doi.org/10.1016/j.enconman.2018.05.042

[13]. Abu-El-Yazied T. G., Doghiem H. N., Ali A. M., Hassan I. M. Investigation of the aerodynamic performance of Darrieus vertical axis wind turbine. IOSR Journal of Engineering, 4(5), May 2014.

[14]. Sabaeifard P., Razzaghi H., Forouzandeh A. Determination of vertical axis wind turbine optimal configuration through CFD simulations. IPCBEE, vol. 28 (2012), IACSIT Press, Singapore.

[15]. Nachida K. M. Évaluation du gisement énergétique éolien - contribution à la détermination du profil vertical de la vitesse du vent en Algérie. Thèse de doctorat, Université Abou Bekr Belkaid de Tlemcen, 2006.

[16]. Boudia S. M. Optimisation de l'Évaluation Temporelle du Gisement Énergétique Éolien par Simulation Numérique et Contribution à la Réactualisation de l'Atlas des Vents en Algérie. Thèse de doctorat, Université Abou Bekr Belkaid de Tlemcen.

[17]. Chellali F., Khellaf A., Belouchrani A., Recioui A. A contribution in the actualization of wind map of Algeria. Renewable and Sustainable Energy Reviews, 15 (2011), 993–1002.

[18]. Benali O. Evaluation de potentiel énergétique éolien dans la région sud-est du Sahara algérienne. Mémoire de master, Université Kasdi Merbah Ouargla, 2015.

[19]. Courtecuisse V. Supervision d'une centrale multisources à base d'éoliennes et de stockage d'énergie connectée au réseau électrique. Thèse, ENSAM, 2008.

[20]. Boumahrat M., Gourdin J. Méthodes numériques appliquées. OPU, Algérie, 1983.

[21]. Poitiers F. Etude et commande de génératrices asynchrones pour l'utilisation de l'énergie éolienne. Thèse de Doctorat, Ecole Polytechnique de l'Université de Nantes, France, 2003.

[22]. Chan L. Systèmes de conversion de l'énergie éolienne. IEEE Canadian Review, Summer 2002, pp. 1–5.

[23]. La Verdure N. L'intégration des générateurs éoliens dans les réseaux faibles ou insulaires. Thèse, Institut national polytechnique de Grenoble, France, 2005.

[24]. WMO Technical Note 175. Meteorological aspects of the utilization of wind as an energy source. WMO, Geneva, 1981.

[25]. Eskin N., Artar H., Tolun S. Wind energy potential of Gökçeada Island in Turkey. Renewable and Sustainable Energy Reviews, 12 (2008), 839–851.

[26] Oztopal A., Sahin A. D., Akgun N., Sen Z. On the regional wind energy potential of Turkey. Energy, 25 (2000), 189–200.

[27]. Lu L., Yang H., Burnett J. Investigation on wind power potential on Hong Kong islands. Renewable Energy, 27 (2002), 1–12.

[28]. Danao L. A., Edwards J., Eboibi O., Howell R. A numerical investigation into the influence of unsteady wind on the performance and aerodynamics of a vertical axis wind turbine. Applied Energy, 116 (2014), 111–124.

[29]. El Samanoudy M., Ghorab A. A. E., Youssef S. Z. Effect of some design parameters on the performance of a Giromill vertical axis wind turbine. Ain Shams Engineering Journal (Elsevier), 1 (2010), 85–95.

[30]. Singh M. A., Biswas, Misra R. D. Investigation of self-starting and high rotor solidity on the performance of a three S1210 blade H-type Darrieus rotor. Renewable Energy, 76 (2015), 381–387.

[31]. Claude A., Bois G., Simonet S. Etude numérique instationnaire d'une micro-éolienne à axe vertical. Conférence sur les Energies Renouvelables, 2010.

[31]. Sranpat C., Unsakul S., Choljararux P., Leephakpreeda T. CFD-Based Performance Analysis on Design Factors of Vertical Axis Wind Turbines at Low Wind Speeds. Energy Procedia, 138 (2017), 500–505.

[32]. Celik T., Yildiz T., Baskaya S. Numerical study on the aerodynamic characteristics of the NACA 0018 airfoil at low Reynolds number for Darrieus wind turbines using the Transition SST model. Processes, 9(3), 477, 2021. https://doi.org/10.3390/pr9030477

[33]. Khalid M., Mansoor N., Mehmood F. Performance evaluation of profile modifications on straight-bladed vertical axis wind turbine by energy and Spalart-Allmaras models. Energy, 126 (2017), 706–718. https://doi.org/10.1016/j.energy.2017.03.046

[34]. Essahraoui M. et al. Vertical Axis Wind Turbines: A Comprehensive Critical Review of Aerodynamic Theory, Design Configurations, Performance Analysis, and Future Perspectives. Energies, 19(11), 2544, 2026. https://doi.org/10.3390/en19112544

Received: 10.01.2026
Accepted: 30.06.2026

MACHINE SCIENCE

ISSN: 2227-6912
E-ISSN: 2790-0479

2026, № 1 Pages 13-21

IMPROVING THE CONSTRUCTION OF THE REGENERATOR FOR SEPARATION OF COTTON PIECES FROM THE WASTE CONTENT

Avazbek OBIDOV[1,a*], Shavkat MAMAJANOV[2,b]

[1]*Dean of the Faculty of Mechanics, Namangan State Technical University*

[2]*Associate Professor of the Department of Transportation, Namangan State Technical University*

E-Mail: [a*]obidovazbek66@gmail.com, [b]shmamajanov.a@gmail.com

https://doi.org/10.61413/NNOU9259

Abstract: This article considers the problem of effective separation of cotton linters from waste generated at cotton ginning plants. The shortcomings of existing regenerator devices are analyzed and an improved design is proposed to increase their separation efficiency. The proposed device is based on a combination of mechanical and pneumatic effects. As a result of the research, the possibility of increasing the separation efficiency and reducing fiber damage is substantiated.

Keywords: *cotton waste, regenerator, separation efficiency, fiber recovery, pneumatic separation, design.*

INTRODUCTION.

As a result of technological processes in the cotton ginning industry, a large amount of waste is generated. A certain amount of cotton fiber and shreds remain in this waste. Their recovery is of great importance in increasing production efficiency, reducing raw material losses, and ensuring economic efficiency. The separation process in existing regenerator devices is not sufficiently perfect. The main problems are:

- low separation efficiency;
- mechanical damage to the fiber;
- high energy consumption.

Therefore, improving the design of the regenerator device is an urgent issue.

Scientific research on the development of technologies for cleaning cotton raw materials from various impurities is carried out by leading scientific centers and universities in the world with a developed textile industry. As a result of this research work, significant scientific achievements have been achieved by improving the technology and equipment for cleaning cotton raw materials, including: the US company Lummus has developed systems for automating the technological processes in which cotton raw materials cleaning machines operate, and in the USA and Australia, effective technologies for cleaning cotton from large and small impurities have been created. Large-scale research is also being carried out in Uzbekistan in this regard, including the Tashkent Institute of Textile and Light Industry, the Cotton Industry Scientific Center, and the Namangan State Technical University, where new machines for these technologies have been developed based on theoretical and experimental research. In the world, including in Uzbekistan, research is being conducted to create cotton ginning machines and technologies, to create a multi-stage regulating system for cleaning cotton raw materials, to create effective technologies for cleaning cotton from foreign impurities, and to develop technological designs for the working bodies of ginning machines, and to develop effective low-wear working bodies for cleaning.

The results of the analysis of modern scientific research on cotton cleaning showed that they were studied in two directions - cleaning cotton from small impurities and cleaning cotton from large impurities. In the 90s of the last century, instead of the PLPH flow lines, UHK cotton cleaning units were introduced, which consisted of four sections, in which cotton raw material was cleaned from small impurities using peg-slatted drums through screens, and from large impurities - with a sawn drum on a grate. The separated impurities fall into a common bunker and are removed from it by a screw equipped with a loading tube with brake valves. As a result, the load on the regenerators increases by 2-3 times as a result of mixing small and large impurities. Under the influence of the screw, small impurities are added to the fluff of the cotton raw material and become difficult to separate. As a result, the cleaning efficiency of the RH type regenerator decreases by 50%, and the contamination of regenerated linters during cleaning of cotton raw materials increases by 70%. As a result, the regenerated linters mix with the cotton raw materials sent for cleaning, making it difficult to clean them from difficult-to-clean fine impurities, and the quality of the fiber decreases by one or two grades.

The recommendations made in 1995 and included in the technological regulation [1] on separate processing of cotton raw materials and regenerated cotton fibers are not implemented in all enterprises for various reasons. Following these recommendations, the quality of raw cotton fiber can be improved by one grade, but the quality of the fiber will decrease by one or two grades due to regenerated fibers. In order to determine the reasons for the decrease in the cleaning efficiency of the RX type regenerator, we will analyze its scheme presented in Fig. 1.

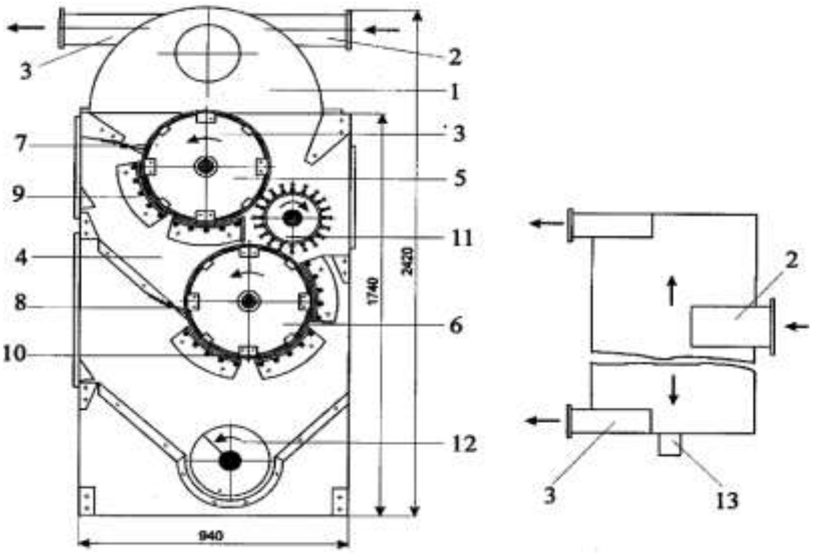

Fig.1. Scheme of regenerator type RX, which regenerates cotton raw materials from the waste of cleaning facilities:
1-pneumoestimator; 2,3-incoming and outgoing nozzles; 4th cleaning section; 5,6-main and regeneration drums; 7,8- sliding brushes; 9,10-colossian bars; 11-separating brush drum; 12-screw for removing impurities; 13-valve tube

The regenerator consists of a pneumatic feeder 1, a semi-cylindrical inlet 2 and outlet 3 pipes located above the cleaning section 4, a main structure 5, regenerating saw drums 6 with sliding brushes 7,8 and grate brushes 9,10, a separating brush drum 11, a screw for removing impurities 12 and a valve tube 13 connected to them.

Some changes were made to the construction of the unit to increase the cleaning and separation efficiency of 1RX type cotton regenerators used in cotton ginning enterprises. The amount of cotton separated in 30 minutes from 8 pieces of the number of planks in the drum is 19.6 kg, when the cotton remaining on the surface of the saw is separated by hand, it is 1.15 kg, and the separation efficiency is calculated to be 94.5%. The number of such planks, the amount of cotton separated in 10, 12 pieces, is increasing in the specified period of time and is 20.6, 23.6 kg. In this case, the separation efficiency is 95.8, 96.1%, and we can see that the number of plates in the separation drum is higher at 10 and 12 pieces. However, it was observed that due to the dense arrangement of 12 slats in the drum, the electric motor was under stress due to the difficulty of air passage through them during rotation, so the number of slats in the drum was left at 10.

STUDY OF THE INFLUENCE OF THE ANGLE OF INCLINATION OF THE BARS ON THE SEPARATION EFFICIENCY.

Experiments were conducted by installing a rubber-slatted drum prepared for the experiment in a 1PX regenerator and changing the angle of inclination of the slats along the axis relative to the center of the drum to 10^0, 15^0, 20^0, 25^0. In this case, the number of slats was recommended to be 10-12 based on experiments, and the experiments were carried out with 10 slats installed. With the installation of 12 slats, the separation efficiency increased due to the dense arrangement of the slats in the drum, which increased the air resistance in it, which led to an increase in the load on the electric motor (Fig. 2).

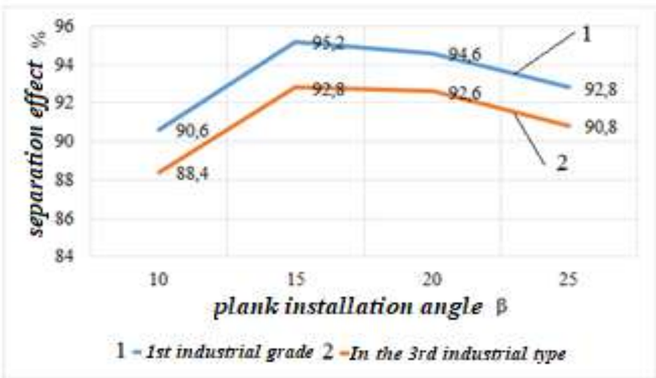

Fig.2. Effect of Slope Angle on Separation Efficiency of Placing Planks Towards the Center of the Separating Drum

The experiments were carried out in triplicate and the average results are presented in Figure 2. The experiments were conducted using raw cotton of the Nam-77 selection variety of I and III industrial varieties of the 2nd class, which was accepted at the enterprise. The impurity of the II industrial variety cotton is 4.8%, the moisture content is 8.2%, and the impurity of the III industrial variety cotton is 10.6%, the moisture content is 9.8%.

From Figure 3, we can see that the separation efficiency of cotton pieces in the waste composition separated from cotton of the I-industrial grade was 90.6% at a slope angle of 10° to the center of the drum, 95.2% at 15°, and the separation efficiency decreased to 94.6% and 92.8% after the angle increased to 20-25°. In the III-industrial grade, the separation efficiency was also high at a slope angle of 15-20°, 92.8-92.6%, and decreased at 250°. Here, the increase in the slope angle of the plank on the drum affected the increase in the angle of separation of cotton pieces from the saw, indicating that the planks in the extreme slope condition reduced the separation of cotton pieces on the saw surface.

Considering the moisture content of cotton, it has been observed in many experiments that the moisture content of the waste from cotton gins is high [2]. High moisture makes it difficult to separate the cotton that has been ginned, so the experiments were continued by changing the angle of inclination of the slats towards the center of the drum. The rotation speed of the separating drum was kept at 945 rpm. The results of the experiment are presented in Figures 3-5 below.

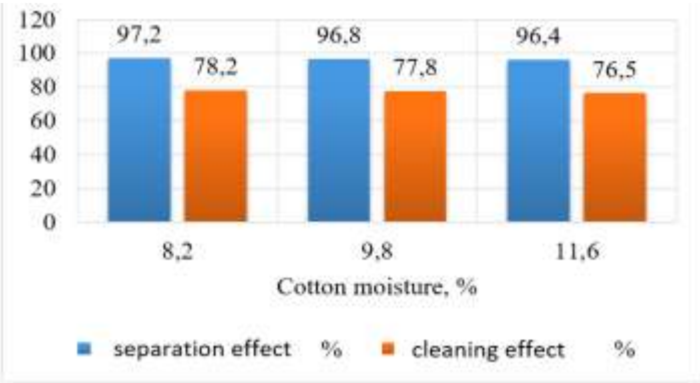

Fig.3. Effect of the angle of inclination of the board at 10 degrees on the efficiency of cotton moisture separation and cleaning

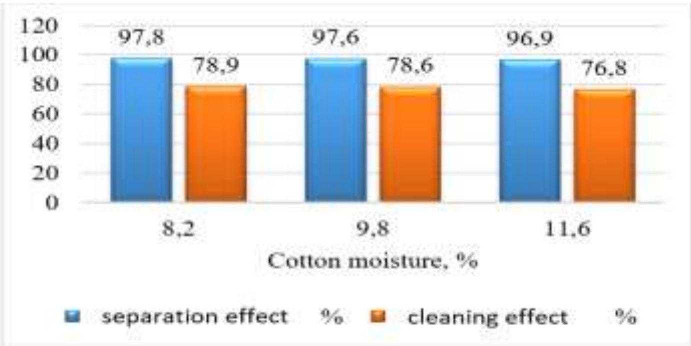

Fig.4. Effect of the angle of inclination of the board at 15 degrees on the efficiency of cotton moisture separation and cleaning

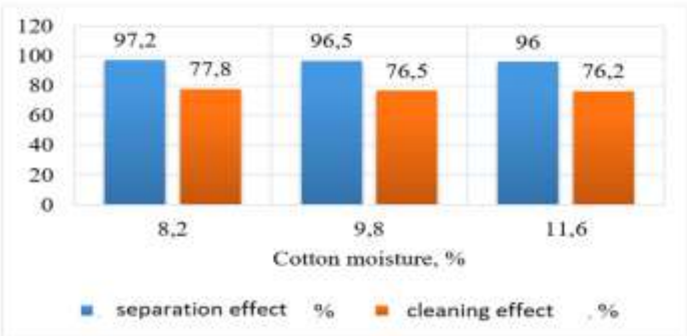

Fig. 5. Effect of the angle of inclination of the board at 20 degrees on the efficiency of cotton moisture separation and cleaning

In the histogram in Figure 3 above, when the angle of deviation of the planks towards the center of the drum is set to 100, the efficiency of separating cotton pieces from the surface of the saw is 97.2% at a moisture content of 8.2%, the cleaning efficiency is 78.2%. It is 77.8, 76.5%. In the histograms in Figures 4-5, the increase in humidity also leads to a decrease in the separation and cleaning efficiency, but if we pay attention to the histogram in Figure 4, we can observe the effect of the angle of inclination of the bar on the cleaning and separation efficiency, where the separation efficiency at an angle of inclination of 150 is 97.8% at a cotton moisture content of 8.2%, which is 0.4% higher than the angle of inclination of the bar at 100 and 200, the separation efficiency at a cotton moisture content of 9.8% is 97.6%, which is 0.8 and 1.1% higher than the angle of inclination of 100 and 200, and the separation efficiency at a cotton moisture content of 11.6% is 96.9%, which is 0.5 and 0.9% higher than the angle of inclination of 100 and 200. we can see that is higher than . We can see that the cleaning efficiencies are also high. Thus, the separation and cleaning efficiencies of 150 were achieved.

DETERMINATION OF THE ROTATION SPEED OF THE SEPARATING RUBBER-SLAT DRUM.

The rotation speed of the separating drum has a significant effect on the efficiency of separating cotton pieces from the saw surface, and in this case, we determine it by changing the angle of inclination of the slats towards the center of the drum. We also study the effect of the angle of inclination of the slats on the cleaning efficiency. The experiments were carried out by setting the rotation speed of the rubber-slat separating drum to 750, 950, 1150 rpm.

The experiments were conducted on the I-sanoat variety processed at the enterprise. Laboratory analyzes showed that the initial impurity of cotton was 7.8%, and its moisture content was 8.9%. During the experiment, it was determined that the amount of cotton pieces separated from the cotton cleaning system of the UHC was in the range of 18.6-20.5%. The experimental results are presented in Figures 6-8.

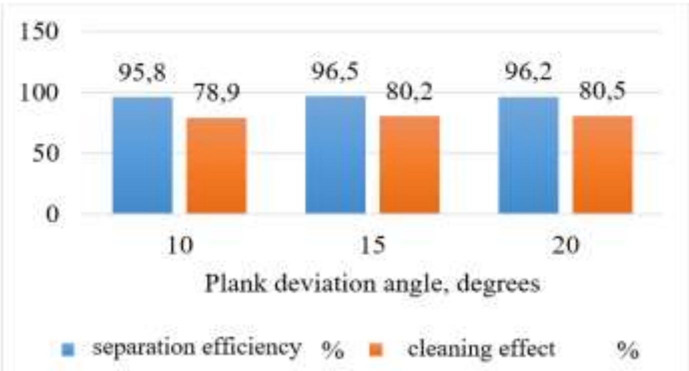

Fig. 6. Effect of variation of deflection angle on separation and cleaning efficiency of slatted drum at 750 rpm

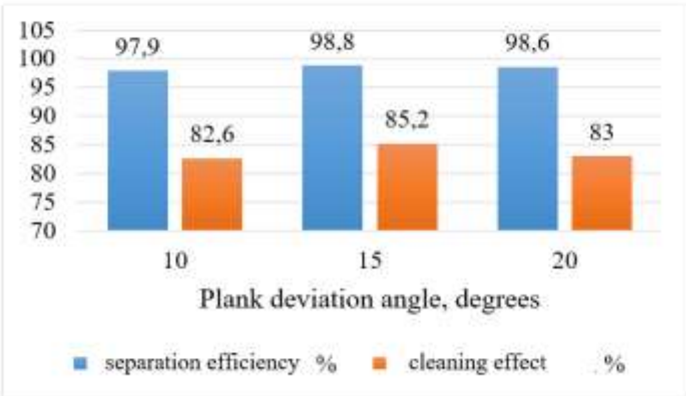

Fig. 7. Effect of variation of deflection angle on separation and cleaning efficiency of slatted drum at 950 rpm

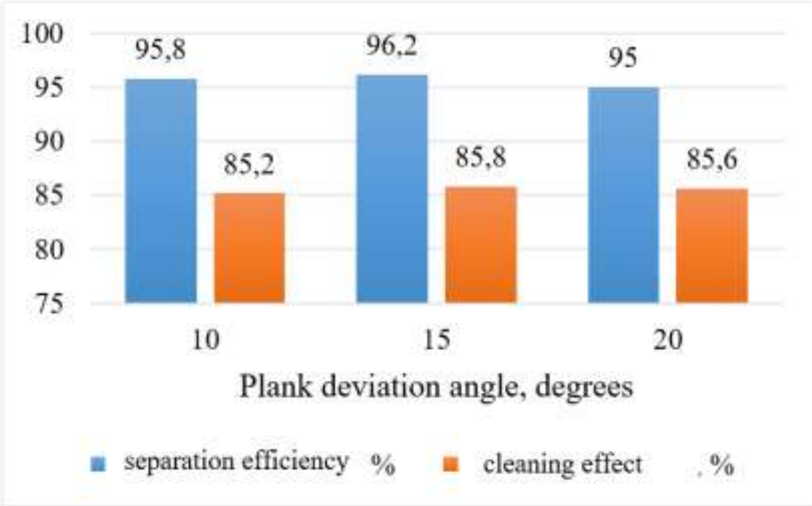

Fig.8. Effect of variation of deflection angle on separation and cleaning efficiency of slatted drum at 1150 rpm

From the histogram in Figure 7 above, it can be seen that the efficiency of separating the plates at 10^0, 15^0, 96.5%, and 20^0 at the angle of deviation of the plates towards the center of the drum at the rotation speed of the rubber-plate separation drum at 750 rpm was 96.2%. In this case, the cleaning efficiency was 78.9%, 80.2%, 80.5%. From the histograms in Figures 7-8 and 9, we can see the effect of the change in the rotation speed of the slatted drum and the changes in the angle of deviation of the slats on the change of the separation efficiency and cleaning efficiency, in which in Figure 8, the rotation speed of the slatted drum at 950 rpm compared to the separation efficiency at 750 rpm is 2.1% in the change of the angles of deviation of the slats. We can see that it is 2.3%, 2.4% higher and 2.1%, 2.6%, 3.6% higher compared to 1150 rpm, and the cleaning efficiency also showed higher values at 950 rpm and 1150 rpm. We can formulate a theory that increasing the rotation speed of the slatted drum to 950-1150 rpm leads to a decrease in the separation efficiency and an increase in the cleaning efficiency, which leads to the separation of small impurities due to the formation of a fan during the movement of cotton on the surface of the slat, but it should also be recognized that with an increase in speed, the saw will not have time to separate the cotton from the surface.

DETERMINING THE DISTANCE BETWEEN THE RUBBER-SLATTED DRUM SLATS AND THE SAW.

The distance between the separating slats and the saw also has a significant effect on the removal of cotton pieces from the surface of the saw teeth of the regenerator's cleaning saw drum. In brush separating drums, the distance between the saw and the saw is set to 0-2 mm [3]. In our case, if the slats of the rubber-slatted drum are brought too close to the saw teeth, the saw teeth can cause the rubber to be worn, so the distance between the slats and the saw was determined based on experiments to be 2-5 mm [5]. Previous studies have placed the slats along the axis of the drum and were mostly used in cotton ginning machines [6-8]. In the 1RX regenerator, in addition to separating the cotton from the saw blade and directing it towards the center, the cleaning efficiency is also increased by increasing the cleaning repetition while the separated cotton moves along the blade surface. Therefore, we study the effect of changing the angle of inclination of the blades towards the center of the drum on the separation and cleaning efficiency of the saw blade and the amount of cotton pieces in the waste.

During the experiments, the impurity of the I-Industrial grade cotton being processed was 5.6%, the moisture content was 8.6%, and the amount of cotton pieces in the waste coming from the waste conveyor in the UHC cleaning system to 1RX was analyzed, and it was found to be 20.6%.

During the experiments, the amount of waste coming out of the 1RX regenerator was measured and the amount of seeded cotton in it was determined, and the regeneration effect was calculated. During the experiment, the angle of deviation of the plank towards the center of the drum was set to 10^0-15^0-20^0 (tables 1-3).

Table 1. Regeneration efficiency index at 10^0 depending on the distance between the separating plate drum and the saw and the angle of installation of the plate to the drum of the cotton regenerator

Distance between the plank and the saw, mm	Waste separated from 1RX regenerator, kg	Amount of cotton separated with waste, kg	The amount of cotton in the waste, %	Regeneration efficiency %
2	110,5	4,8	4,3	95,6
4	109,6	4,2	3,8	96,1
6	112,4	5,5	4,8	95,1

Table 2. Regeneration efficiency index at 15° between the distance between the separating plate drum and the saw of the cotton regenerator and the angle of installation of the plate to the drum

Distance between the plank and the saw, mm	Waste separated from 1RX regenerator, kg	Amount of cotton separated with waste, kg	The amount of cotton in the waste, %	Regeneration efficiency %
2	112,0	4,2	3,7	96,2
4	114,2	3,9	3,4	96,5
6	111,3	4,8	4,3	95,6

Table 3. Regeneration efficiency index at 20° depending on the distance between the separating plate drum and the saw blade of the cotton regenerator and the angle of attachment of the plate to the drum

Distance between the plank and the saw, mm	Waste separated from 1RX regenerator, kg	Amount of cotton separated with waste, kg	The amount of cotton in the waste, %	Regeneration efficiency %
2	110,8	4,5	4,0	96,0
4	112,6	4,2	3,7	96,2
6	110,5	5,0	4,5	95,4

From the above tables 1-3, it can be seen that when the angle of installation of the separating slats to the center of the drum is set to 10^0, the amount of cotton seeds in the waste composition separated from the 1PX regenerator is 4.8 kg at a distance of 2 mm between the slat and the saw, and the regeneration efficiency is 95.6%, which is 0.6% higher than that of the current regenerator. At a distance of 4 mm between the slat and the saw, the amount of cotton seeds in the waste composition is 4.2 kg, and the regeneration efficiency is 96.1%. However, when the distance is increased to 6 mm, the regeneration efficiency decreases to 95.1%. Therefore, we can conclude that the cotton seeds pass between the slats and the saw blades due to the excessive increase in the distance.

From the experimental results, we can see that in Table 3, the regeneration efficiency increased by 96.2%, 96.5%, and 95.6% when the angle of the bar to the drum was 15^0 and the distance between the bar and the saw was changed, and the regeneration efficiency increased by 96.0%, 96.2%, and 95.4% when the angle of the bar to the drum was 20^0 (Table 3).

Considering the experimental results, a high regeneration efficiency was achieved when the angle of the bar to the drum was 15^0 and the distance between the bar and the saw was 4 mm. Therefore, we will continue the experiments and consider the effect on the separation efficiency.

During the experiments, the regenerator was stopped at each variant of the plank installation angle and spacing, and the cotton pieces remaining on the surface of the saw were separated and the separation efficiency was calculated (Fig. 9).

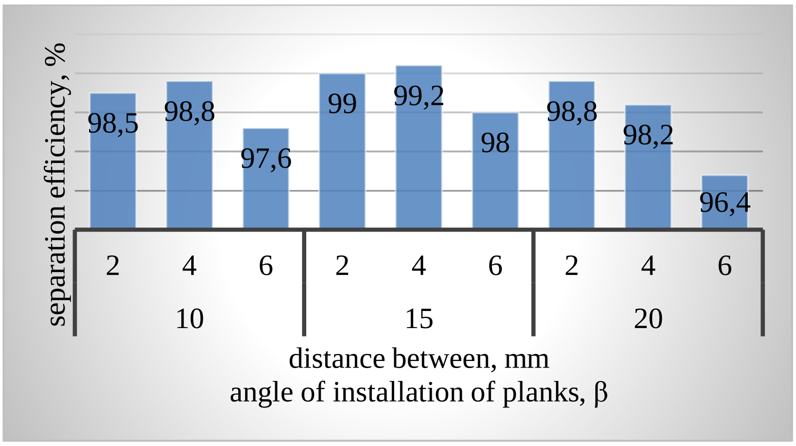

Fig. 9. The effect of the distance between the planks and the saw and the angle of the planks on the cutting efficiency

As can be seen from Figure 9 above, the efficiency of separating the planks from the saw teeth decreases as the distance between the saw and the plank changes from 2 mm to 6 mm. The separation efficiency is high at an angle of 15° to the drum and a distance between the plank and the saw of 4 mm, reaching 99.2%.

RESULTS AND CONCLUSIONS.

In order to effectively separate the cotton lint from the waste generated by cotton gins and reduce the level of contamination, the 1RX regenerator was improved as follows:

-The cotton intake pipe of the 1RX regenerator was changed, i.e., directing the waste cotton to both ends of the drum smoothes its spread along the surface of the saw drum;

-To effectively separate the cotton stuck in the saw drum, a rubber-slatted drum was used, with the slats placed at an angle to the center of the drum. This increases the separation efficiency and directs the cotton toward the outlet pipe;

-Reducing the distance between the rollers in the lower regeneration drum reduces the amount of cotton lint going into the waste.

From the experiments conducted to determine the number of rubber strips in the separation drum, it was found that the amount of cotton separated with the number of strips of 10 and 12 increased over the specified time interval and amounted to 20.6 and 23.6 kg. The separation efficiency was 95.8 and 96.1%, respectively, and the number of strips in the separation drum was higher with the number of strips of 10 and 12. However, due to the dense arrangement of the 12 strips in the drum, it was observed that the voltage on the electric motor decreased due to the difficulty of air passage between them during rotation, so the number of strips in the drum was left at 10.

The effect of the angle of deviation of the plank on the drum on the cleaning and separation efficiency was studied, in which the separation efficiency at the angle of deviation 150 was 97.8% at the cotton moisture content of 8.2%, and the deviation angle of the plank was 0.4% higher than at the angle of deviation of the plank at 10^0 and 20^0, the separation efficiency was 97.6% at the cotton moisture content of 9.8%, and the deviation angle at the angle of 10 and 20^0 We can see that it is higher by 0.8 and 1.1% compared to , the separation efficiency at 11.6% cotton moisture is 96.9%, and the deviation angle is higher by 0.5 and 0.9% compared to 10^0 and 20^0.

As a result of the experiment, a high separation efficiency of 99.2% was achieved when the angle of attachment of the plank to the drum was 15^0 degrees and the distance between the plank and the saw was 4 mm.

REFERENCES

[1]. Obidov, A., Shamshitdinov, M. Reactive power compensation and start-up energy waste reduction of linter device electric motor. E3S Web of Conferences, 2024, 515, 03013

[2]. A.A.Obidov M.M.Sultanov. To research the method of separating fibers suitable for spinning on a needle drum. International scientific and practical conference CUTTING EDGE-SCIENCE. June 29-30, 2020 Shawnee, USA, 128-131 P.

[3]. A Obidov, S Khamidov, I Muhammadjonova. Research removal of impurities by cleaning in the drum section of the fiber separation device - AIP Conference Proceedings, 2023.

[4]. Avazbek Azamatovich Obidov and Mirzaolim Mirzarakhmatovich Sultanov. Study of Technological Parameters of Fiber Separation Device. International Journal of Psychosocial Rehabilitation. 2020, Volume 24 - Issue 5, 6400-6407 P.

[5]. Borodin P.N., et al. Development of a stripping drum with metal strips for saw-toothed cleaners of raw cotton. Report, on topic 9807, JSC Scientific and Production Center "Paxtasanoatilm", Tashkent, 1999.

[6]. U.T. Abdullaev, H.K. Karimov, F.A. Veliev, I.A. Khalilov, I.F. Allakhverdieva, Experimental Evaluation of Boundaries Strength of Dense and Sparse Areas of Fabric with Variable Density by Weft, Izvestiya Vysshikh Uchebnykh Zavedeniy Seriya Teknologiya Tekstilnoy Promyshlennosti, Issue 2025(2), Pages 428–432

[7]. I.A. Khalilov, G.Z. Dzhabbarova, Analysis of Winding Mechanism with Dispersion of Winding Structure Defects by Periodic Changes of the Winding Drum Diameter, Izvestiya Vysshikh Uchebnykh Zavedeniy Seriya Teknologiya Tekstilnoy Promyshlennosti, Issue 2025(2), Pages 216–222

[8]. Obidov A.A. Improvement of the technology of cleaning and sorting of ginned seeds. Dissertation of Candidate of Technical Sciences. - Tashkent: TITLI, 2007. - 200 p.

Received: 03.02.2026
Accepted: 11.06.2026

MACHINE SCIENCE

ISSN: 2227-6912
E-ISSN: 2790-0479

2026, № 1 Pages 22-32

FEATURES AND FUNCTIONAL CAPABILITIES OF A MODERN CNC SYSTEM FOR IMPLEMENTING AUTOMATIC GRINDING CYCLES

Leonid SHIPULIN[1,a], Dmitriy ARDASHEV[1,b], Nizami YUSUBOV[2,c], Heyran ABBASOVA[2,d*]

[1]*Department of Automation Engineering, South Ural State University, Chelyabinsk, Russia*
[2]*Department of Mechanical Engineering Technology, Azerbaijan Technical University, Baku, Azerbaijan*

E-mail: [a]shipulinlv@susu.ru, [b]ardashevdv@susu.ru, [c]nizami.yusubov@aztu.edu.az, [d*]abbasova.heyran@aztu.edu.az

https://doi.org/10.61413/PKOF5853

Abstract: Modern mechanical engineering imposes increased requirements on the accuracy, surface quality, and productivity of finishing processes, among which grinding holds a key position. The enhancement of stability and efficiency in grinding operations is achieved through the use of Computer Numerical Control (CNC) machines equipped with automatic cycle systems. However, insufficient systematization of knowledge about the built-in cycles of modern CNC systems complicates their justified selection and effective application in production process planning. The aim of this research is the analysis and classification of the built-in automatic cycles of the Siemens Sinumerik 802D sl CNC system, focused on grinding operations, to assess their functional purpose and areas of rational application. The methodological basis of the work was a systematic analysis of the technical and reference documentation for this specific CNC system, as well as a review of scientific publications in the field of grinding technology. As a result of the study, a classification of automatic cycles was developed, structured by purpose into three groups: workpiece surface machining cycles, grinding wheel dressing and profiling cycles, and auxiliary cycles. A detailed analysis of the most technologically significant group – the machining cycles (CYCLE405, CYCLE410, CYCLE411, CYCLE412, CYCLE413, CYCLE414, CYCLE415, CYCLE451) – was conducted. Their clear specialization by the type of geometry being processed (short and long cylindrical surfaces, conical surfaces, faces, radii) and the applied grinding methods (with longitudinal feed, plunge, multi-pass, with oscillation) has been established. It was revealed that a key advantage of these cycles is the implementation of the classic three-stage processing scheme (roughing, finishing, spark-out), which minimizes the influence of elastic deformations and thermal effects and allows for the independent assignment of cutting conditions for each stage. The results of the work make it possible to formalize the process of selecting the optimal automatic cycle based on the part geometry, required surface quality, and characteristics of the grinding tool, thereby reducing process planning time and minimizing the influence of the subjective human factor.

Keywords: *grinding, automated processing cycles, classification of grinding cycles, production process planning, process design.*

INTRODUCTION

Modern mechanical engineering is characterized by increasing requirements for the quality, accuracy, and productivity of part manufacturing. One of the key finishing processes is grinding, upon which the final operational characteristics of products directly depend. Computer numerical control (CNC) grinding machines equipped with automatic cycle systems make it possible to significantly improve the stability and efficiency of this process [1-7]. However, the design of optimal machining cycles that ensure the simultaneous achievement of high accuracy, surface quality, and productivity remains a complex scientific and technical task [8-14]. The relevance of this study is driven by the need to develop and systematize approaches to using automatic control cycles for CNC grinding machines in order to minimize the subjective human factor and maximize the technological capabilities of the equipment. The aim of this work is to analyze and structure the built-in automatic cycles of the Siemens Sinumerik 802D SL CNC system for grinding operations, as well as to evaluate their functional purpose and areas of effective application.

Numerous studies are devoted to the optimization and automation of grinding processes. The fundamental works of S. Malkin and his colleagues [15, 16] laid the foundation for the optimization of grinding cycles by addressing process control issues to minimize machining time and prevent defects. Research in the field of adaptive control, such as the works of G. Xiao and S. Malkin [17], demonstrates the possibilities of online optimization of cutting parameters. The works of Russian scientists, such as P.P. Pereverzev and D.Yu. Pimenov [18], and V.I. Guzeev [19], consider methods for optimizing NC programs and designing cycles based on the rigidity of the machining system. The theoretical foundations for assigning machining allowances, which are a critical parameter for cycle design, are detailed in the works of V.M. Kovan [20] and reflected in the normative literature [21]. Despite the significant volume of research, most of the works focus on the theoretical optimization of individual parameters, while a comprehensive analysis of the standard cycles embedded in modern CNC systems, their comparative characteristics, and practical recommendations for their selection depending on the geometry of the machined surface are insufficiently represented in the literature. Existing manuals for CNC systems, such as those for Siemens Sinumerik [22], are primarily descriptive in nature and do not contain a systematized analysis from a technological point of view.

Thus, there is a problem of insufficient systematization of knowledge regarding the built-in automatic grinding cycles of modern CNC systems, which complicates their justified selection and effective use in the technological preparation of production. It is hypothesized that the classification and detailed analysis of the parameters of standard control system cycles will make it possible to formalize the process of their selection for typical grinding operations, thereby increasing the rationale behind the development of NC programs.

The methodological basis of the research is systems analysis. The work was carried out by studying and summarizing data from the technical and reference documentation for the Siemens Sinumerik 802D SL CNC system [22], as well as analyzing scientific publications in the field of grinding technology and machine tool control. The automatic cycles were classified by their intended purpose (machining cycles, dressing cycles, auxiliary cycles) and by the type of machined surfaces. For machining cycles, a detailed breakdown was performed according to parameters such as the number of machining stages (roughing, finishing, spark-out), applied grinding methods (traverse grinding, plunge grinding, multi-pass grinding), and the types of grinding wheels used.

Stages of machining at the inter-operational level

The first level of dividing machining into stages lies in the fact that the production of any mechanical engineering product involves a series of sequential technological operations to transform its geometric, physical, and chemical properties. The formation of almost any geometric feature occurs in several stages. To obtain accurate holes, an initial hole is drilled, which is then core-drilled and reamed. When machining external cylindrical surfaces, rough, semi-finish, finish, and fine turning are performed. When milling surfaces, both roughing and finishing operations are also carried out. All this indicates that practically all edge-cutting machining processes are carried out in several stages.

The division of machining into various operations is carried out due to their different functional purposes. In roughing operations (drilling, turning, milling, etc.), the goal is to remove as much machining allowance as possible using maximum cutting parameters, thereby ensuring maximum productivity. In finishing operations, the defective layer formed during roughing is removed from the part's surface, and the required parameters for the accuracy and surface quality of the product are achieved 23–25].

The question of how to divide the total machining allowance into roughing and finishing parts is one of the key issues in mechanical engineering technology. When answering this question, two conflicting conditions must be taken into account. On the one hand, the roughing allowance should be as large as possible, since this stage is the most productive. On the other hand, the finishing allowance must be sufficient to remove the defective layer and form a new high-quality surface.

The assignment of machining allowances in production is carried out as follows. Based on the type of workpiece (casting, forging, rolled stock), the total allowance for the entire machining process—necessary to compensate for errors during the execution of the entire set of machining steps—is determined according to the corresponding normative and technical document [26–29]. Next, the total allowance is divided into inter-operational allowances using a calculative-analytical method and normative data [30].

The theoretical foundations of the principle of assigning allowances for edge-cutting machining, set forth in the standards [30], are summarized and presented in the work of V.M. Kovan [20]. The author proposes a calculative-analytical method for assigning allowances, which is based on determining the minimum necessary allowance per step, which includes the thickness of the defective layer, surface roughness, form error, and setup error. The author considers errors in form, setup, and machining, and provides methodologies for their calculation. Based on these methodologies and the calculative-analytical method, normative data is formed [20].

STAGES OF MACHINING WITHIN A TECHNOLOGICAL OPERATION

The second level consists of dividing machining into stages within a technological operation, including through the use of CNC system features. As an example, let us consider the division of a technological operation into stages within a turning operation on a CNC lathe. Modern CNC systems have the ability to specify a standard turning cycle. The codes G70 (finish turning), G71 (longitudinal turning), G72 (face turning), and G73 (contour turning) are allocated for this purpose. The strategy for using these codes is as follows.

The contour of the finished surface is defined in the NC program, and the blocks of the recorded contour are numbered. Next, in the blocks of the NC program, the code G71, G72, or G73 is declared along with all necessary parameters and the numbers of the starting and ending blocks of the NC program that contain the finished surface contour. The CNC system automatically calculates the coordinates of the roughing passes with a specified step (Fig. 1). If finishing is required, the G70 code is placed in the program, specifying the exact same starting and ending block numbers containing the final contour.

When using one of the rough turning cycles (G71, G72, or G73) in combination with the G70 finish turning cycle, it is possible to set different feed rates, cutting speeds, and depths of cut for these stages. Thus, one can speak of a certain similarity to a simple two-stage machining cycle with varying cutting parameters within a single technological operation, distributed between two steps: rough and finish turning.

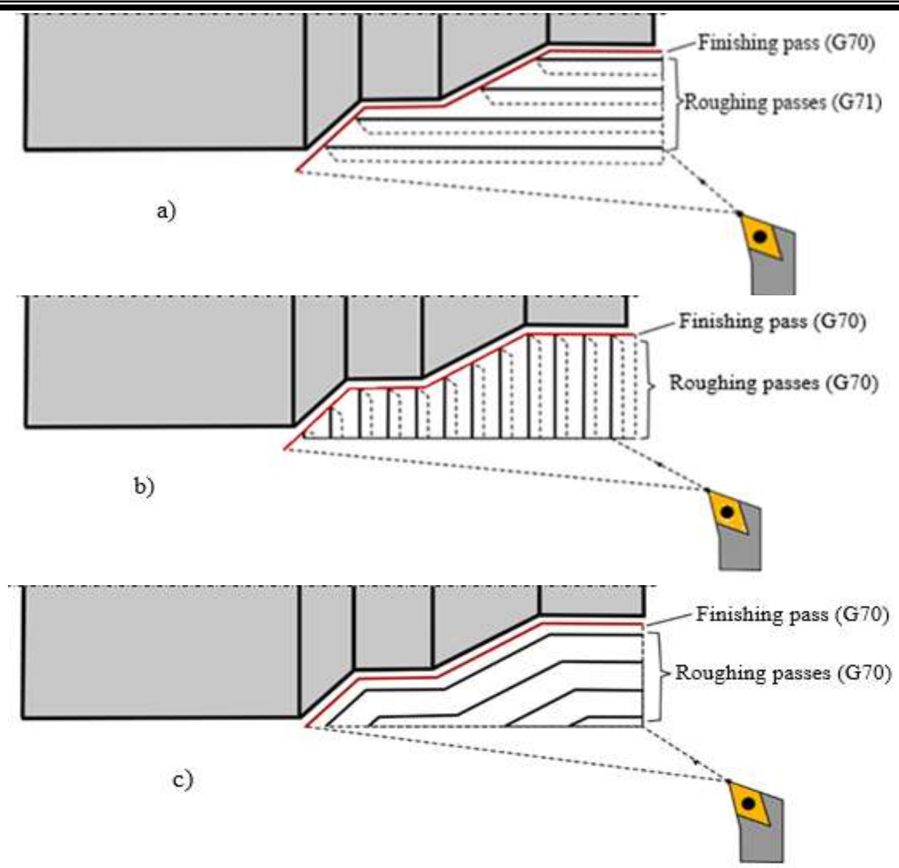

Fig. 1. Standard Turning Cycles: a) Longitudinal Rough Turning Cycle G71; b) Facing Rough Turning Cycle G72; c) Pattern Repeating Cycle G73

On modern CNC cylindrical grinding machines, machining can be carried out in the form of automatic cycles. The emergence of automatic cycles is related to the fact that edge-cutting machining is carried out in phases, meaning it exhibits a certain stage-by-stage nature. Let us consider two levels of dividing machining into stages.

Considering the second level of dividing a technological operation into stages as applied to grinding, it should be said that the machining is carried out in the form of an automatic cycle. An automatic cycle is generally understood as the sequence of relative movements of the grinding wheel and the workpiece, during which the workpiece is machined in a grinding operation. In its simplest form, an automatic cycle consists of two (roughing and finishing) or three (roughing, finishing, and spark-out) stages. Each stage has a different functional purpose: at the roughing stage, the majority of the allowance is removed at a high removal rate; at the finishing stage, the defective layer remaining after roughing and the rest of the allowance are removed; at the spark-out stage, the requirements for high accuracy and low surface roughness are achieved. In a general sense, automatic machining cycles can be applied in operations of external cylindrical grinding, internal cylindrical grinding, peripheral surface grinding, face surface grinding, profile grinding, and other types.

AUTOMATIC MACHINING CYCLES OF CNC GRINDING MACHINE CONTROL SYSTEMS

The Siemens Sinumerik 802D SL CNC system for cylindrical grinding machines provides the following built-in automatic cycles for the movement of the machine's working elements.

The "CYCLE405" cycle is designed for taper grinding, which can be carried out using two methods: traverse grinding (Fig. 2, a) and multiple plunge grinding (Fig. 2, b). The cycle is specified in the form of cutting parameters for the roughing, finishing, and spark-out (fine finishing) stages, and there is an option to set intermediate dressing. By default, each stage is implemented as traverse grinding, but it is possible to specify the machining as multiple plunge grinding at the roughing stage; at the roughing and finishing stages; or at all stages.

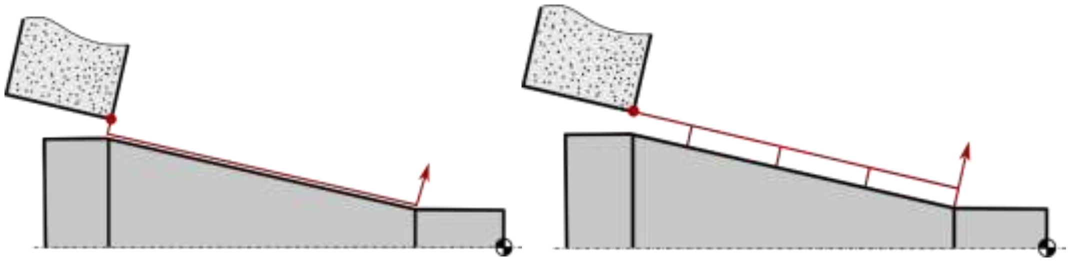

a) b)

Fig. 2. Cone grinding with CYCLE405: a) with longitudinal feed; b) with multi-plunge grinding

The "CYCLE406" cycle is designed for positioning the grinding wheel along the Z-axis (Fig. 3). The cycle specifies the starting position to which the grinding wheel is automatically brought during the execution of the cycle; then, the grinding wheel is fed to the face of the workpiece-either via manual feed by the operator or automatic feed until contact is detected by a sensor-to position the grinding wheel relative to the workpiece along the Z-axis. After making contact with the workpiece, a specified number of spark-out revolutions is executed. This cycle is intended for setup rather than machining, so it should not be considered an automatic machining cycle.

The "CYCLE407" cycle is designed to define an obstacle diameter and allows the grinding wheel to be directed to a safe position during interruptions, for example, during intermediate tool dressing (Fig. 4). For this purpose, an X coordinate is specified in the cycle to which the tool is retracted, followed by its safe movement along the Z-axis. This cycle is intended for setup rather than machining, so it should not be considered an automatic machining cycle.

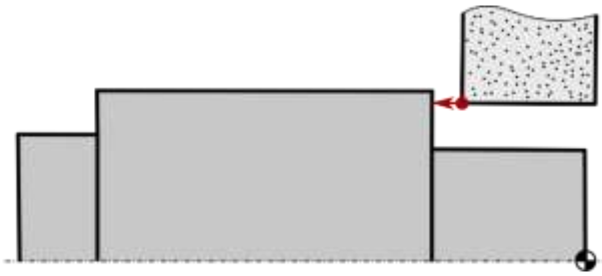

Fig. 3. Positioning the workpiece relative to the grinding wheel in the Z-axis using CYCLE406

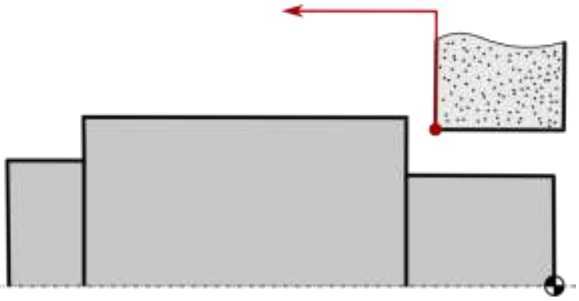

Fig. 4. Definition of an obstacle for the X-axis using CYCLE407

The "CYCLE410" cycle is designed for the plunge grinding of cylindrical surfaces. The cycle is applied only in cases where the width of the machined surface is less than the width of the grinding wheel. The cycle is specified as a set of cutting parameters for the roughing, finishing, and spark-out (fine finishing) stages. During the plunge, it is possible to set either a straight plunge feed or a plunge with oscillation along the Z-axis (Fig. 5). Grinding can be carried out using either a straight-profile wheel or an inclined wheel with a conical profile.

The "CYCLE411" cycle is designed for multiple plunge grinding along the length of the workpiece (Fig. 6). The cycle is applied in cases where the width of the grinding wheel is less than the width of the machined surface, meaning that to machine the entire surface, it is necessary to plunge into the workpiece multiple times using a plunge feed. The cycle is specified as a set of cutting parameters for the roughing, finishing, and spark-out (fine finishing) stages; the amount of overlap between the current and previous positions of the grinding wheel is also specified. The roughing stage is always carried out in the form of multiple plunge grinding, while the finishing and spark-out stages are performed as traverse grinding. In this case, grinding can be carried out using either a straight-profile wheel or an inclined wheel with a conical profile.

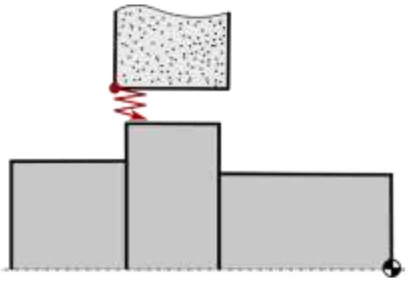

Fig. 5. Plunge grinding with oscillation using CYCLE410

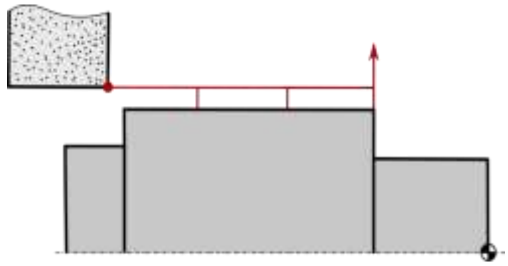

Fig.6. Multi-plunge grinding using CYCLE411

The "CYCLE412" cycle is designed for the plunge grinding of a face. The cycle is specified as a set of cutting parameters and allows the face to be rough ground, or rough and finish ground; there is also an option to set spark-out (fine finishing). During plunging, it is possible to set either a straight plunge feed or a plunge with oscillation along the X-axis (Fig. 7). Grinding can be carried out using either a straight-profile wheel or an inclined wheel with a conical profile.

The "CYCLE413" cycle is designed for the plunge grinding of a cylindrical surface with an angular feed at a 45° angle without machining the adjacent face (Fig. 8). The cycle is applicable in cases where the size of the grinding wheel exceeds the size of the machined surface. It is possible to set the cycle parameters to implement roughing, finishing, and fine finishing stages. Machining can be carried out using either a straight-profile wheel or an inclined wheel with a conical profile.

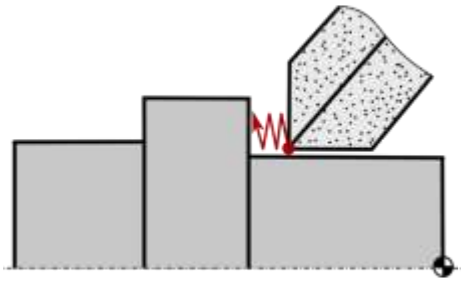

Fig. 7. Plunge face grinding using CYCLE412

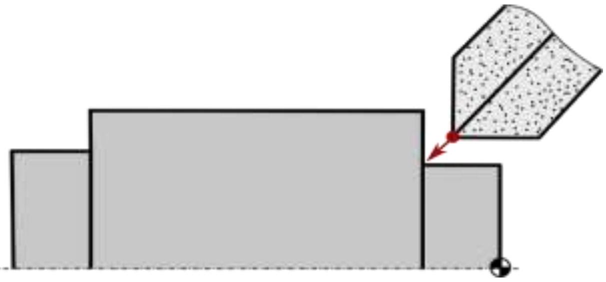

Fig. 8. Plunge grinding of a cylindrical surface without face contact using CYCLE413

The "CYCLE414" cycle is designed for the rough grinding of an internal or external radius (Fig. 9). Radius grinding is carried out in a single pass, which is due to the lack of high accuracy requirements for radii. Therefore, this cycle is applicable for grinding radii, but it should not be considered a scientific cycle.

The "CYCLE415" cycle is designed for grinding a cylindrical surface with traverse feed (Fig. 10). The cycle is applied when the width of the grinding wheel is less than the width of the machined surface. It is possible to machine the surface: rough; rough and finish; rough, finish, and with spark-out. Radial feed can be applied either per single working stroke of the tool or per double working stroke. Machining can be carried out using either a straight-profile wheel or an inclined wheel with a conical profile.

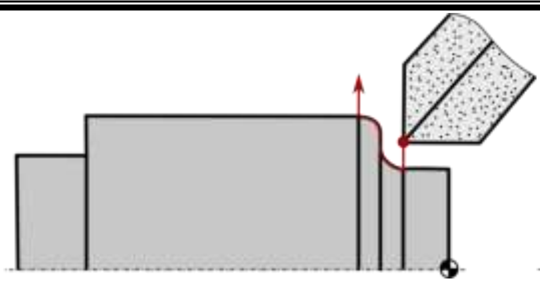

Fig. 9. Grinding of external and internal radii using CYCLE414

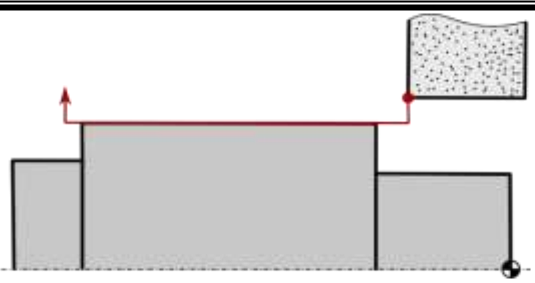

Fig. 10. Cylindrical grinding with longitudinal feed using CYCLE415

The "CYCLE416" cycle is designed for specifying the dressing and profiling of the grinding wheel (Fig. 11). The cycle allows for the dressing and profiling of the geometry of two types of grinding wheels (straight and inclined), as well as those with a corner radius or a corner chamfer. To define the cycle, parameters are set: the dressing depth for each surface of the grinding wheel and the dressing mode. At the same time, the tool parameters are read in the program from the entered information about the grinding wheels. During dressing, the removed amount is accounted for in the wear parameters of the active tool offset. Despite the importance of this cycle, it does not entirely fall under the scope of this research.

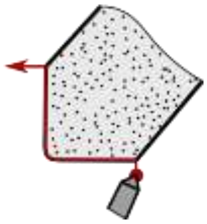

Fig. 11. Grinding wheel dressing and profiling using CYCLE416

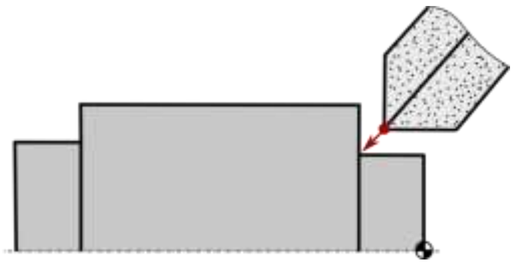

Fig. 12. Plunge grinding of a cylindrical surface and face using CYCLE451

The "CYCLE420" cycle is designed for specifying the dressing and profiling conditions when machining a batch of workpieces. The distinguishing feature of CYCLE420 compared to CYCLE416 is that the former is launched when a specified number of workpieces has been machined, whereas the latter is launched exactly when called in the NC program. To define the cycle, parameters are set: the dressing depth for each surface of the grinding wheel, the dressing mode, and the number of workpieces after which the dressing and profiling cycle will be triggered. The cycle must be specified at the beginning of the NC program.

The "CYCLE430" cycle is designed for specifying the dressing of a profile grinding wheel using a profile roller. After dressing, the amount of the removed layer is accounted for in the wear parameters of the active tool offset. The dressing is triggered after machining the number of workpieces specified in the cycle.

The "CYCLE446" cycle is designed for selecting the peripheral speed of the grinding wheel. At the same time, a check of the maximum peripheral speed and the rotational speed is performed for all wheels mounted on the spindle. If the peripheral speed or rotational speed is exceeded, a warning message is displayed, and the value is limited to the corresponding maximum.

The "CYCLE450" cycle is designed for specifying technological parameters: the type of feed programming per stroke and the selection of the feed rate for traverse grinding.

The "CYCLE451" cycle is designed for plunge grinding with an angular feed of a cylindrical surface and its adjacent face (Fig. 12). The cycle is applicable in cases where the dimensions of the grinding wheel exceed the dimensions of the machined surfaces. It is possible to set the cycle parameters to implement roughing, finishing, and fine finishing stages. Machining can be carried out using either a straight-profile wheel or an inclined wheel with a conical profile.

Thus, the standard cycles of the Siemens Sinumerik CNC system have been reviewed, which include: workpiece surface machining cycles, grinding wheel dressing cycles, and auxiliary cycles. The workpiece surface machining cycles and general information about them are summarized in Table 1.

Table 1. Summary of Machining Cycles for the Siemens Sinumerik CNC System

Cycle code	Machined surfaces	Machining method description	Grinding wheel types used
CYCLE405	External conical surface	Grinding is performed as a cycle that includes roughing, finishing, and spark-out stages. Machining during these stages is carried out either as multiple plunge grinding or as traverse grinding (longitudinal feed grinding).	Straight-profile grinding wheel (PP / Type 1); tapered-profile grinding wheel (2P)
CYCLE410	Short external cylindrical surface	Grinding is performed as a cycle that includes roughing, finishing, and spark-out stages. Machining at each stage is carried out as straight plunge grinding or with oscillation along the machined surface.	Straight-profile grinding wheel (PP); tapered-profile grinding wheel (2P)
CYCLE411	Long external cylindrical surface	Grinding is performed as a cycle that includes roughing, finishing, and spark-out stages. Machining at the roughing stage is always carried out as multiple plunge grinding along the length of the workpiece, while the finishing and spark-out stages are performed as traverse grinding.	Straight-profile grinding wheel (PP); tapered-profile grinding wheel (2P)
CYCLE412	End face	Grinding is performed as a cycle that can include: roughing only; roughing and finishing; or roughing, finishing, and spark-out stages. Machining at each stage is carried out as straight plunge grinding or with oscillation along the machined surface.	Straight-profile grinding wheel (PP); tapered-profile grinding wheel (2P)
CYCLE413	Short external cylindrical surface	Grinding is performed as a cycle that can include: roughing only; roughing and finishing; or roughing, finishing, and spark-out stages. Machining is carried out as angular-feed plunge grinding at an angle of 45° without machining the end face.	Straight-profile grinding wheel (PP); tapered-profile grinding wheel (2P)
CYCLE414	Radiused surfaces (fillets)	Radius grinding is performed using circular interpolation with a constant feed rate of the grinding wheel.	Tapered-profile grinding wheel (2P)
CYCLE415	Long external cylindrical surface	Grinding is performed as a cycle that can include: roughing only; roughing and finishing; or roughing, finishing, and spark-out stages. Machining is carried out as traverse grinding. Radial feed is applied per working stroke or per double working stroke of the tool.	Straight-profile grinding wheel (PP); tapered-profile grinding wheel (2P)
CYCLE451	Short external cylindrical surface and adjacent end face surface	Grinding is performed as a cycle that includes roughing, finishing, and spark-out stages. Machining is carried out as angular-feed plunge grinding.	Straight-profile grinding wheel (PP); tapered-profile grinding wheel (2P)

RESULTS AND DISCUSSION

As a result of the systematic analysis of the technical documentation and scientific publications, a classification of the built-in automatic cycles of the Siemens Sinumerik 802D SL CNC system, designed for cylindrical grinding operations on CNC machines, has been developed. All considered cycles were structured by their intended purpose into three main groups: 1) workpiece surface machining cycles; 2) grinding wheel dressing and profiling cycles; 3) auxiliary cycles. The most extensive and technologically significant is the first group, a detailed analysis of which made it possible to identify their key characteristics and areas of rational application.

As follows from the data presented in Table 1, the machining cycles (CYCLE405, CYCLE410, CYCLE411, CYCLE412, CYCLE413, CYCLE414, CYCLE415, CYCLE451) possess a clear specialization based on the type of geometry being machined. It has been established that the system offers flexible solutions for machining short (CYCLE410, CYCLE413, CYCLE451) as well as long cylindrical surfaces (CYCLE411, CYCLE415), conical surfaces (CYCLE405), faces (CYCLE412), and radii (CYCLE414). An important result is the identification of two fundamentally different machining strategies embedded in the cycles: traverse grinding and plunge grinding (including multi-pass and oscillating plunge). The choice between them directly depends on the ratio of the width of the grinding wheel to the machined surface, which is consistent with the fundamental principles of grinding technology presented in the works of S. Malkin [15, 16].

A key advantage of the analyzed cycles is their multi-stage nature. The vast majority of the machining cycles implement a classic three-stage scheme: roughing, finishing, and spark-out (fine finishing) stages. This fully corresponds to the theoretical foundations of machining staging discussed in the introduction. At the roughing stage, the main part of the allowance is removed with maximum productivity; at the finishing stage, the defective layer is removed and the required dimensions are achieved; and at the spark-out stage, high levels of accuracy and surface finish are ensured. Such a division makes it possible to minimize the influence of negative factors such as elastic deformations of the machining system and thermal effects, which was noted in the studies by V.I. Guzeev [19] and P.P. Pereverzev [18]. The ability to independently set cutting parameters (feeds, speeds) for each stage provides the process engineer with a tool for fine-tuning the process, analogous to the principles used in turning cycles (G71, G72).

The obtained results allow formalizing the process of selecting an automatic cycle depending on the technological task. For example, for grinding a long cylindrical surface when the wheel width is insufficient, it is advisable to use CYCLE411, which combines multiple plunge grinding at the roughing stage with traverse grinding at the finishing and fine finishing stages. For the simultaneous machining of a cylindrical surface and its adjacent face when a large grinding wheel is available, CYCLE451 is the optimal solution. The identified specialization of the cycles refutes a universal approach and emphasizes the need for their justified selection, which reduces the risks of defects and increases process stability.

The discussion of the results would be incomplete without mentioning the dressing cycles (CYCLE416, CYCLE420, CYCLE430). Although they do not directly perform machining, their correct application is critically important for maintaining the geometric accuracy and cutting ability of the grinding wheel throughout the entire operation. The integration of these cycles into the NC program, especially with an automatic trigger after machining a specified batch of workpieces (CYCLE420), is a practical implementation of the adaptive control principles discussed in the works of G. Xiao and S. Malkin [17].

Thus, the conducted analysis and the proposed classification systematize the disparate information regarding the standard grinding cycles of the Siemens Sinumerik 802D SL. The results of the work make it possible to reduce the time for the technological preparation of production by formalizing the selection of the optimal machining cycle depending on the part geometry, the required surface quality, and the characteristics of the grinding tool. This helps to reduce the subjective factor during programming and to increase the efficiency of using high-tech equipment. In further research, experimental verification of the developed recommendations and their adaptation for other modern CNC systems are planned.

REFERENCES

[1]. Al-Ahmari A.M.A. Predictive machinability models for a selected hard material in turning operations. Journal of Materials Processing Technology, 2007, Vol. 190(1), pp. 305-311.

[2]. Koshin A.A. Obrabotka na tokarnykh stankakh: naladka, rezhimy rezaniya. Spravochnik (Processing on Turning Machines: Adjustment and Cutting Mode: Handbook). Siti-Print, 2012.

[3]. Bogatenkov S.A., Sazonova N.S., Yusubov N.D., Abbasova H.M., Badalova B.B., Bazhenov R.I. Decision-making in the conditions of introduction of automated design systems of technological processes. SOCAR Proceedings Special, 2022, No. 1, pp. 006–010.

[4]. Aouici H., Yallese M.A., Chaoui K., Mabrouki T., Rigal J.F. Analysis of surface roughness and cutting force components in hard turning with CBN tool: Prediction model and cutting conditions optimization. Measurement, 2012, Vol. 45(3), pp. 344-353.

[5]. Yusubov N., Abbasova H., Khankishiyev I. Development of a planning theory for multi-tool machining with the possibilities of modern CNC machine tools. Forschung im Ingenieurwesen, 2021, Vol. 85(2), pp. 661–678.

[6]. Guzeev V., Yusubov N., Abbasova H., Dadashov R. Optimization of the number of machining stages workpieces for mechanical engineering parts. Machine Science, 2024, No. 2, p. 4-12

[7]. Yusubov N., Ardashev D., Abbasova H., Dadashov R. The influence of cutting conditions and tool wear on machining efficiency in CNC machine tools. Machine Science, 2025, No. 1, pp. 4–19.

[8]. Pereverzev P., Pimenov D. Optimization of control programs for numerically controlled machine tools by dynamic programming. Russian Engineering Research, 2015, Vol. 35(2), pp. 135–142.

[9]. Guzeev V., Nurkenov A. Designing the plunge-grinding cycle on the basis of the rigidity of the technological system. Russian Engineering Research, 2015, Vol. 35(2), pp. 150–153.

[10]. Bogatenkov S.A., Sazonova N.S., Yusubov N.D., Mammadov P.V., Bazhenov R.I. Increasing the productivity of multitool machining on automated lathes by optimizing the machining plan. Russian Engineering Research, 2021, Vol. 41(11), pp. 1071–1074.

[11]. Yusubov N.D., Abbasova H.M. Full factorial models of dimensional accuracy of multi-tool machining on automatic turning machines. Bulletin of the South Ural State University. Series: Mechanical Engineering Industry, 2019, Vol. 19(1), pp. 56–67.

[12]. Simon S., Yusubov N.D., Amirli S.F., Amirov F.G. Hardness of surface layers obtained after waterjet cutting of chromium–nickel steel workpieces. Russian Engineering Research, 2025, Vol. 45(12), pp. 1714–1718.

[13]. Yusubov N., Abbasova H., Dadashov R. Modeling of machining accuracy of conical surfaces on CNC machine tools. Proceedings, 2025, Vol. 2, pp. 59–67.

[14]. Balabanov I., Movlazade V., Yusubov N., Abbasova H., Dadashov R., Huseynov R. Development

of a parametric model for calculating cutting forces in external cylindrical turning of 20CrMn steel (1.7147) using an SNMG 15 06 16-PR 4425 insert. Reliability: Theory and Applications, 2025, Vol. 20(7), pp. 335–342.

[15]. Malkin S., Koren Y., Ber A. Off-Line Grinding Optimization with a Micro-Computer. CIRP Annals, 1980, Vol. 29(1), pp. 213–216.

[16]. Malkin S. Grinding Cycle Optimization. CIRP Annals, 1981, Vol. 30(1), pp. 223–226.

[17]. Xiao G., Malkin S. On-Line Optimization for Internal Plunge Grinding. CIRP Annals — Manufacturing Technology, 1996, Vol. 45(1), pp. 287–292.

[18]. Pereverzev P., Akintseva A. Optimal internal grinding cycles in multidimensional control-parameter space. Russian Engineering Research, 2016, Vol. 36(11), pp. 974–978.

[19]. Guzeev V.I. Improving the efficiency of integrated technological processes at the stages of design and implementation. Science-Intensive Technologies in Mechanical Engineering, 2014, No. 7 (37), pp. 36-41.

[20]. Kovan V.M. Fundamentals of Machine-Building Technology. Moscow: Mashgiz, 1953. 400 p.

[21]. Kosilova A.G. (Ed.) Handbook of a Mechanical Engineering Technologist. In 2 vols. Vol. 1. Moscow: Mashinostroenie, 1985. 656 p.

[22]. SIEMENS SINUMERIK 802D SL. Cylindrical Grinding: Programming and Operating Manual. Software Version 1.4. Available at: https://cache.industry.siemens.com/dl/files/125/28436125/att_76624/v1/802DSL_BPRS_0709_ru_ru-RU.pdf (accessed: 04.06.2021).

[23]. Ivester R., Danai K., Malkin S. Optimization of cylindrical plunge grinding by recursive constraint bounding. American Society of Mechanical Engineers, Dynamic Systems and Control Division, 1995, Vol. 57-1, pp. 529–537.

[24]. Lapshin V.P., Turkin I.A., Khristoforova V.V. An example of experimental evaluation of the influence of wear on the components of the cutting force in metal turning. STIN, 2020, No. 4, pp. 41-44.

[25]. Childs T.H.C., Sekiya K., Tezuka R., et al. Surface finishes from turning and facing with round nosed tools. CIRP Annals. 2008. Vol. 57. P. 89–92.

[26]. GOST 2590-2006 Hot-rolled steel round bars. Size assortment. Moscow: Standartinform, 2012.

[27]. GOST R 53464-2009. Castings from metals and alloys. Dimensional tolerances, mass tolerances and machining allowances (with Amendments No. 1, 2). Moscow: Standartinform, 2010.

[28]. GOST 7062-90. Forgings of carbon and alloy steel made by press forging. Moscow: IPK Publishing House of Standards, 2003.

[29]. GOST 7505-89. Steel die forgings. Tolerances, allowances and forging draft. Moscow: Standartinform, 2003.

[30]. Kosilova A.G., Meshcheryakov R.K., Kalinin M.A. Machining Accuracy, Workpieces and Allowances in Mechanical Engineering. Moscow: Mashinostroenie, 1976. 288 p.

Received: 04.12.2025
Accepted: 04.06.2026

MACHINE SCIENCE

ISSN: 2227-6912
E-ISSN: 2790-0479

2026, № 1 Pages 33-39

INVESTIGATION OF UNIFORM WEAR DISTRIBUTION ON BRAKE SHOES IN DRUM BRAKE MECHANISMS USING FLOATING BRAKE SHOE DESIGN

Farhad SHIRZADOV[1,a*], Yadullah BABAYEV[1,b], Orkhan HUSEYNOV[2,c]

[1]Azerbaijan Technical University, Baku, Azerbaijan
[2]The University of Alabama in Huntsville, Alabama, USA

E-mail: [a]farhad.shirzadov@aztu.edu.az, [b]yadullah.babayev@aztu.edu.az, [c]orkhan.huseynov@uah.edu*

https://doi.org/10.61413/EBUZ5569

Abstract: One of the most important mechanisms ensuring the safe operation of machines and mechanical systems is the braking system. The primary cause of brake failure is wear of brake shoes. This paper investigates the improvement of a drum brake mechanism in which friction linings experience non-uniform wear over the entire contact surface. In contrast to conventional approaches, a movable rod connecting the ends of the brake shoes is introduced, and the force distribution over the friction surface together with shoe displacements are simulated using SOLIDWORKS software. Based on the simulation results, the proposed design increases the contact area between the friction linings and the drum, thereby promoting more uniform wear compared with conventional configurations. The proposed construction can be applied to lifting and transporting machines equipped with drum brake mechanisms.

Keywords: *drum brake mechanism; brake shoe wear; numerical simulation; tribology; hydraulics*

INTRODUCTION

The performance and reliability of drum brake mechanisms have been subjects of extensive investigation in both automotive and industrial applications. Achieving uniform contact pressure distribution and minimizing non-uniform wear of brake shoes constitute fundamental challenges that directly influence braking efficiency, operational safety, and component service life. Numerous studies have demonstrated that inadequate contact conditions at the brake shoe–drum interface not only reduce braking effectiveness but also accelerate material deterioration, thereby increasing maintenance demands and operational costs.

One of the principal research directions in drum brake analysis has focused on understanding the contact pressure distribution between brake shoes and drums. Söderberg and Andersson conducted comprehensive numerical investigations using finite element analysis to simulate wear and contact pressure distribution at the pad-to-rotor interface in disc brakes, demonstrating that general-purpose finite element software can effectively predict wear patterns under steady-state drag conditions through implementation of a generalized Archard wear law [1]. Their three-dimensional finite element model revealed that contact pressure distribution plays a decisive role in determining the useful life of braking components and overall system behavior. Similarly, analytical approaches have been employed to characterize steady wear states in drum brakes. The analytical expressions for contact pressure distribution in drum brakes, derived from variational principles by minimizing wear dissipation power, indicate that steady-state pressure distributions can be expressed in terms of sine functions of angular position, providing critical insights into the transition from transient to steady wear conditions [2]. These findings underscore the significance of accurate pressure modeling in predicting long-term tribological performance.

The tribological behavior of friction materials constitutes another essential aspect of drum brake performance. Recent investigations have examined composite brake pad materials under variable operational conditions to evaluate the influence of applied load and rotational speed on the coefficient of friction. Results demonstrate that the coefficient of friction increases progressively from approximately 0.697 at low contact pressures to 0.795 under maximum applied loads, attributable to enhanced interfacial interactions, mechanical interlocking of surface asperities, and tribo-film stabilization [3]. These tribological characteristics are particularly critical in heavy-duty applications where elevated contact stress and sustained thermal exposure demand superior friction material performance. Furthermore, comprehensive reviews of friction material behavior in disk-brake systems emphasize that structural changes in contact surfaces significantly affect tribological properties, thereby influencing braking system stability and reliability [4]. Understanding the evolution of these interfacial properties under realistic operating conditions remains paramount for optimizing brake lining formulations and improving service longevity.

Finite element simulation has emerged as an indispensable tool for analyzing the mechanical behavior of brake assemblies under complex loading scenarios. Detailed finite element analyses of brake shoes under static loading conditions have revealed that structural design significantly influences stress distribution and deformation patterns. In one notable study, the maximum stress observed in brake shoe structures reached 418.09 MPa under operational loads, exceeding the allowable stress threshold and indicating potential structural inadequacy. Subsequent structural modifications, including thickening and chamfering of the main beam, successfully reduced peak stresses to 288.97 MPa, thereby achieving a safer design margin [5]. These simulation-driven design improvements illustrate the value of computational approaches in refining brake component geometry to enhance durability and prevent premature failure. Moreover, advanced multi-physics coupling frameworks that simultaneously address transient heat conduction, nonlinear stress distribution, and wear evolution provide comprehensive insights into the degradation mechanisms governing brake drum performance. Such integrated simulation strategies enable quantitative assessment of material fatigue life and facilitate more accurate prediction of maintenance intervals [6].

In addition to computational modeling, experimental investigations have provided valuable validation of analytical predictions and have revealed practical challenges associated with non-uniform wear. Field observations indicate that in conventional single-cylinder drum brake mechanisms, wear typically initiates near the hydraulic actuator and progresses toward the pivot region of the shoe, often resulting in complete lining depletion near the actuator while substantial material remains unused near the pivot. This severe non-uniformity not only diminishes material utilization efficiency but also compromises braking effectiveness by reducing the effective contact area between the shoe and the drum. Studies focusing on brake shoe geometry and optimization have emphasized that proper selection of contact angle, lining length, and shoe support configuration can substantially alter contact pressure distribution and improve wear uniformity[7]. Mathematical models incorporating both elastic deformations and preliminary contact geometry have demonstrated that conventional rigid-body assumptions fail to capture the actual contact behavior, thereby highlighting the necessity of including material compliance in predictive models [8].

The optimization of brake shoe design to promote uniform wear and enhance braking torque has been addressed through various engineering strategies. One approach involves reconfiguring the location of shoe rotation pins to maximize braking moment based on steady-state pressure distributions, thereby improving mechanical efficiency [2]. Alternative strategies include the introduction of auxiliary adjustment mechanisms and modified hydraulic actuation schemes to ensure more consistent contact along the entire friction surface. However, practical implementation of such modifications has often been hindered by increased structural complexity, elevated maintenance requirements, and economic constraints. Consequently, achieving a balance between improved performance and practical feasibility remains an ongoing challenge in brake system development.

In conclusion, the literature reveals a multifaceted research landscape addressing the tribological, thermal, and mechanical challenges inherent in drum brake mechanisms. While significant progress has been made in characterizing contact pressure distributions, modeling wear behavior, and employing advanced simulation techniques, the problem of achieving uniform wear and optimized contact conditions in a practical, cost-effective manner remains an area of active investigation. The integration of analytical modeling, computational simulation, and experimental validation continues to drive innovation toward more durable, efficient, and reliable drum brake systems.

PROPOSED DESIGN CONCEPT AND RESEARCH OBJECTIVES

The operating principle of the proposed simple design, intended to ensure uniform wear over the friction surface of the brake shoes, is based on installing a movable rod between the shoe ends located opposite the working hydraulic cylinder. Owing to the braking force, the shoe whose friction lining is more severely worn rotates about the contact line between the shoe and the brake drum, thereby pressing the opposite shoe against the drum, as illustrated in Fig. 1.

During braking, the working hydraulic brake cylinder (1) forces the shoe (2) against the drum (5). In a drum brake mechanism, because wear depth increases toward the region near the hydraulic actuator, a contact point is formed between the worn and unworn regions of the friction lining. Under braking conditions, the shoe rotates about this point and generates a moment M_2 proportional to the lever arm a_2 of the braking force. This moment produces an additional force in the movable rod (3), depending on both the braking-force lever arm a_2 and the distance a_3 between the shoe pivot and the movable rod, thereby pushing the rod laterally. Which of the two shoes—left or right—compresses the opposite one depends, for equal braking forces, on the respective lever arms and on the direction of drum rotation.

From a static standpoint, an initial analysis might suggest that the shoe with the more severely worn friction lining would dominate because of the larger effective force lever arm, leading to preferential wear of a single shoe throughout the service life. To clarify this mechanism, a specific static case is considered. If the upper region of the right shoe is more heavily worn than that of the left shoe, the force generated by this shoe on the movable rod will exceed the force produced by rotation of the left shoe, as shown in Fig. 1. Under such conditions, wear will occur in the upper region of the right shoe, while both the upper and lower regions of the left shoe will also participate in contact. This situation is considered more efficient than that of conventional designs, in which only the upper portions of the shoes are in contact with the drum. In contrast, the proposed configuration can statically provide three distinct contact regions between the shoes and the drum instead of two, thereby promoting more uniform utilization of the friction lining material.

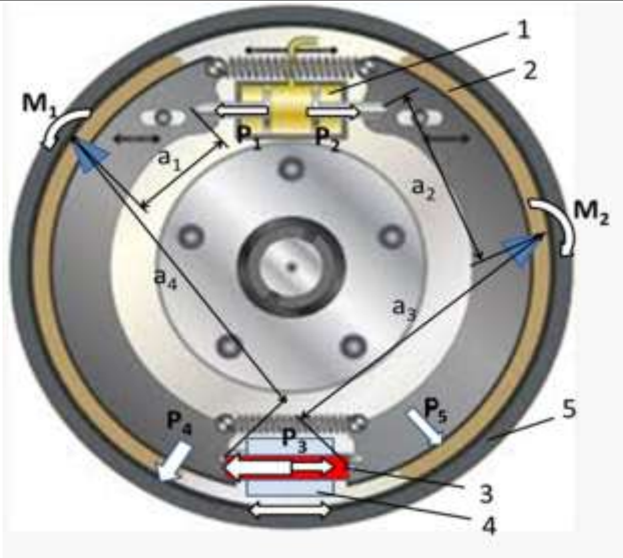

Fig.1. Schematic of the floating brake-shoe design. 1 – working hydraulic cylinder; 2 – brake shoe; 3 – movable rod installed between the shoe ends; 4 – groove of the movable rod; 5 – brake drum; $M_1$and M_2– moments causing rotation of the shoes; a_1, a_2, a_3,and a_4– force lever arms; $P_1$and P_2– hydraulic forces; P_3, P_4,and P_5– forces acting on the shoes and the drum.

FINITE ELEMENT SIMULATION AND COMPARATIVE ANALYSIS

The simulation procedures were carried out under static conditions using the SOLIDWORKS software package. In general, the solution of engineering problems in numerical simulation environments consists of three stages. In the first stage, referred to as preprocessing, the geometric model of the object is constructed. The second stage, known as processing, involves introducing the computational parameters into the program and performing calculations under prescribed boundary conditions. The final stage, postprocessing, is devoted to presenting the results of the analysis to the user in graphical form.

In accordance with these stages, the physical model of the investigated object was created using three-dimensional modeling tools and subsequently discretized into a finite-element mesh, as shown in Fig. 2. For clarity of visualization, certain portions of the brake drum were removed in order to illustrate the contact interaction more distinctly.

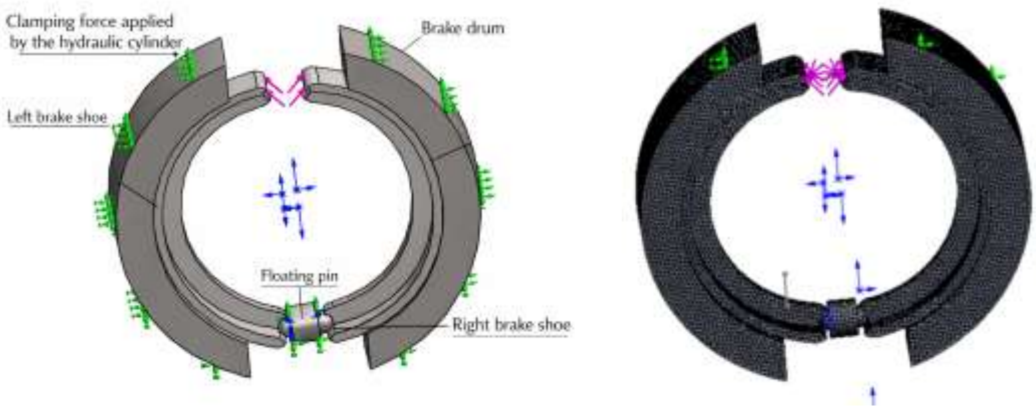

Fig.2. Three-dimensional simplified representation of the drum brake mechanism and discretization of the geometric model into finite elements.

Numerical simulation based on the finite element method relies on an iterative computational procedure that gradually converges toward realistic results. Prior to analysis, the geometric model is subdivided into small finite elements, and calculations are performed at the nodal points where these elements intersect. Each element represents a small portion of the material and carries its mechanical properties. In modern simulation software packages, the selection of element type and shape is performed automatically by the computer in accordance with user-defined requirements. The accuracy of the solution depends to a significant extent on the proper selection of these elements.

In the present study, the objective is to ensure a larger static contact area between the brake shoes and the drum. For this reason, the rotational motion of the drum is neglected, and it is treated as a rigid stationary body. When a force is applied to the upper portions of the brake shoes through the hydraulic actuator, the shoes rotate slightly in opposite directions about the contact line (or point) until they press against the drum, thereby forcing the movable rod toward the opposite side of the drum.

To evaluate the effectiveness of the proposed configuration, separate simulations were carried out for both the conventional and the newly developed designs, and the obtained results were assessed comparatively.

The results of the simulation for the conventional configuration indicate that the contact area between the brake shoe and the drum—and thus the braking force—is concentrated only in the upper region of the shoe, as illustrated in Graph 1. This condition not only reduces braking effectiveness but also leads to non-uniform surface wear of the shoes, thereby decreasing the reliability of the mechanism and increasing maintenance and repair costs.

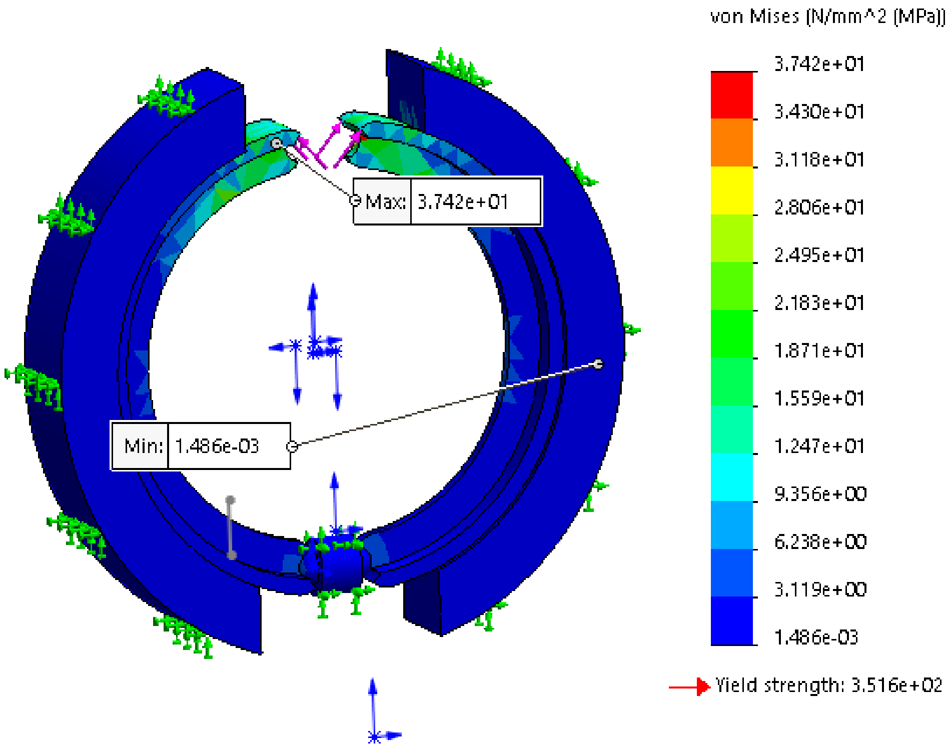

Graph 1. Contact pressure distribution between the brake shoe and the drum in the conventional design (with a fixed rod).

With the introduction of the movable rod at the lower support region of the shoes, contact between the lower portions of the shoes and the drum is also established, as shown in Graph 2. Because the shoe with greater wear in its upper region generates a higher moment, the opposite shoe is pressed more firmly against the drum and consequently develops a larger contact area than the other shoe. In this manner, the alternating moments acting between the shoes promote more uniform wear and, owing to the increased effective contact area, provide higher braking efficiency compared with the conventional configuration.

According to the numerical results presented on the right-hand side of Graph 2, the corresponding stress distribution is depicted on the left-hand image. As noted earlier, in the proposed new configuration the contact during braking does not occur solely at the upper regions of the shoes, but also extends to both the upper and lower left contact areas, thereby further contributing to improved load distribution and wear uniformity.

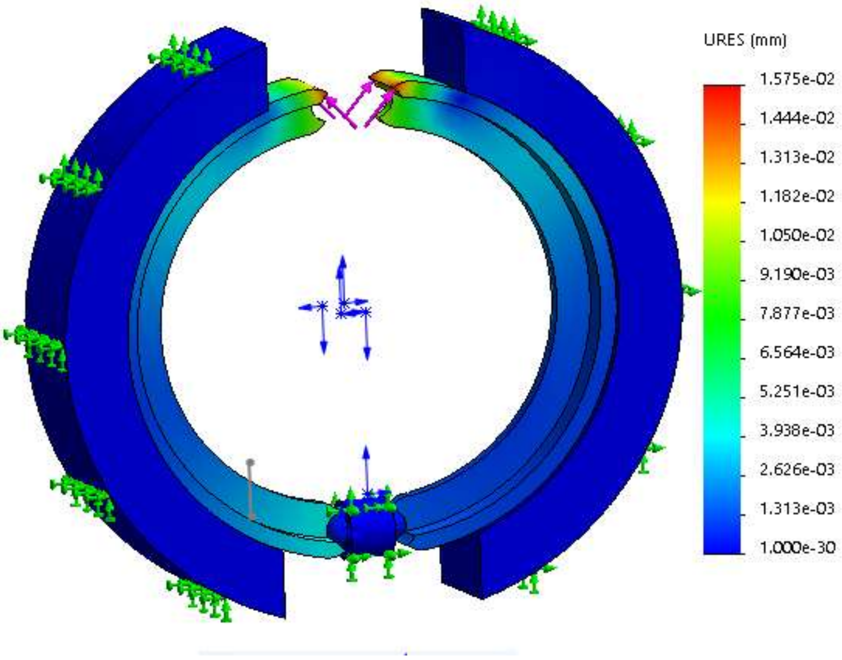

Graph 2. Displacement of the brake shoe surface and contact pressure distribution at the shoe–drum interface in the improved design.

CONCLUSION.

This study demonstrates that increasing the effective contact area of brake shoes in widely used drum brake mechanisms can enhance braking efficiency and operational safety, enable lightweight design by achieving the same braking performance with a more compact structure, extend maintenance intervals, improve productivity of mechanical systems, promote more efficient utilization of brake lining material, and reduce repair costs.

In the proposed configuration, an additional movable rod is installed within a groove fixed to the housing at the shoe ends opposite the working hydraulic cylinder. This arrangement causes the shoes to rotate with different moments depending on the effective lever arms associated with the worn regions of the friction surfaces, thereby increasing their contact area with the drum. As a result, more uniform wear of the shoes is promoted and braking effectiveness is improved through enlarged contact zones. This potential behavior was evaluated under static conditions using the SOLIDWORKS simulation environment, and visualization of the results indicated that, in comparison with conventional designs, the floating action introduced by the movable rod can theoretically increase the contact area.

The practical significance of the proposed construction should be confirmed through experimental investigations conducted on prototypes developed in accordance with the suggested scheme. Furthermore, dynamic design considerations—such as additional forces generated by drum rotation, the use of pistons with different diameters within a single hydraulic actuator, and the assignment of modified geometric parameters to the shoes consistent with the new configuration—may further enlarge the effective contact area and enable more efficient utilization of lining material through periodic interchange of the shoes during maintenance operations.

REFERENCES

[1]. Barecki, Z., & Scieszka, S. F. (1987). A mathematical model of the brake shoe and path system for post type drum brakes. R&D Journal, 3, 13–17.

[2]. Essam, M. A., Faragallah, M. M., Abdeltawab, N. M., & Ali, M. (2026). Tribological characteristics of composite brake pads under variable conditions. Scientific Reports, 16, Article 1634. https://doi.org/10.1038/s41598-025-33326-7

[3]. Ilie, F., & Cristescu, A.-C. (2022). Tribological behavior of friction materials of a disk-brake pad braking system affected by structural changes—A review. Materials, 15(14), Article 4745. https://doi.org/10.3390/ma15144745

[4]. Liu, N., Zheng, Z. C., Wu, Y. L., Kong, X. G., & Ding, H. (2015). Finite element analysis of drum brake assembly. Chemical Engineering Transactions, 46, 1057–1062. https://doi.org/10.3303/CET1546177

[5]. Páczelt, I., Baksa, A., & Mróz, Z. (2020). Analysis of steady wear state of the drum brake. Open Access Library Journal, 7, 1–16. https://doi.org/10.4236/oalib.1106432

[6]. Söderberg, A., & Andersson, S. (2009). Simulation of wear and contact pressure distribution at the pad-to-rotor interface in a disc brake using general purpose finite element analysis software. Wear, 267(12), 2243–2251.

[7]. Wang, Y., Yang, X., Huang, Y., Sun, C., & Shi, W. (2025). Thermo-stress-wear multiphysics coupling mechanism in drum brakes: A comparative study on material fatigue life through simulation and experiment. Tribology International, 212, Article 110904. https://doi.org/10.1016/j.triboint.2025.110904

[8]. Zheng, B., Zhang, J., & Liu, W. (2018). Finite element analysis of brake shoe based on ANSYS Workbench. In Proceedings of the 2018 2nd International Conference on Artificial Intelligence: Technologies and Applications (ICAITA 2018) (pp. 89–92). Atlantis Press. https://doi.org/10.2991/icaita-18.2018.23

Received: 02.06.2026
Accepted: 10.06.2026

MACHINE SCIENCE

ISSN: 2227-6912
E-ISSN: 2790-0479

2026, № 1 Pages 40-48

WAYS TO INCREASE THE PRODUCTIVITY OF THE SEED SORTING DEVICE

Avazbek OBIDOV[1,a*], Abrorjon ABDULLAEV[2,b]

[1]Dean of the Faculty of Mechanics, Namangan State Technical University
[2]Associate Professor of the Department of Technological Machinery and Equipment, Namangan State Technical University

E-mail: [a]obidovazbek66@gmail.com, [b]abdullayevabror738@gmail.com*

https://doi.org/10.61413/REQH3949

Abstract: This article analyzes ways to increase the productivity of the seed sorting device. During the study, existing technologies and seed sorting equipment used in manufacturing enterprises were studied, and their advantages and disadvantages were identified. Furthermore, based on the literature analysis, the main factors influencing the seed sorting process have been scientifically substantiated. As a result of theoretical and applied research, a new technical solution aimed at increasing the efficiency of the sorting process was proposed. The design of the developed improved sorting device and its operating principle are described, and it has been proven through experimental tests that the device's productivity has increased significantly. The results obtained showed that the device is effective for use in agriculture and serves to improve the quality of seeds.
Keywords: *seed sorting, seed, sorting device, productivity, improvement, efficiency, technological process, design, theoretical research, practical experience, innovative solution, agricultural machinery.*

INTRODUCTION

The primary raw material of the global textile industry is cotton fiber, with approximately 23–24 million tons of cotton fiber produced annually on a global scale. Due to the intensive growth of the population, the consumption of cotton fiber and the demand for it are expected to increase in the future. Therefore, on a global scale, identifying and eliminating factors negatively affecting product quality during cotton cultivation, improving its consumer properties, cotton preparation, and primary processing—specifically during the processes of harvesting, transportation, drying, and cleaning of cotton impurities—and creating automated, resource-saving technologies that reduce production costs remain important tasks [1].

In world production, the creation of cotton varieties with high consumer properties, the preparation of high-quality seeds, the development of standard techniques and technologies that positively affect the production process, and the improvement of existing technologies at enterprises are of particular importance. In this regard, one of the important tasks is the implementation of scientific research in the fields of radically changing seed quality indicators, high germination, and the production of seed seeds with uniform and uniform chemical treatment indicators. High quality indicators of seed cotton are ensured by technological systems for its sorting and high-quality treatment. To improve the quality of sorting, in addition to improving the equipment, the uniform feeding of seeds to sorting units is of great importance. To achieve an increase in the quality indicators of prepared seeds by increasing the productivity of sorting devices implemented in seed preparation workshops, it is important to improve the working components of the units and create new equipment.

Foreign scientists Sh. Barampuram, G. Allen, S. Krasnyansky, V.S. Mor, Jyoti Jhawar, and others have conducted scientific research on improving the techniques and technologies for processing and preparing seeds; domestic scientists M.N. Bushuev, A.I. Schleicher, D.K. Kasimov, V.G. Rakipov, S. Tukhtaboev, V.Kh. Tuychiev, Kh.T. Akhmedkhodzhaev, R.K. Dzhamalov, A.Yu. Tursunov, R.Kh. Dzhuraev, and others have conducted scientific research [2,3,4,5].

However, to date, several scientific and technical problems have not been fully resolved through the results of research work on seed sorting and cleaning technologies and equipment used in foreign and domestic cotton ginning enterprises, as well as on increasing the efficiency of their working parts.

ANALYSIS OF THEORETICAL AND PRACTICAL RESEARCH

One of the main requirements for cotton ginning enterprises to increase the efficiency of seed preparation technology remains the preparation of high-quality seeds while preserving the natural physical and mechanical properties of the seeds. During the technological process of seed sorting at the cotton ginning plant, it is observed that various impurities and foreign impurities, as well as unripe seeds, are mixed into the incoming seed mass. As a result, the quality indicators of seed production are decreasing.

Based on the analysis of the research results and the observation of seed preparation technologies operating at the enterprise, it was proposed to improve the USM-A seed sorting device operating at the enterprise.

In the improved seed seed sorting device, special hoppers are installed for sucking seeds through the air and separating impurities, empty seeds, and industrial seeds into fractions, and the sorting of seeds is controlled using a movable screwdriver. The newly proposed improved seed sorting device increases the efficiency of trapping small impurities, empty and broken seeds, and prevents the mixing of small impurities, empty and broken seeds with dust air[6,7,8,9].

The operation of the new device is carried out under the influence of a horizontal air flow. Due to changes in air velocity in the sorting chamber, sorting is carried out according to aerodynamic parameters.

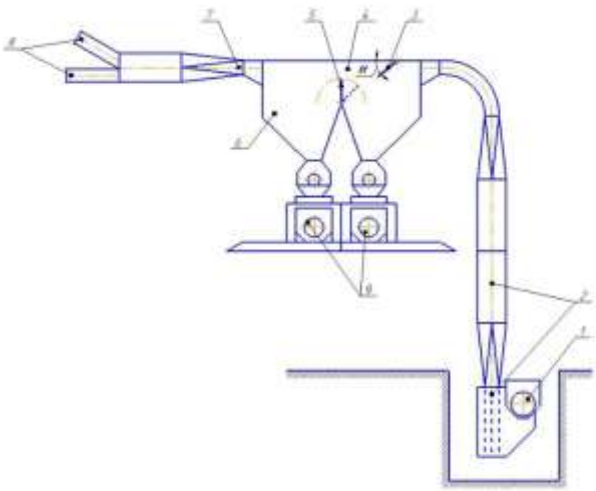

Fig.1. Technological scheme of the improved seed seed sorting device

1-collecting conveyor, 2-seed suction pipe, 3-seed barriers ,4 - separation chamber, 5 - mobile diverter, 6 - hoppers, 7-air suction pipe, 8-dust air pipe, 9-vacuum valves;

In the proposed seed sorting device operating in a horizontal air stream:

a) maximum cleaning of seeds from various impurities;

b) separation of seeds into optimal fractions by selecting air velocities;

c) creating opportunities for selecting selected seed seeds depending on their mass.

In the mathematical equation describing the pattern of seed movement under the influence of airflow in the working chamber, the following simplifications were adopted:

- seeds moving in the airflow do not affect each other (point 1);

- seeds with masses m1 and m2 moving under the influence of airflow have a certain elastic bond with each other (point 2);

- in both cases, the seeds were taken as a material point with a certain flight coefficient - K_{ch} and aerodynamic drag coefficients - $K_{chk.}$

Let us investigate the movement of the seeds in the sorting chamber relative to the XOY - Cartesian coordinate system (Fig. 2). Let the velocity of the air flow entering the chamber be V0, the velocity inside the chamber be V_x, and the laws of motion for the seeds inside the chamber be x (t), y (t)[10,11,12].

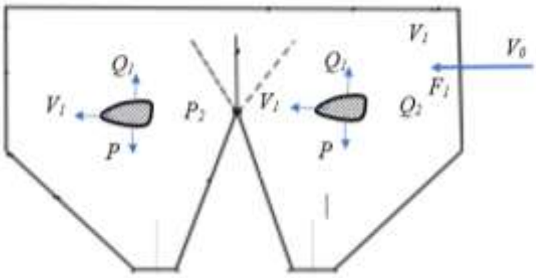

Fig.2. Diagram of seed movement in the sorting chamber and the forces acting upon it

Cotton seeds can differ from each other in terms of completeness, quality, immaturity, and degree of fuzziness. During the movement (flight) of the cotton seeds being sorted, air resistance forces Q_{ix}, Q_{iy}, and P-gravity forces act in a given direction.

We shall formulate the equations of motion for cotton seeds based on the principle of the existing methodology, taking into account the aforementioned forces. The seeds differ from each other in their mass and do not possess elastic bonds. In this case, the law of movement of cotton seeds is expressed by the following system of differential equations:

$$\left\{\begin{aligned} m_i\ddot{x}_i &= c_i\left(V_x - \dot{x}_i\right) \\ m_i\ddot{y}_i &= -\left(c_{ki}y_i + c_{pi}\dot{y}\right) - m_i g \end{aligned}\right\} \quad i=1,2,3 \tag{1}$$

Here: - coefficients of resistance to seed flight.

In this case, let the seeds with masses m_1 and m_2 have a mutually elastic bond.

In this work, we consider the vertical-horizontal positions of two-component and interconnected cotton seeds.

For these cases, the law of movement of cotton seeds is expressed using the following system of differential equations:

$$\left.\begin{aligned} m_1\ddot{x}_1 &= v_{x0} - c_{k1}\dot{x}_1 + c_{x0}\left(x_2 - x_1\right) \\ m_2\ddot{x}_2 &= v_{x0} - c_{k2}\dot{x}_2 + c_{x0}\left(x_1 - x_2\right) \\ m_1\ddot{y}_1 &= -m_1 g + c_p\dot{y}_1 + c_k\left(y_1 - y_2\right) \\ m_2\ddot{y}_2 &= -m_2 g + c_p\dot{y}_2 + c_k\left(y_2 - y_1\right) \end{aligned}\right\} \tag{2}$$

According to the theoretical analysis, using a system of differential equations for two cases, taking into account the corresponding initial conditions and the elasticity and aerodynamic resistance coefficients, we create a special program and determine the values numerically[13,14,15].

For the first case, when seeds are considered as discrete material points without interconnections, the graphs of their movement patterns in the sorting chamber are taken in various variations, and some results are presented in the first table (Fig. 3, Table 1). As seen from this table and the graph in the figure, the change in the elasticity coefficient (c'=const) has a smaller effect on the flight distance along the length of the seed sorting chamber. This situation is justified by the fact that due to the small mass of cotton seeds, the influence of elastic forces during the movement process is insufficient. However, the increase or decrease in the seed flight resistance coefficient (s_k=const) is one of the main factors factors affecting the seed flight distance [16].

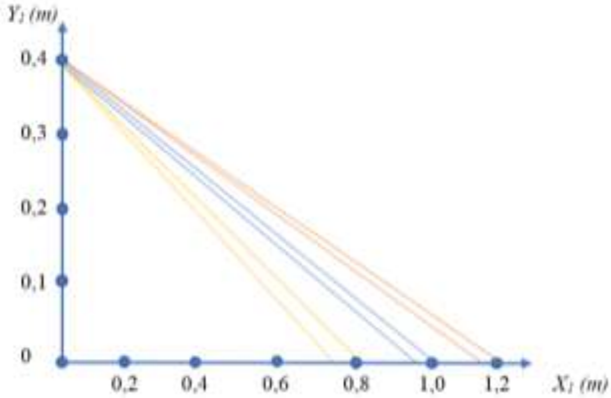

Fig.3. The graph representing the movement patterns of seeds that are not interconnected but have a certain connection

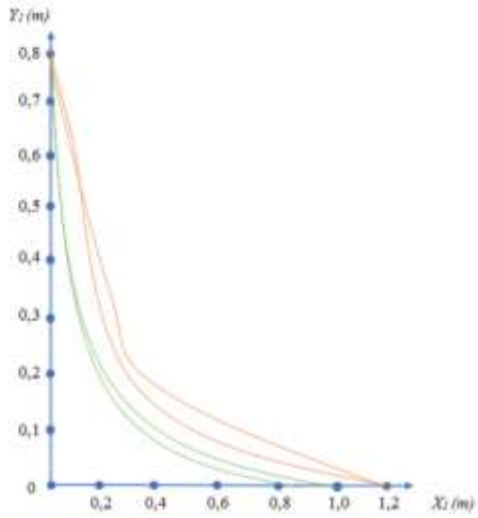

Figu.4. The graphs of the dependence of the flight distance on the decrease in the coefficient of elastic resistance of the seeds.

Depending on the mass value of the cotton seeds, it was observed that technical seeds fall within the intervals of 0.45<x<0.60 m along the length of the sorting chamber. It is known from practice that when cotton seeds have a certain fuzziness, their volatility coefficient increases. This circumstance is of great importance in the selection process. Table 1 shows the relationship between the values of seed mass and the flight distance depending on the change in air velocity.

Table 1.Dependence of the takeoff distance on seed mass and air velocity.

Seed mass (kg)	*Initial velocities*			
	υ_0=12 m/s	*υ_0= 16 m/s*	*υ_0 =18 m/s*	*υ_0 =20 m/s*
0,001	0,41	0,49	0,55	0,60
0,002	0,39	0,44	0,49	0,55
0,003	0,36	0,40	0,44	0,52
0,004	0,34	0,38	0,42	0,50

Table 2.Dependence of the flying distance on mass when the speed of interconnected seeds is constant.

υ_0 = 18 m/s				
m (kg) / x(m)	$m_1 = 0{,}001$ $m_2 = 0{,}002$	$m_1 = 0{,}001$ $m_2 = 0{,}003$	$m_1 = 0{,}002$ $m_2 = 0{,}003$	$m_1 = 0{,}003$ $m_2 = 0{,}004$
x_1 x_2	0,94 0,87	0,81 0,79	0,80 0,74	0,78 0,71

For the second case, it is somewhat difficult to sort the seeds because they are not fully hairless. From this, it can be concluded that they are interconnected in a certain way. Tables 2 and 3 show the results of graphs representing the laws of motion of seeds differing in mass when they are in an elastic bond.

Table 3.Change in the flight distance of interconnected seeds with constant speed, variable mass, and resistance coefficient

υ_0 = 18 m/s			
m(kg)	$m_1 = 0{,}001$, $m_2 = 0{,}002$, c_k=0,02		
x(m)	c_p =0,01	c_p =0,02	c_p =0,03
x_1	1	1,2	1,36
x_2	0,92	1,16	1,28
x(m)	c_p =0,005	c_p =0,007	c_p=0,009
x_1	0,84	0,92	1,00
x_2	0,76	0,88	0,88
	c_p=0,2	c_p =0,2	c_p=0,2
x(m)	c_k=0,01	c_k =0,02	c_k =0,03
x_1	1,20	1,20	1,21
x_2	1,15	1,16	1,16

In both cases, the laws of motion are basically the same, and the seed flight distances are highly dependent on the change in the cp-coefficient and less dependent on the change in ck. That is, the degree of seed fuzziness is one of the important factors in the sorting process. Furthermore, the air velocity entering the sorting chamber plays a special role in seed sorting. The above results allow for the selection of seed fractionation distances under the influence of horizontal air currents. Based on the results, it is possible to set the parameters of two receiving chambers for sorted cotton seeds in the design of the sorting chamber.

In each of the conducted experiments, the device was tested in several variants, taking into account compliance with seed seed sorting regulations and the negative phenomena occurring in currently used devices. After conducting the tests, the results were obtained, and work was carried out to develop a design intended for use in production.

It is known that the regulation for seed production is PDQI 44-2002, which provides for the introduction of new modern machinery and equipment into the technology of seed production at cotton ginning plants. Amendments and additions have been made to this regulation according to PDI 07-2008, which provides for the use of modern machinery and the introduction of new technologies at cotton ginning enterprises.

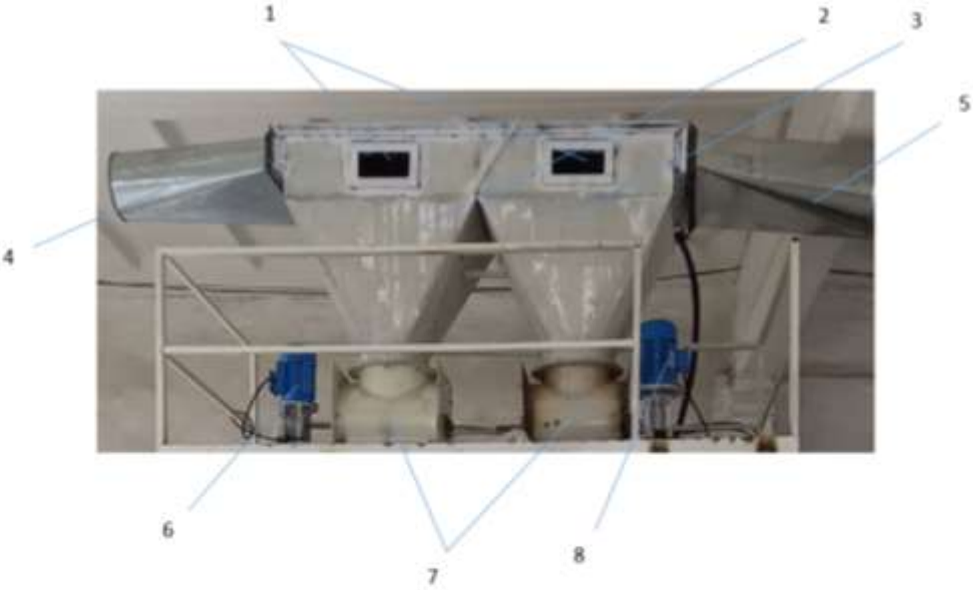

Fig. 4. Seed sorting device
1-observation slit; 2-seed chamber; 3-technical seed chamber; 4-inlet pipe; 5-outlet pipe; 6-seed chamber electric motor; 7-vacuum valves; 8-technical seed chamber electric motor;

The design of the seed sorting device intended for implementation in production was manufactured at Jizzakh Kenteks LLC in the Jizzakh region.

Device 1-observation slit; 2-seed chamber; 3-technical seed chamber; 4-inlet pipe; 5-outlet pipe; 6-seed chamber electric motor; 7-vacuum valves; The 8-technical seed chamber consists of electric motors (Fig. 4).

The seed seed sorting device operates as follows. Seeds intended for sowing are supplied to the working chambers using air from inlet pipe 4. Here, the seed mass enters the chamber 2 intended for the first seeds, and as a result of the loss of pressure, the ripe seeds fall into this chamber. The remaining mass—empty and immature seeds—continues its movement and enters chamber 3 for technical seeds, where it separates from the air and enters the chamber. This device is equipped with 2 vacuum valves 7 driven by electric motors 6, 8, which serve to separate the seed fractions entering the chambers from the air and transfer them to the next process. The progress of the process is monitored using observation slits 1. Additionally, a seed screen is installed between the chambers, the angle of inclination of which is adjusted depending on the sorting state of the fractions.

The fractions released from the chamber into which the technical seeds separated in the sorter are passed through a vacuum valve and sent to the warehouse through a seed screw, while the seed seeds are sent for further cleaning and treatment processes.

The new device has been tested at Jizzakh Kenteks LLC in the Jizzakh region.

During the production trials, the technological process was carried out without violations, in compliance with safety regulations and other requirements. Based on the operating principle of the new device, it can be concluded that the device has the capability to effectively sort ginned seeds into 3 fractions (a heavy impurity chamber is also installed in the lower part of the device, corresponding to the technology of the USM device).

The testing of the new device under production conditions was carried out according to the existing regulations. Production studies were conducted using the industrial grade S-6524, first and second grades, with a moisture content of 7-8%, impurity of 1.1–1.8%, and seed fuzziness of 8–9%. Sampling after the device was performed according to available methods. The technical characteristics of the device are presented in Table 4.

Table 4. Technical specifications of the seed seed sorting device

№	Indicator name	Unit of measurement	Quantity
1.	Device performance, until	kg/h	4000
2.	Sorting device length	mm	1200
3.	Width of sorting device	mm	600
4.	Device height	mm	1400
5.	Mini gin for separating fibrous seeds number of machine saws	grain	42
6.	Number of fractions to be separated in the sorting device	grain	3
7.	Camera size: Chamber 1 (for heavy mixtures) 2nd chamber (for seeds) 3rd chamber (for industrial seeds)	mm	 600x250 600x600 600x600
8.	Air velocity - pipeline - on camera	m/s	 24 18
9.	Seed screen size	mm	600x200
10.	Power requirement: - for vacuum valves (2 units) -For VTS ventilator	kW	 4,4 11

Experiments were conducted primarily by varying the angle of inclination of the seed screen (Fig. 5), as well as depending on other factors affecting sorting efficiency. The experiments were repeated three times, and the average of the results obtained was taken.

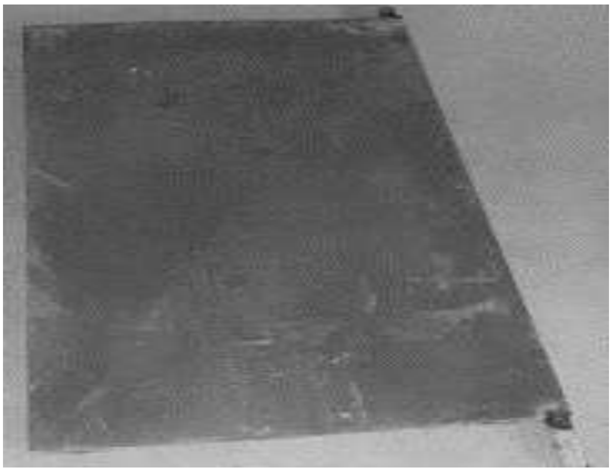

Fig.5. Seed screen view

Production tests were conducted on both machines with identical productivity (2000; 3000; 3500; 4000 kg/h), the S-6524 selection variety, and the R-2 generation of seeds were used alternately in both units, with three repetitions of the experiments. The analyses were conducted under the conditions of the production process of a seed-processing plant. Seed indicators: fuzziness – 8-9%, impurity – 1-1,8%, mechanical damage – 3.9%, moisture – 7-8%, 1000-seed weight – 98-99 grams.

It should be noted that currently used seeds sorting units of the CHSA type operate with a maximum productivity of 3000 kg/h and operate with an efficiency of 70-88% for fractions. It was concluded that the main reason for this is the vertical placement of the sorting chambers. To compare the results of the experimental work, the results of the same type of CHSA devices were accepted for research.The results of the preliminary tests are presented in Table 5.

Table 5.Results of testing the results of theoretical research under industrial conditions.

Air speed, m/s	Seed barrier slope angle, degree	Camera width, mm	Performance, %		
			Seed seeds chamber	Technical seeds chamber	Camera 2 seed fractions
14	30	400	90	97	10
		600	94	98	6
		800	93	98	7
16		400	90	98	10
		600	95	98	5
		800	94	97	6
18		400	94	97	6
		600	97	98	3
		800	95	98	5

From this experiment, it can be seen that the best efficiency is ensured at an air velocity of 18 m/s and a chamber width of 600 mm at a seed guard inclination of 300.

When sorting seeds, primary attention is paid to the total weight of the selected seeds (per 1000 seeds); the weight of the seed mass demonstrates the reliability of the sorting. Furthermore, it should be taken into account that fractions not belonging to this fraction are deposited in the seed chamber, whereas in previously used units, this indicator was significantly lower; specifically, cases were observed where empty seeds accounted for about 10% of the seed composition.

CONCLUSION.

As a result of this research, scientific and practical solutions aimed at increasing the productivity of the seed sorting device were developed. An analysis of the conducted literature and the study of existing technologies showed that existing sorting units have a number of shortcomings that negatively affect operational efficiency. Based on theoretical and practical research, an improved design aimed at eliminating these shortcomings has been proposed.

The developed sorting device was tested, and it was found that its productivity and sorting quality have significantly increased. As a result of the device's application, the quality indicators of the seed seeds improved, ensuring an increase in the efficiency of the production process. At the same time, the implementation of the proposed technical solution into practice serves to ensure the rational use of resources, increase labor productivity, and ensure economic efficiency in agricultural enterprises.

REFERENCES

[1].Decree of the President of the Republic of Uzbekistan No. UP-60 dated January 28, 2022. New Uzbekistan for 2022–2026. Aydarov Sh.G. "Research on the sorting of eaten seeds." cotton in an electronic drum separator," Abstract 1973, Yangiyul, 23 pp.

[2].P. Shaimov. "Sorting of pubescent cotton seeds in a dielectric drum separator," Cand. Sci. (Eng.) Dissertation, 1995.

[3]. Yusubaliev A., Kurbonboev T. O. Increasing the clarity of separation of cotton seeds in a dielectric device // Problems of modern science and education. 2016. No. 33. P. 22-24.

[4].Niyazkulov A. A. Sorting of naked cotton seeds on a dielectric sizing machine: diss. Cand. Sci.

(Eng.). Moscow, 1987. 251 p.

[5].Akhmedkhodjaev Kh. T., Karimov A. I., Obidov A. A. Study of vibration movement of cotton seeds on parallel-spinning vibrating carriages. // Journal of Textile Problems. - Tashkent, 2003. - No. 4. - P. 65-67.

[6].Akhmedkhodjaev Kh. T., Obidov A. A. On the issue of studying a vibrating sorter equipped with vibrating feeders. // I International Scientific and Technical Conference of the Institute of Technical Agrochemistry: Abstracts of the reports. - Ivanovo, 2003. - P. 158-159.

[7].Oripov N., Turdaliyev Kh., Abdullaev A. Improving the technology of cleaning cotton seeds from small impurities. International Scientific Conference "The Role of International Farmers in the Implementation of Innovative Technologies in the Integration of Agricultural Production, Science and Education," NamSI, September 25-26, 2020.

[8].Sarimsakov A., Abdullaev A. Improving Seed Sorting Technology. International conference on the topic: "Economic, innovative, and technological problems of increasing production efficiency based on the deep processing of raw materials in cotton-textile clusters and international experience." 2022. May 27-28. 2 volumes

[9].Obidov A., Abdullaev A. The technology of preparing seed cotton improvement. Collection of articles from the international scientific and technical conference "Scientific-intensive innovative technologies and solutions to urgent problems in the textile and light industries." Volume 1, April 26-27, 2023, pp. 46-50.

[10].Abudullayev A. Analysis of Experimental Works on Improving the Seed Selection Process. International Journal of Scientific Trends- (IJST) ISSN: 2980-4299, Volume 2, Issue 10, October, 2023, 33-39 P.

[11].Obidov A., Abudullayev A. Theoretical justification of the efficient operation of the seed sorting device. Engineering, Scientific Research Publishing. 2023, 15, 720-728

[12].Logachev K.I., Posokhin V.N. Calculation of flow near a round suction nozzle. News of universities. Aviation engineering. - 2004. - No. 1.-P. 29-32.

[13].I.A. Khalilov, G.Z. Dzhabbarova, Analysis of Winding Mechanism with Dispersion of Winding Structure Defects by Periodic Changes of the Winding Drum Diameter, Izvestiya Vysshikh Uchebnykh Zavedeniy Seriya Teknologiya Tekstilnoy Promyshlennosti, Issue 2025(2), Pages 216–222

[14].U.T. Abdullaev, H.K. Karimov, F.A. Veliev, I.A. Khalilov, I.F. Allakhverdieva, Experimental Evaluation of Boundaries Strength of Dense and Sparse Areas of Fabric with Variable Density by Weft, Izvestiya Vysshikh Uchebnykh Zavedeniy Seriya Teknologiya Tekstilnoy Promyshlennosti, Issue 2025(2), Pages 428–432

[15].Harmats D.E., Tuychiev V.Kh. "SPS sorter for pubescent cotton seeds." Fan Publishing House, Tashkent, 1983, p. 8.

[16].Obidov A., Abdullaev A. Theoretical substantiation of the effective operation of a seed sorting device. Namangan Institute of Textile Industry Scientific and Technical Journal "Science and Innovation in the Textile and Fashion Industry," No. 1.

Received: 16.01.2026
Accepted: 23.06.2026

MACHINE SCIENCE

ISSN: 2227-6912
E-ISSN: 2790-0479

2026, № 1 Pages 49-60

THEORETICAL SUBSTANTIATION OF THE PARAMETERS OF CUTTING WORKING ELEMENTS OF A COTTON TOPPING APPARATUS FOR COTTON CULTIVATED UNDER INTENSIVE TECHNOLOGY USING A TWIN-ROW PLANTING SCHEME

Shavkat RAVSHANOV[1,a*], Kobuljon ERMATOV[2,b], Dilsabo CHORIEVA[3], Nigora OQYOLOVA[2]

[1]Research Institute of Agricultural Mechanization, Yangiyol, Uzbekistan
[2]Andijan State Technical Institute, Andijan, Uzbekistan
[3]Karshi State Technical University, Karshi, Uzbekistan

E-Mail: [a]ravshanovshavkat78@mail.ru, [b]ermatov1960@mail.ru*

https://doi.org/10.61413/AEBV1753

Abstract: The article presents a theoretical justification of the parameters of the working elements of a cutting apparatus for mechanical cotton topping under intensive cultivation with a $76 \times 10 cm$ double-row planting scheme. It is shown that under double-row planting, one rotor interacts simultaneously with cotton plants in two rows; therefore, the number of blades, rotational speed, blade-tip speed, spacing of cutting traces, rotor radius, and hydraulic drive power must be determined with regard to the two-row technological load. Based on the analysis of sources, it was established that the diameter of the upper cotton stem in the topping zone mainly ranges from $3{,}5$ to $4{,}8 mm$, while a range of $4-6 mm$ is reasonable for design calculations with a safety margin. Theoretical calculations showed that at an operating speed of $1{,}4-1{,}7\,m/s$, a two-blade rotor operating at $450 rpm$ is insufficient for high-quality topping. For a four-blade rotor, the following rational parameters were justified: rotational speed of $600-750 rpm$, rotor radius of $0{,}18-0{,}22 m$, and blade-tip speed of $11-17\,m/s$.

Keywords: *cotton, topping, intensive technology, double-row planting, cutting apparatus, rotor, knife, rotational speed, hydraulic drive.*

INTRODUCTION

The agrotechnical operation of cotton topping is an important process aimed at limiting the plant's apical growth, redistributing nutrients from vegetative to generative organs, and accelerating boll formation. In cotton-growing practice, topping is performed manually, mechanically, or chemically, with chemical topping based on the use of plant growth regulators. However, under intensive-technology conditions-characterized by higher plant density, denser planting schemes, and shorter optimal windows for the operation-there is a growing need for high-performance, precisely adjustable, and low-damage mechanical topping equipment.

In Uzbekistan, the adoption of intensive cotton cultivation technologies is becoming increasingly important. According to the Ministry of Agriculture of the Republic of Uzbekistan, in Andijan region the cotton variety "Xin Lu Zao-52" was sown using a double-row scheme of $76 \times 10 cm$ with a density exceeding $240{,}000\, plants/ha$, with the technological process organized based on Chinese agrotechnology [1].

This planting scheme changes the requirements placed on the working elements of the topping apparatus. Whereas in conventional single-row schemes the cutting apparatus mainly acts on plants in a single row, under the double-row $76\times10cm$ scheme the rotor axis is positioned between two rows, and a single rotor simultaneously covers cotton plants in both rows. Therefore, the number of blades, rotor rotational speed, cutting step, and rotor radius must be justified not on the basis of values adopted for conventional schemes, but with regard to a dense two-row plant flow.

In early mechanical topping machine designs, priority was given to simplicity, reliability, and field repairability. For example, mechanical topping devices of the ChVKh-4 type were used to some extent in cotton-growing regions, and their working process has been described in scientific and technical sources [2,3]. However, under intensive technology conditions, the requirements for accounting for plant density, stem and leaf mass, inter-row spatial constraints, precise topping-height control, and avoidance of plant damage increase significantly. Therefore, theoretical re-justification of the cutting working element parameters of a modern topping apparatus is a relevant task.

MATERIALS AND METHODS

The study used methods of theoretical analysis, kinematic calculation, geometric modeling, and generalization of biomechanical indicators from the literature. The following initial conditions were adopted for calculations:

-planting scheme - double row $76\times10cm$;

-distance between rows within the double row - $0,10m$;

-distance of each row from the rotor axis - $0,05m$;

-unit travel speed - $1,4-1,7\,m/s$;

-spacing between plants along the row - $0,10-0,11m$;

-stem diameter in the topping zone for design calculation - $0,004-0,006m$;

-knife installation height - $0,8-1,1m$.

The following main criteria were used to evaluate the cutting apparatus's operation:

q - plant flow per rotor, $plants/s$;

Δl - distance between consecutive cutting traces, m;

v_u - linear speed of the knife tip, m/s;

$\lambda = v_u/v_a$ -ratio of knife-tip speed to unit travel speed;

R - rotor radius, m;

P - power required for the cutting rotor, kW.

EFFECT OF THE DOUBLE-ROW PLANTING SCHEME ON CUTTING APPARATUS OPERATION

In the double-row $76\times10cm$ scheme, two cotton rows are located $10cm$ apart. If the cutting rotor axis passes between the two rows, each row is located $5cm$ from the rotor axis.

In this case, the rotor's working element covers not one but two rows, located to the left and right of the rotor axis. Therefore, the plant flow per rotor is determined by:

$$q = \frac{kv_a}{s},\ plants\Big/s \qquad (1)$$

where:

v_a - unit travel speed, m/s;

s -spacing between cotton plants along the row, m;

k - coefficient showing that one rotor services two rows, $k=2$.

From expression (1), it follows that at $v_a = 1{,}4-1{,}7\,m/s$ and $s=0{,}10-0{,}11m$, the plant flow is $q = 25{,}5-34\,plants/s$.

Consequently, one rotor interacts with approximately $25-34$ cotton plants per second. This shows that the technological load on the cutting apparatus is significantly higher than in a conventional single-row working process.

STEM DIAMETER IN THE TOPPING ZONE AND CUTTING RESISTANCE

The study by İ. Aydın and S. Arslan established that in the upper part of the cotton plant, at the $0-15cm$ section, the average stem diameter is $4{,}35mm$, the cutting force is $73N$, moisture content is 72%, maximum cutting stress is $4{,}94MPa$, and specific cutting energy is $0{,}069\,J/mm^2$. At the section $15-30cm$ lower, the stem diameter increased to $5{,}79mm$, cutting force to $121N$, and specific cutting energy to $0{,}078\,J/mm^2$ $[4]$.

Studies by Y. Xu, X. Han, and other authors note that in the apical part of the cotton plant, the average stem diameter was $3{,}49-4{,}78mm$, average cutting force was $15{,}94N$, and maximum cutting force was $30{,}56N$ $[5]$.

Based on these data, for theoretical calculations of the topping apparatus's working elements, the stem diameter in the cutting zone is conservatively adopted within the range $d = 0{,}004m - 0{,}006m$ for design purposes.

The cross-sectional area of the stem is determined by:

$$A = \frac{\pi d^2}{4} \tag{2}$$

Calculations using this expression show that $A = 12{,}56-28{,}27mm^2$.

The study by F.G. Pekitkan, R. Esgici, and others also shows that as the cotton stem's cross-sectional area increases, cutting force and energy increase: at a cross-sectional area of $13{,}84mm^2$, cutting force was $47{,}28N$ and energy was $16{,}76N\cdot cm$, while at $29{,}20mm^2$ these values reached $102{,}30N$ and $41{,}97N\cdot cm$ respectively $[6]$.

Therefore, the use of the stem diameter range $d = 0{,}004-0{,}006m$ in theoretical calculations to ensure reliability and power margin is scientifically justified.

KINEMATIC JUSTIFICATION OF THE NUMBER OF BLADES AND ROTATIONAL SPEED

To ensure clean topping by the cutting apparatus, the distance between consecutive cutting traces of the rotor blades must not equal or exceed the spacing between cotton plants. Otherwise, the knife may skip individual stems, bend them, or cause crushing instead of a clean cut.

The cutting-action frequency of the blades is determined by:

$$f = \frac{zn}{60}, s^{-1} \tag{3}$$

where:

- z - number of blades on the rotor;

- n - rotor rotational speed, rpm.

Distance between consecutive cutting traces:

$$\Delta l = \frac{v_a}{f} = \frac{60 v_a}{zn}, m \tag{4}$$

For a clean cut, it is advisable to maintain the condition $\Delta l \leq 0,5 - 0,7s$, i.e., the distance between knife traces should not exceed 50-70% of the spacing between cotton plants along the row. If $s = 0,10 - 0,11m$, the rational cutting-trace step should be within $\Delta l = 0,05 - 0,07m$. In a dense double row, this condition becomes even stricter, since a single rotor processes the plant flow of two rows.

The results of a calculated comparison of rotors with 2, 4, and 6 blades using expression 50-70% (4) are given in Table 1. The analysis shows that for a two-blade rotor, a rotational speed of $450 rpm$ is insufficient for a double cotton row. At $v_a = 1,7 m/s$, the distance between cutting traces is $0,113m$, which equals or exceeds the spacing between plants along the row $(0,10 - 0,11m)$. As a result, the knife cannot consistently act on each plant, and topping quality decreases.

Moreover, although a two-blade rotor can operate in the $650 - 850 rpm$ range, increasing the rotational speed sharply raises dynamic load, vibration, and forces acting on the bearings. For a six-blade rotor, cutting traces become denser, but the design becomes more complex, and mass and balancing requirements increase. Therefore, from the standpoint of technological efficiency and structural reliability, the four-blade rotor is the most rational option.

Table 1. Comparison of rotor kinematic indicators for different numbers of blades and rotational speeds

Number of blades z, pcs.	**Rotational speed n, rpm**	**Δl at v_a = 1.4 m/s, m**	**Δl at v_a = 1.7 m/s, m**	**Assessment**
2	450	0.093	0.113	Insufficient for double row
2	650	0.065	0.078	Borderline condition
2	850	0.049	0.060	Satisfactory, but dynamic load high
4	450	0.047	0.057	Kinematically satisfactory
4	650	0.032	0.039	Rational
4	750	0.028	0.034	Rational for quality cut
6	450	0.031	0.038	Good, but design becomes complex

LINEAR BLADE-TIP SPEED AND THE KINEMATIC REGIME COEFFICIENT

The cleanliness of stem cutting depends not only on the number of blades and rotational speed, but also on the linear speed of the blade tip. The blade-tip speed is determined as follows:

$$v_u = \frac{2\pi R n}{60} \tag{5}$$

where:

v_u - linear blade-tip speed, m/s;

R - rotor radius, m;

n - rotor rotational speed, rpm.

Table 2 presents calculated blade-tip speed results for an adopted rotor radius $R = 0,18m$.

Table 2. Change in blade-tip speed and kinematic regime coefficient as a function of rotor rotational speed

Rotational speed, rpm	Blade-tip speed v_u, m/s	$\lambda = v_u/v_a$ at v_a = 1.7 m/s
450	8.48	4.99
600	11.30	6.65
650	12.25	7.21
750	14.14	8.32
850	16.02	9.42

Analysis of Table 2 shows that as rotor rotational speed increases, the linear blade-tip speed and the kinematic regime coefficient λ increase proportionally. At $450 rpm$, $\lambda = 4{,}99$, which is insufficient for high-quality topping of cotton in double rows. In this case, the relative speed of the blade's action is low, increasing the likelihood of stem bending or displacement before cutting.

When rotational speed is increased to $600-850 rpm$, blade-tip speed reaches $11{,}3-16 m/s$, and the kinematic regime coefficient reaches $6{,}65-9{,}42$. In this case, the knife's action time is reduced and impact-cutting conditions improve. As a result, stem bending decreases, and topping quality and stability improve.

Additionally, increasing the rotor radius to $0{,}20-0{,}22m$ allows the blade-tip speed to reach $12{,}6-17{,}3 m/s$. This value exceeds the unit travel speed $(1{,}4-1{,}7 m/s)$ by several times and ensures active kinematic action of the blade on the stem. This reduces inertial and elastic deformations during cutting and decreases the likelihood of pre-cut stem displacement.

However, as rotor radius increases, its moment of inertia and energy consumption also increase, and dynamic loads on bearings and transmissions intensify. Furthermore, a larger-radius rotor increases the apparatus's mass and dimensions, and in double cotton rows may exert excessive mechanical action on the plants. Therefore, an increase in rotor radius must be evaluated not only from a technological-effect standpoint but also with regard to structural and energy constraints.

Accordingly, for a topping apparatus for intensive double-row cotton planting, the condition $\lambda = 6-10$ is considered rational, meaning the linear blade-tip speed should be at least $6-10$ times greater than the unit travel speed.

ROTOR RADIUS, CUTTING WIDTH, AND STRUCTURAL CONSTRAINTS

The general geometric condition for determining rotor radius can be written as:

$$R \geq b/2 + \delta_\gamma + a - k_\gamma \tag{6}$$

where:

R - rotor radius, m;

b - distance between the two rows of cotton in the double row, m;

δ_γ -margin for lateral deviation of plants and the unit from the row axis, m;

R - additional margin for covering leaf-stem mass, m;

k_γ -correction value accounting for the guiding action of row dividers, m. It indicates by how much the row dividers shift the apical part of the cotton plants toward the cutting zone. In calculations, it can be taken as $k_\gamma = 0{,}02-0{,}04m$.

If row dividers are not accounted for, the rotor radius should be $R \geq 0{,}10-0{,}13m$. However, in practice row dividers bring the apical part of the plants closer to the rotor's center and partially compensate for their lateral deviation. Therefore, the condition for effective coverage can be estimated as $R \geq 0,07 - 0,11m$.

However, this value reflects only the minimum geometric coverage. Considering the need to ensure sufficient linear blade-tip speed, plant oscillation, the angled entry of plants to the blades via the row dividers, and technological margin in the working process, it is advisable to adopt a rotor radius within $R = 0,17 - 0,19m$. At this radius, the total cutting width of the rotor is $B = 2R = 0,34 - 0,38m$

Such a rotor radius provides reliable coverage of the apical part of plants located in a double row with a *10 sm* inter-row spacing. In this case, the row dividers preliminarily bring deviated and unevenly positioned cotton stems into the working zone of the blades, which improves the completeness of cutting and allows more efficient use of the rotor's active zone.

JUSTIFICATION OF ROW DIVIDER PARAMETERS

Row dividers are an important structural element that directs cotton plants into the cutting zone and stabilizes their interaction with the blades. Their parameters are determined based on the double-row planting scheme, the rotor's cutting width, and the condition of centered plant feeding into the cutting zone $[4,5,6]$. In modern topping machines, the row divider, rotor knife, hydraulic drive, and height-adjustment mechanisms operate as a unified system $[5,7]$. In the 3MDZ-4 machine, a separating-guiding device operates together with the topping and spraying systems; the device width is $470mm$, the minimum rotational speed of the disc-knife shaft is $716rpm$, and field-test results showed a topping rate of 91% $[8]$. In agricultural machinery, plant-guiding mechanisms are considered an important unit that affects work quality and technological stability $[10]$.

Row dividers are placed at the front of the cutting apparatus, ahead of the blades in the direction of unit travel. They must guide cotton plants into the cutting zone in stages. Therefore, their working surface must be smooth and shaped so as not to damage the plant.

The inlet section of the row divider must be sufficiently wide, since in field conditions cotton plants are not positioned strictly vertically or uniformly. The outlet section, conversely, must be narrower and correspond to the blade's working zone. This allows cotton plants to be fed into the cutting zone in a compact form.

When designing row dividers to ensure staged guidance of plants into the cutting zone and their compact feeding relative to the blades, the following condition must be met:

$$B_k > B_o > B_{ch} \tag{7}$$

where:

B_k - inlet width of the row divider, m;

B_o - average width in the guiding zone, m;

B_{ch} - outlet width, i.e., width in the cutting zone, m.

The inlet section of the row divider must cover not only the double row width of $0,10m$, but also the lateral deviation of cotton plants, unit deviation from the row, and the distribution of leaf-stem mass.

Therefore:

$$B_k \geq b + 2\left(\delta_\gamma + a\right) \tag{8}$$

where:

$b = 0,10m$ - distance between rows in the double row;

$\delta_\gamma = 0,03-0,05m$ - margin for lateral deviation of the unit and frame oscillation;

$a = 0,02-0,03m$ - margin for covering leaf-stem mass.

From expression (8), it follows that the minimum geometric coverage is $B_k \geq 0,20-0,26m$. However, in practice, a technological margin of $0,04-0,08m$ is added for smooth plant guidance and to compensate for row irregularities, so it is reasonable to adopt $B_k = 0,28-0,34m$.

The outlet width of the row divider must ensure compact feeding of the apical part of double-row plants into the rotor's effective cutting zone and is determined by:

$$B_c \geq b + 2c \tag{9}$$

where:

$c = 0,01-0,03m$ - lateral margin for stem diameter, leaf mass, and guidance error.

From expression (9), it follows that B_c should be $0,12-0,16m$.

The overall narrowing angle of the row divider is justified by the condition of smooth, centered guidance of cotton plants into the cutting zone. For the double-row planting scheme, with $B_k = 0,28-0,34m$ and $B_c = 0,12-0,16m$, the overall narrowing angle is best chosen within $\beta = 15-25^o$ to avoid excessive elongation of the row divider and sharp bending of plants, while ensuring their staged entry into the rotor's cutting zone. In this case, the angle of each side wall relative to the direction of unit travel is $\alpha = \beta/2 = 7,5-12,5^o$.

The length of the guiding section is determined as follows:

$$L_y = \frac{B_k - B_c}{2\tan(\alpha)} \tag{10}$$

or

$$L_y = \frac{B_k - B_c}{2\tan(\beta/2)} \tag{11}$$

Calculations using expression (11) with the given values show that the rational length of the guiding section is $L_y = 0,35-0,50m$.

If the outlet section of the row divider is positioned too close to the knife, plant matter may become jammed between the knife and the divider, creating a hazardous zone for the rotor. If it is positioned too far away, the guided plants may spread apart again before entering the knife zone.

Therefore, the distance from the outlet section of the row divider to the knife's action zone is estimated by the following condition:

$$l_p = v \cdot t_s \tag{12}$$

where:

$v_a = 1,4-1,7\, m/s$ - unit travel speed;

$t_s = 0,05-0,09s$ - time during which the plant retains a guided position before entering the cutting zone.

Consequently, adopting a time of $t_s = 0,05-0,09s$ for cotton tops to enter the cutting zone in a guided state, the distance l_p is $0,008-0,15m$.

ASSESSMENT OF CUTTING FORCE, ENERGY CONSUMPTION, AND HYDRAULIC DRIVE

The energy expended on cutting the stem depends on stem diameter, cross-sectional area, moisture content, blade sharpness, cutting angle, and cutting speed. Theoretically, the energy required to cut a single stem can be estimated as:

$$E_c = e_s A \tag{13}$$

where:

E_c -cutting energy for one stem, J;

e_s -specific cutting energy, J/mm^2;

A -stem cross-sectional area, mm^2.

According to İ. Aydın and S. Arslan, the specific cutting energy for the upper part of the cotton plant ($0-15$ section) is $0,069\,J/mm^2$ [4]. Given the value $A = 12.56\text{-}28.27\ mm^2$ established in Section 2, expression (13) yields $E_c = 0,87-1,95J$.

Using the value $q = 25,5-34\ plants/s$ determined in Section 1, the net cutting power is determined by:

$$P_c = \frac{E_c q}{\eta} \tag{14}$$

where:

$\eta = 0,75-0,85$ - overall efficiency of the drive and cutting process.

Calculations using expression (14) show that the theoretical power directly expended on cutting stems is within: $P_c = 15,3-82,9W$.

It should be noted that this range characterizes only the useful cutting power and does not account for additional losses and operational loads that arise under real operating conditions. During topping, the rotor's energy consumption is additionally affected by rotor and blade inertia, bearing friction, hydraulic losses in the drive, blade interaction with leaf-stem mass, unit oscillation, uneven plant feeding, blunting of cutting edges, and stem bending/displacement before the moment of cutting.

Accordingly, the hydraulic motor power for a single rotor should be selected not based on minimum theoretical cutting power, but with regard to technological and structural margin. For practical calculation, it is advisable to adopt a working power of one cutting rotor within: $P_r = 0,8-1,5kW$, and when selecting a hydraulic motor with a reliability margin - $P_r = 1,5-2,2kW$.

At a rotor rotational speed of $n = 650rpm$, the angular velocity is $\omega = 68,1rad/s$. In this case, to provide power $P_r = 1,5-2,2kW$, the required torque is within: $M = 22-32,3N \cdot m$.

Therefore, for a single cutting rotor of the cotton topping apparatus, it is rational to use a hydraulic motor providing a torque of $22-35N \cdot m$ in the $600-750rpm$ range. For a four-rotor apparatus, the total power on the working-element shafts will be approximately $6-9kW$, and accounting for losses in the hydraulic system- $8-12kW$. This power level ensures stable rotor rotational speed and quality cutting of the apical part of the plants.

For an apparatus designed to work on double rows, it is structurally advisable to use an individual hydraulic drive for each rotor. This eliminates the need for complex mechanical transmissions, reduces the influence of vibrations and backlash, ensures independent operation of sections, and allows the rotational speed of each cutting element to be adjusted according to operating conditions.

To provide a rotational speed of $600-750rpm$ and a torque of $22-35N \cdot m$, gear-type or high-speed hydraulic motors with a displacement of about $16-25cm^3/rev$ can be used. The working fluid flow rate per section is approximately $10-18\,L/\min$, and for a four-rotor apparatus- $40-70\,L/\min$. With higher pump output, the hydraulic system must include regulation and protection devices: throttle regulators, a safety valve, flow distribution between sections, and a return line for excess oil to the tank.

INFLUENCING FACTORS AND RESULTING CRITERIA

The quality of mechanical cotton topping under intensive double-row technology is determined not only by rotor rotational speed or number of blades, but also by the mutual influence of agrobiological, kinematic, structural, and operational factors. Therefore, when evaluating cutting apparatus parameters, a systematic "factor-process-result" approach should be used (Table 3).

Table 3 Assessment of cutting apparatus parameters based on the "factor-process-result" system

Factor group	Main factors	Effect on resulting criteria
Agrobiological factors	stem diameter, stem moisture, plant height, leaf-stem mass, varietal characteristics	cutting force, cutting energy, probability of incomplete cutting and damage
Kinematic factors	unit speed, number of blades, rotational speed, blade-tip speed	distance between cutting traces, frequency of blade action on stem, degree of cutting cleanliness
Structural factors	rotor radius, blade shape, row-divider width, gap between sections	stability of stem entry to the blade, absence of contact between rotors, jamming risk
Operational factors	accuracy of row entry, frame oscillation, hydraulic-motor speed stability, blade sharpness	cutting-height stability, energy consumption, reliability

The following indicators are appropriate as resulting criteria:

K_t - topping completeness, $\%$;

K_{ch} - proportion of incompletely cut stems, $\%$;

K_s - degree of damage to fruiting branches and bolls, $\%$;

∇H - deviation of cutting height, cm;

N_r - power consumed per rotor, kW;

W - unit productivity, ha/h.

The resulting criteria are not independent of one another. For example, as unit travel speed increases, productivity W increases, but the plant flow per rotor also increases. If the blade's action frequency is insufficient, this leads to an increase in K_{ch} and a decrease in topping completeness K_t.

Increasing rotor rotational speed reduces ∇l and improves K_t. However, at excessively high frequency, dynamic loads, damage K_s, energy consumption N_r, and blade wear all increase.

Row-divider parameters simultaneously affect K_t, K_{ch} and K_s. With sufficient inlet width, scattered cotton plants are guided into the cutting zone; with a rational outlet width and narrowing angle, stems are fed to the blades in compact form. However, if the outlet section is excessively narrow or the angle is too large, plant mass is compressed, fruiting branches are damaged, and K_s

increases.

Therefore, optimal cutting apparatus parameters should be selected based on the following comprehensive condition:

$$K_t \to \max,\ K_{ch} \to \min,\ K_s \to \min,\ \ \mathrm{V}H \to \min,\ N_r \to \textit{ rational value},\ W \to \max$$

Here, for N_r, a "rational" rather than "minimum" value is required. If power is too low, the rotor's rotational speed will not be stably maintained; if power is too high, energy consumption and structural mass increase.

This approach allows the cutting apparatus to be evaluated not only by geometric dimensions, but also by technological outcomes-topping cleanliness, minimal damage, cutting-height stability, and energy efficiency.

Recommended parameters

Based on the analysis and theoretical studies conducted, the recommended parameters of the working elements of the cutting apparatus for mechanical topping of cotton grown under intensive technology with the double-row $76\times10cm$ scheme are given in Table 4.

Table 4 Recommended parameters of cutting apparatus working elements for mechanical topping of cotton grown under the double-row scheme

No.	Parameter	Recommended value
1	Planting scheme	double row $76\times10cm$
2	Unit travel speed	$1,4-1,7\,m/s$
3	Spacing between plants along the row	$0,10-0,11m$
4	Plant flow per rotor	$25-34\,plants/s$
5	Stem diameter	$0,004-0,006m$
6	Number of blades	$4\,pcs$
7	Rotor rotational speed	$600-750rpm$
8	Rotor radius	$0,18-0,22m$
9	Linear blade-tip speed	$11-17\,m/s$
10	Distance between cutting traces	$0,028-0,039m$
11	Knife installation height	$0,8-1,1m$
12	Working power per rotor	$0,8-1,5kW$
13	Hydraulic motor power with margin	$1,5-2,2kW$
14	Hydraulic motor torque	$20-35N\cdot m$
15	Drive type	individual hydraulic motor per rotor

CONCLUSION

The theoretical studies conducted showed that the parameters of the cutting apparatus for topping cotton grown under intensive technology with the double-row $76\times10cm$ scheme must be determined with regard to the two-row plant flow, the biomechanical properties of the apical part of the stem, the rotor's kinematic regime, row-divider parameters, and the apparatus's structural constraints.

It was established that at a unit travel speed of $1,4-1,7\,m/s$ and a plant spacing of $0,10-0,11m$

along the row, the flow per rotor is $25{,}5-34\,plants/s$. For design calculations, it is advisable to adopt a stem diameter in the topping zone within $4-6mm$. Kinematic analysis showed that a two-blade rotor at $450rpm$ does not provide the required frequency of action on the plants, whereas a four-blade rotor at $600-750rpm$ produces a cutting-trace step of $0{,}028-0{,}043m$, sufficient for a stable, quality cut.

For a practical apparatus design, the following are rational: rotor radius of $0{,}17-0{,}19m$, cutting width of $0{,}34-0{,}38m$, row-divider inlet width of $0{,}28-0{,}34m$, outlet width of $0{,}12-0{,}16m$, narrowing angle of $15-25^{\circ}$, and guiding-section length of $0{,}35-0{,}50m$. For a single rotor, it is recommended to use a hydraulic motor with a power of $1{,}5-2{,}2kW$ and a torque of $20-35N\cdot m$. Overall, a four-blade rotor with an individual hydraulic drive and row divider is a rational structural-technological solution for mechanical cotton topping under an intensive double-row planting scheme.

REFERENCES

[1]. Ministry of Agriculture of the Republic of Uzbekistan. Agrotechnologies bring field results only when properly implemented [Electronic resource] // Official website of the Ministry of Agriculture of the Republic of Uzbekistan.-2025.

[2]. 2.Раев Б.Г. Чеканка хлопчатника приспособлением ЧВХ-4. — Ташкент: Госиздат УзССР, 1961. — 51 с.

[3]. 3.Гадоева М. Механизированная чеканка хлопчатника. — Душанбе: Таджикгосиздат, 1963. — 15 с.

[4]. 4.Aydın İ., Arslan S. Mechanical properties of cotton shoots for topping // Industrial Crops and Products.-2018.-Vol. 112.-P. 396–401. DOI: 10.1016/j.indcrop.2017.12.036.

[5]. 5.Xu Y., Han C., Zhang J., Hu B., Ma X., Mao H. Innovative Designs for Cotton Bionic Topping Manipulator // Agriculture.-2024.-Vol. 14, No. 9.-Article 1469. DOI: 10.3390/agriculture14091469.

[6]. 6.Pekitkan F.G., Esgici R., Elicin A.K., Sessiz A. The change of shear force and energy of cotton stalk depend on knife type and shear angle // Scientific Papers. Series A. Agronomy.-2018.-Vol. LXI, No. 1.-P. 360–366.

[7] 7.Ахметов А.А., Ахмедов Ш.А., Батыров Р.М., Рузимов Ж.К. Чеканочный агрегат на базе трактора с регулируемым клиренсом // Фундаментальные и прикладные научные исследования: актуальные вопросы, достижения и инновации: сборник статей XVIII Международной научно-практической конференции, 15 декабря 2018 г., Пенза. В 2 ч. Ч. 1. Пенза: МЦНС «Наука и Просвещение», 2018. — С. 87–89.

[8] 8.Li Xia, Wang Weixin, Zhang Ruoyu, Song Haitang, Li Mingzhi, Ge Yun, Zhao Yongman. Cotton topping machine with automatic height adjustment: patent CN201078930Y, China; patent holder: Shihezi University.-Filed 16.07.2007; published 02.07.2008.-Electronic resource.

[9] 9.Wang Chunyao, Jiang Yongxin, Min Lei, Chen Fa, Sun Wenlei, Zhou Jianping. Cotton topping machine cutting device: patent CN201315766Y, China; patent holders: Xinjiang University; Agricultural Mechanization Research Institute, Xinjiang Academy of Agricultural Sciences.-Filed 29.07.2008; published 30.09.2009.-Electronic resource.

[10] 10.Peng Qiangji, Kang Jianming, Song Yumin, He Qinghai. Design of 3MDZ-4 self-propelled cotton topping and spraying combined machine // Transactions of the Chinese Society of Agricultural Engineering.-2019.-Vol. 35, No. 14.-P. 30–38. DOI: 10.11975/j.issn.1002-6819.2019.14.004.

[11] 11.Xu Y., Han C., Qiu S., You J., Zhang J., Luo Y., Hu B. Design and Experimental Evaluation

of a Minimal-Damage Cotton Topping Device // Agriculture.-2024.-Vol. 14, No. 12.-Article 2341. DOI: 10.3390/agriculture14122341.

[12] A 12.Persson S. Mechanics of Cutting Plant Material.-St. Joseph, Michigan: American Society of Agricultural Engineers, 1987.-ASAE Monograph No. 7.

[13] 13.Bai J., Ma S., Wang F., Xing H., Ding Z., Hu J. Key technologies on crop dividers of sugarcane harvester: a review // 2021 ASABE Annual International Virtual Meeting.-St. Joseph, Michigan: American Society of Agricultural and Biological Engineers, 2021.-Paper No. 2100613. DOI: 10.13031/aim.202100613.

Received: *15.02.2026*
Accepted: *03.07.2026*

MACHINE SCIENCE

ISSN: 2227-6912
E-ISSN: 2790-0479

2026, № 1 Pages 61-69

INTEGRATED MULTISCALE COMPUTATIONAL MODELS OF ALUMINUM-BASED MATRIX NANOCOMPOSITES REINFORCED WITH CERAMIC PARTICLES

Farid JAFAROV

Azerbaijan State Oil and Industry University, Baku, Azerbaijan

E-mail: jafarovfarid3@gmail.com

https://doi.org/10.61413/HCIU2194

Abstract: Particle-reinforced aluminum matrix nanocomposites offer significant potential for advanced structural applications due to their enhanced stiffness, strength, and wear resistance. However, the simultaneous optimization of mechanical performance and damage tolerance remains a critical challenge, primarily due to the complex interplay between reinforcement content, particle morphology, spatial distribution, and interfacial behavior. In this study, an integrated multiscale computational framework is proposed to systematically investigate and optimize the mechanical behavior of ceramic particle–reinforced aluminum composites. The framework combines representative volume element (RVE)-based finite element modeling, molecular dynamics (MD) simulations, and phase-field approaches within a unified predictive architecture. Microstructural descriptors such as particle volume fraction, size distribution, morphology, agglomeration statistics, and interfacial properties are explicitly quantified and incorporated into statistically controlled RVE ensembles. The results demonstrate that nanoscale dispersion quality and interfacial mechanics govern the transition between strengthening and embrittlement. The proposed approach enables the construction of structure–property design maps that identify optimal reinforcement windows maximizing strengthening while limiting brittleness and defect sensitivity. This study establishes computational modeling as a viable alternative to extensive experimental campaigns for the design of aluminum-based nanocomposites.
Keywords: *aluminum matrix nanocomposites; particle reinforcement; multiscale modeling; finite element method; molecular dynamics; phase-field modeling; structure–property relationships*

INTRODUCTION

Aluminum-based composite materials are widely studied in the aerospace, automotive, and energy industries for their advantages, including low density, high specific strength, and corrosion resistance. The strength, impact toughness, and wear resistance of these materials can be significantly increased by adding ceramic particles. However, the introduction of nanoparticles, in particular, is often accompanied by a decrease in ductility and an increased risk of brittle fracture [1].

The combined effects of multiple microstructural parameters shape macroscopic mechanical behavior. Traditional homogenization and analytical models cannot fully capture these interactions and are limited in their ability to provide reliable predictions for real-world process conditions. Therefore, statistical descriptions of microstructure and multivariate computational approaches play a crucial role in modern materials design [2].

This work aims to develop an integrated computational model that quantitatively describes the relationship between microstructure and properties and determines the optimal reinforcement design parameters for nanocomposites reinforced with aluminum particles.

The scientific novelty of this study lies in the systematic assessment of the influence of the amount, size, morphology, and distribution of reinforcing particles on mechanical properties. To this end, the following research objectives were defined:

1) Analysis of the limitations of existing modeling approaches;

2) Quantitative assessment of the influence of nanoscale dispersion on material deformation and damage;

3) Integration of SEM, MD, and phase field models into a single multidimensional framework;

4) Determination of optimal design parameters that ensure a balance between strengthening and brittleness.

QUANTITATIVE DESCRIPTION OF THE MICROSTRUCTURE

The mechanical properties of particle-reinforced aluminum-based composite materials directly depend on their microstructural properties. Therefore, it is crucial to characterize the reinforcing phase not only qualitatively but also quantitatively, using microstructural parameters. Quantitative description of the microstructure enables us to determine cause-and-effect relationships between the material's mechanical properties and its microstructural parameters, thereby improving the accuracy with which real-world systems are represented in computational models.

The strengthening phase is characterized by the following key microstructural parameters: volume fraction, particle-size distribution, morphology, and spatial distribution. Each of these parameters has a distinct impact on the composite's strengthening mechanisms and fracture processes [3].

The volume fraction of reinforcing particles is one of the most important structural parameters of a composite material. Increasing the volume fraction generally increases the composite's stiffness and strength. This effect is primarily due to the load transfer mechanism and the presence of the hard ceramic phase. However, adding excessive amounts of the reinforcing phase can lead to increased interparticle interactions, stress concentration, and increased process porosity. This can lead to embrittlement and premature failure of the composite material. Therefore, determining the optimal volume fraction is considered an important step in the design of composite materials.

The size and size distribution of reinforcing particles significantly influence the strengthening mechanisms of a composite. As particle size decreases, the distance between particles decreases, creating additional barriers to dislocation movement. The Orowan strengthening mechanism explains this phenomenon and leads to increased material strength. However, very small nanoparticles exhibit a sharp increase in surface area, which can increase susceptibility to agglomeration and pose additional challenges in manufacturing [4].

Particle size distribution is characterized not only by average size but also by variance and extreme values. A broad size distribution can sometimes lead to localized stress concentrations due to the presence of large particles and can accelerate the failure process.

The morphology of reinforcing particles is one of the important structural properties affecting the mechanical properties of a composite. Morphology is typically described by parameters such as aspect ratio, sphericity, and angularity

Spherical particles generally provide a more uniform stress distribution and reduce the likelihood of stress concentration. Angular or non-spherical particles can lead to increased stress concentration. On the other hand, particles with a high aspect ratio can enhance the load transfer mechanism, but can also lead to anisotropic mechanical behavior of the material [5].

The distribution of particles within a material's structure is one of the main factors determining the mechanical stability of a composite. Ideally, reinforcing particles should be uniformly distributed within the matrix. However, in real materials, particle agglomeration is often observed. The following parameters can characterize the distribution within the structure:

- distribution of distances between adjacent particles;
- proportion of agglomeration;
- distribution of agglomerate sizes.

Agglomerates create localized zones of hardening within the material, where stress concentrations develop. This increases the likelihood of microcracking and reduces the composite's overall strength.

Quantitative description of the microstructure allows for a more accurate representation of real materials in computational models [6]. Based on these parameters, statistically controlled representative volume elements (RVEs) are constructed, and the influence of various microstructural configurations on mechanical behavior is investigated. This approach enables establishing relationships between microstructural parameters and macroscopic mechanical properties, as well as determining optimal reinforcement design parameters. Based on these parameters, statistically controlled RVE ensembles are created, and the cause-and-effect relationships of microstructure influences are separately studied.

COMPUTATIONAL MODELING METHODS

Finite Element Method. SEM is used as the primary tool for virtual mechanical testing of microstructures. The models account for nonlinear constitutive behavior, periodic boundary conditions, and interfacial cohesion laws. This approach allows us to determine the conditions for damage initiation and the formation of localized deformations.

The finite element method (FEM) is one of the most widely used computational techniques in modern materials science and engineering analysis. It is used to analyze the mechanical behavior of materials with complex geometries and heterogeneous microstructures. In particle-reinforced aluminum composites, FEM is considered a particularly effective tool for studying stress distribution, plastic deformation localization, and damage initiation mechanisms at the microstructural level [7].

The basic principle of the scanning electron microscopy (SEM) approach is to divide a continuous medium into small elements. Mechanical balance equations are solved for each of these elements, resulting in the determination of stress and strain fields for the entire system. Since the matrix and reinforcing particles in composite materials have different mechanical properties, an accurate description of the microstructure is of great importance.

In scanning electron microscope (SEM) models, the microstructure of a composite material is typically described using a representative volume element (RVE). An RVE is considered a small volume reflecting the statistical properties of the actual material. The size, shape, and distribution of reinforcing particles within this volume are taken into account. This approach enables analysis of the influence of microstructure on macroscopic mechanical behavior.

In representative volume element (RVE) models, particles are explicitly modeled, and the interface between the matrix and reinforcing phase is defined separately. This interface plays a key role in stress transfer and damage initiation under mechanical loading.

The behavior of composite materials is often accompanied by the onset of plastic deformation after the elastic phase. Therefore, SEM models employ nonlinear constitutive models for the matrix material. These models describe elastic-plastic behavior, the effects of hardening, and the evolution of deformation. Ceramic particles are typically modeled as elastic and brittle materials [8].

Representative volume element (RVE) models use periodic boundary conditions to simulate the infinite microstructure of a real material. These conditions ensure the consistency of strains and stresses on the model's external surfaces and account for the microstructure's repetitive nature. The use of periodic boundary conditions guarantees more realistic and reliable modeling results.

Figure 1 shows a microstructural diagram demonstrating the random distribution of ceramic particles within a representative volume element (RVE) and a local agglomeration zone. The figure depicts a random distribution of particles in the matrix. This distribution is intended to simulate the microstructural properties observed in real composite materials. The different particle sizes reflect the size distribution present in real materials. This statistical distribution enables a more accurate assessment of the influence of microstructural parameters on mechanical properties. The figure also shows an area in which particles are clustered, referred to as an agglomeration zone. Agglomeration results from the uneven distribution of particles within the matrix and can lead to stress concentrations in composite materials. Such areas are critical to the material's mechanical stability and often serve as initiation sites for microcracks

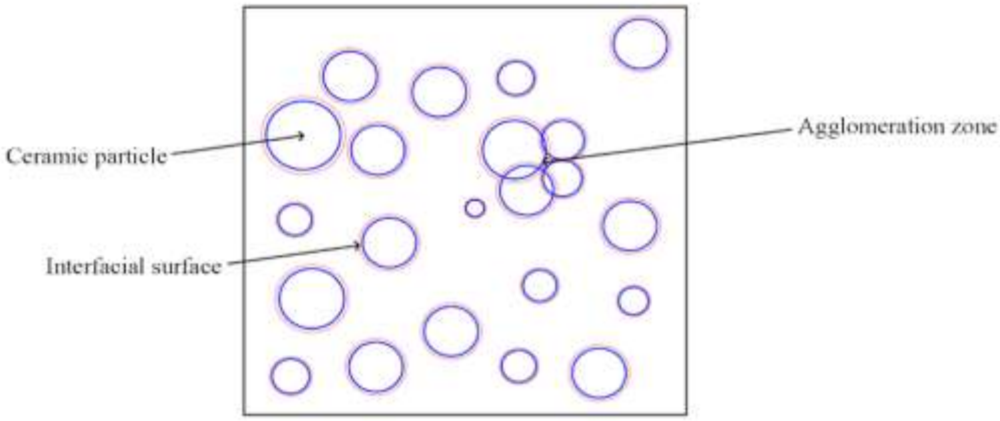

Fig. 1. Representative Volume Element (RVE) microstructure model.

In composite materials, damage often initiates at the interface between the matrix and reinforcing particles. Therefore, in SEM models, behavior at the interface is described by cohesive zone models. These models enable the simulation of separation processes under tension and shear at the interface. Cohesive laws account for the maximum stress and interfacial separation energy, enabling analysis of the mechanisms of microcrack initiation and propagation [9].

Scanning electron microscopy (SEM) results reveal the distribution of stress and strain fields within the material. Stress concentrations are observed, in particular, at particle corners and in agglomeration zones. These zones are considered potentially critical for the onset of failure. Analysis of local strain fields provides deeper insight into the mechanisms of composite strengthening and embrittlement.

Figure 2 shows the effect of the amount of reinforcing phase on the local stress level in particle-reinforced composite materials. As the graph shows, with increasing volume fraction of reinforcing particles, the maximum stress observed within the material also tends to increase. When the volume fraction is zero, i.e., when the material consists solely of the matrix phase, the maximum stress is approximately 140–150 MPa. With the addition of reinforcing particles, the mechanism of mechanical load distribution within the matrix changes, and stress concentrations begin to form around the particles.

As the volume fraction increases in the range of 2–4%, the maximum stress increases rapidly, and this increase is mainly explained by the fact that hard ceramic particles perform the load transfer function within the matrix. At this stage, the particles restrict the movement of dislocations, and as a result, plastic deformation of the material becomes difficult. This process can also be associated with the Orowan strengthening mechanism. As the volume fraction increases to 4–6%, the rate of increase in stress becomes relatively constant. At this stage, a more complex stress distribution between the matrix and the strengthening phase occurs, and the interaction between the particles begins to intensify. This process leads to the formation of local stress fields within the microstructure. When the volume fraction reaches 8–10%, the maximum stress increases to values of approximately 260 – 265 MPa. At this stage, since the amount of the strengthening phase is already quite large, the distance between the particles decreases, and stress concentration is observed more strongly. At the same time, an excessive amount of particles can increase the likelihood of agglomeration and increase the risk of embrittlement of the material [10].

Thus, the graph shows that increasing the volume fraction of reinforcing particles increases the composite's strength, but this effect is limited. Excessive increases in volume fraction can lead to increased stress concentration, microcrack formation, and material embrittlement. Therefore, selecting the optimal volume fraction of the reinforcing material is critical to the design of composite materials. The graph demonstrates a direct relationship between the amount of the reinforcing phase and the stress level in particle-reinforced composite materials. This result confirms that microstructural parameters significantly affect the mechanical behavior of composite materials and underscores the importance of selecting optimal design parameters.

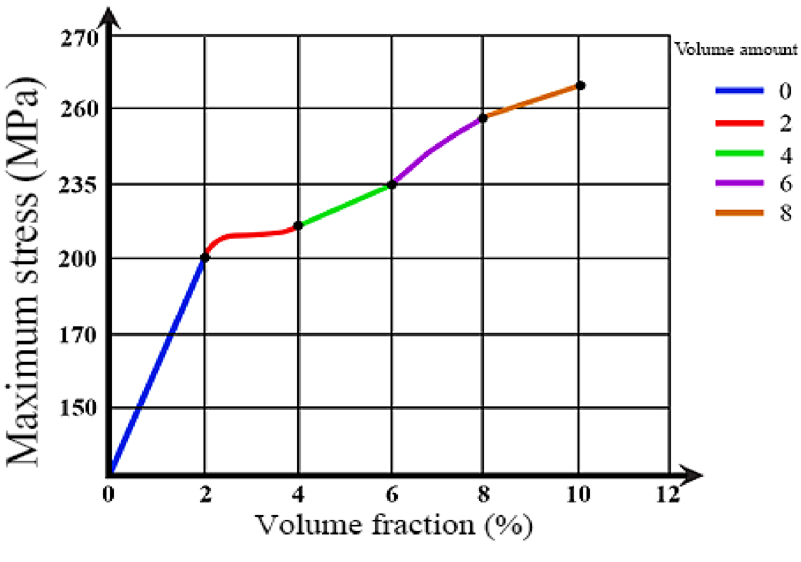

Fig.2. Dependence of stress concentration on the volume fraction of particles.

Molecular Dynamics. Molecular dynamics (MD) simulations are used to evaluate interfacial bond strengths, dissociation energies, and dislocation-particle interactions at the atomic level. The results obtained play a key role in calibrating the interfacial parameters used in SEM models.

Molecular dynamics (MD) simulation is one of the most important computational methods for studying the behavior of materials at the atomic scale. This method enables fundamental investigation of the microstructure and mechanical properties of materials by modeling interactions among atoms and molecules according to classical mechanics. In particle-reinforced aluminum nanocomposites, MD simulation plays a key role, particularly in studying the mechanics of interfacial interactions between the matrix and reinforcing particles.

Within the MD approach, atomic motion is computed using Newton's second law, and interatomic potential functions govern interactions. These potential functions describe the material's chemical and physical properties and determine the energy states of the atoms. For aluminum-matrix composites, the embedded-atom potential or other suitable interatomic potential models are typically employed [11].

The interfacial region between the aluminum matrix and ceramic reinforcing particles plays a key role in the composite's mechanical behavior. Molecular dynamics (MD) simulations can be used to evaluate the cohesive strength and separation energy of this interfacial region at the atomic level. The interactions between atoms and the separation process under mechanical loading applied along the interfacial region are modeled. This analysis yields parameters, including the maximum tensile stress and the separation energy of the interfacial region. These parameters serve as important inputs for calibrating cohesive-zone models within finite-element models. Thus, the results obtained at the atomic level are compared with macroscopic mechanical models.

One mechanism for strengthening composite materials is the blocking of dislocations by reinforcing particles. Molecular dynamics simulations reveal how dislocations behave near particle boundaries and the mechanisms that limit their motion. The results indicate that the size, morphology, and interfacial bond strength of the particles directly influence dislocation motion. Analysis of the interaction between dislocations and particles provides deeper insight into the Orowan strengthening mechanism. These processes, observed at the atomic level, are considered one of the main reasons for the increase in macroscopic strength of the composite [12].

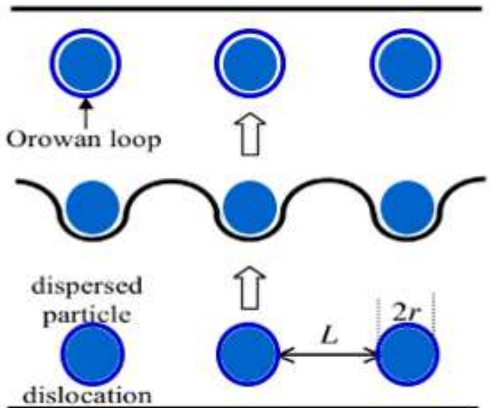

Fig.3. Orowan amplification mechanism.

Figure 3 illustrates the mechanism by which dispersed particles in a metal matrix impede the movement of dislocations. Dispersed particles are distributed within the crystal lattice and restrict the free movement of dislocations, which are the main carriers of plastic deformation. As shown, the lower part exhibits a dislocation line and dispersed particles in front of it. L denotes the distance between these particles, and the particle radius is $2r$. When a dislocation reaches these particles, it cannot pass through them and is forced to go around them. The middle part shows the bending (twisting) of the dislocation line around the dispersed particles. This phenomenon is called the Orowan mechanism. After a dislocation passes between particles, under the action of tension, it forms a closed dislocation ring behind them. The upper part shows the Orowan loop formed as a result of this process. These loops remain around the dispersed particles and further complicate the movement of subsequent dislocations. As a result, the material's strength, resistance to plastic deformation, and yield strength increase. The effectiveness of this mechanism depends primarily on the size of the dispersed particles (r) and the distance between them (L). The smaller and closer the particles, the more complex the dislocation movement and the stronger the strengthening effect of the material.

Thus, the movement of dislocations of dispersed particles distributed in the metal matrix is limited by the Orowan mechanism, which leads to strengthening of the material [12].

Molecular dynamics modeling also enables the study of the organization of the interfacial structure at the atomic scale and potential chemical reactions. In some cases, reaction layers form between the aluminum matrix and ceramic particles. These layers affect the mechanical strength of the interfacial surface and the overall stability of the composite. Atomic-level analysis enables the determination of the atomic arrangement at the interface, the distribution of potential energy, and the formation of residual stresses. These data are of great importance for predicting the long-term mechanical behavior of the composite material [13].

One of the most important applications of molecular dynamics simulation results is their integration into finite element models. The interface parameters obtained from molecular dynamics simulations are used to calibrate the cohesive laws applied in scanning electron microscopy models. This approach enables the connection between physical mechanisms at the atomic scale and macroscopic mechanical behavior. This integrated multidimensional modeling approach enables more reliable predictions in the design of composite materials and helps significantly reduce the number of experimental studies.

Phase-field models. The phase-field approach is used to describe trends in particle agglomeration, microstructural evolution, and crack initiation and propagation. These models ensure the formation of a microstructure that corresponds to actual process conditions.

Phase-field models are a modern computational approach widely used in materials science to study the formation and evolution of microstructure. This method describes how interfaces and microstructural changes between different phases evolve using continuous field variables. The main advantage of the phase-field approach is that the movement and evolution of interphase surfaces can be tracked explicitly, and these processes do not require separate boundary-tracing algorithms [14].

Phase-field models are particularly important for studying the mechanisms of microstructure formation and particle distribution properties in particle-reinforced aluminum composites. These models can be used to analyze particle distribution in the matrix, agglomeration tendencies, and the thermodynamic stability of the microstructure.

The phase-field approach enables modeling of microstructural changes over time and the interaction among different phases. In this approach, the state of a system is described by one or more phase variables. These variables indicate the distribution of phases in different regions of the material and describe the evolution of the microstructure over time.

For example, during the production of composite materials, particle distribution is influenced by factors such as temperature changes, diffusion processes, and interfacial energy. Phase-field models enable the generation of microstructural configurations suitable for real-world process conditions, accounting for these processes. One of the most important problems in nanoparticle-reinforced composites is particle agglomeration. During agglomeration, particles are unevenly distributed within the matrix, forming localized zones of hardening. These zones increase stress concentration and reduce the material's mechanical stability.

Phase-field models enable the simulation of the development of the agglomeration process, accounting for particle interactions and interfacial energy. These models can be used to determine the conditions under which particles remain uniformly dispersed and those under which agglomeration occurs.

Another important application of phase-field models is the study of crack initiation and propagation. In classical models of fracture mechanics, crack boundaries must be defined and tracked separately. In the phase-field approach, crack existence and propagation are described by a specific phase variable, and crack formation is modeled automatically [15, 16].

This approach allows us to determine how cracks propagate between particles and the matrix, especially in heterogeneous materials, and which microstructural regions are more susceptible to damage. This enables more accurate analysis of the failure mechanisms of composite materials.

Phase-field models are used in conjunction with other computational methods within multidimensional modeling. These models determine the formation of the microstructure and particle distribution, while the finite element method analyzes the mechanical behavior of this microstructure. This integrated approach enables the connection between a material's microstructural properties and its macroscopic mechanical properties. In this regard, phase-field models play an important role in the materials design process and help determine optimal microstructural parameters.

CONCLUSIONS

Computational results indicate that the optimal quantity and size of reinforcing phase particles maximize strengthening; however, agglomeration and poor interphase adhesion lead to premature failure. The quality of the nanodispersion directly influences the distribution of mechanical properties, while extreme microstructural conditions can determine macroscopic behavior.

The obtained design maps of structural properties indicate that optimal reinforcement should be characterized not only by increased strength but also by the preservation of ductility.

This paper presents an integrated multiscale computational model for the design of aluminum particle-based nanocomposites reinforced with reinforcing elements. The proposed approach:

1. Provides improved modeling that takes into account microstructural statistics and interphase mechanics;
2. Quantitatively evaluates the influence of nanoscale dispersion on mechanical behavior;
3. Has the potential to reduce the number of physical tests significantly;
4. Enables rational selection of optimal reinforcing element design ranges.

These results demonstrate that computer modeling is a powerful and reliable scientific tool in the design of aluminum-based nanocomposites.

REFERENCES

[1].Miracle D.B. Metal matrix composites – From science to technological significance. Composites Science and Technology, 2005, Vol. 65, Issues 15–16, pp. 2526–2540. *https://doi.org/10.1016/j.compscitech.2005.05.027*

[2].Chawla N., Chawla K.K. Metal Matrix Composites. Springer, New York, 2013. 417 p.

[3].Torquato S. Random Heterogeneous Materials: Microstructure and Macroscopic Properties. Springer, 2002, 701 p. DOI: 10.1115/1.1483342

[4].Anderson T.L. Fracture Mechanics: Fundamentals and Applications. CRC Press, 2017, 684p https://doi.org/10.1201/9781315370293

[5].Hull D., Clyne T.W. An Introduction to Composite Materials. Cambridge University Press, 2019, 360 p. DOI: 10.1017/9781139050586

[6].Chen L.Q. Phase-field models for microstructure evolution. Annual Review of Materials Research, 2002, Vol. 32, pp. 113–140.

[7].Callister W.D., Rethwisch D. Materials Science and Engineering: An Introduction Wiley, 2018.

[8].Suneev Anil Bansal, Virat Khanna, Pallav Gupta. Metal Matrix Composites: Properties and Applications (Vol. 2), 2022, 288p. https://doi.org/10.1201/9781003194910

[9].Tadmor E., Miller R. Modeling Materials: Continuum, Atomistic and Multiscale Techniques. Cambridge University Press, 2011. DOI: 10.1017/CBO9781139003582

[10].Biner S.B. Programming Phase-Field Modeling. Springer, 2017.

[11].Mamedov A.T., Madzhnunov E.E. Justification of the selection of antifriction materials for bimetallic friction pairs. Scientific works of the Azerbaijan State Maritime Academy No. 1, 2025, pp. 77-81.

[12].Orowan E. Problems of plastic gliding. Proceedings of the Physical Society, 1948, Vol. 52, pp. 8–22.

[13].Fish J., Belytschko T. A First Course in Finite Elements. Wiley, 2007.

[14].Allen M.P., Tildesley D.J. Computer Simulation of Liquids. Oxford University Press, 2017, 383p.

[15].Frenkel D., Smit B. Understanding Molecular Simulation: From Algorithms to Applications. Academic Press, 2002, 628p.

[16].Novikov I.I. Theory of heat treatment of metals. Textbook. 5th ed. - M .: LENAND, 2021 .- 480 p.

Received: 22.12.2025
Accepted: 18.06.2026

MACHINE SCIENCE

ISSN: 2227-6912
E-ISSN: 2790-0479

2026, № 1 Pages 70-80

ENERGY EFFICIENCY OF KAZAKHSTAN'S POWER GENERATION SECTOR: AN ANALYTICAL ASSESSMENT OF CURRENT CHALLENGES AND DEVELOPMENT PRIORITIES

Sergey SHISHKANOV[1,a], Alexandr NIKULSHIN[2,b*], Yelena KUNTUSH[3,c], Zukhra BAYASSILOVA[3,d], Tatyana SIVERSKAYA[3,e]

[1] Saran Solar Power Plant 100 MW, Saran, Kazakhstan
[2] «PV Construction» LLP, Saran, Kazakhstan
[3] Karaganda Industrial University, Temirtau, Kazakhstan

*E-Mail: [a]cpe_shishkanov@mail.ru, [*b]nikulshin2002@mail.ru, [c]ye.kuntush@tttu.edu.kz, [d]z.bayassilova@tttu.edu.kz, [e]t.siverskaya@tttu.edu.kz*

https://doi.org/10.61413/YWMF6034

Abstract: In Kazakhstan's power industry, the predominance of thermal generation, primarily coal-fired power generation, and the significant role of combined heat and power plants make the energy efficiency of the power generation sector a matter of systemic technical and economic importance. This study examines the energy efficiency of Kazakhstan's power generation sector as an integrated characteristic of the conversion of fuel and energy resources into electrical and thermal energy. The purpose of the article is to substantiate the relevance of this issue on the basis of fuel and energy balance data, sectoral materials, and scientific publications addressing key indicators and factors of generation efficiency. The methodological framework includes analysis and synthesis, comparative analysis, structural and logical analysis, and a problem-oriented analytical approach applied to official statistical, sectoral, and scientific sources. The study shows that the considerable gap between total primary energy consumption and final energy consumption, together with conversion processes, auxiliary consumption, and losses within the energy system, increases the importance of efficiency assessment in the generation sector. It is also established that energy efficiency should be evaluated through a set of interrelated indicators, including specific fuel consumption, useful energy output, auxiliary consumption, equipment operating modes, reliability, technical condition, and the parameters of the plant thermal scheme. The article concludes that improving energy efficiency requires an integrated approach combining refined techno-economic assessment, optimization of combined heat and power generation modes, reduction of internal plant consumption, technical modernization, and the use of secondary energy.

Keywords: *energy efficiency, power generation sector, Kazakhstan power industry, thermal power generation, techno-economic assessment, power plant modernization.*

INTRODUCTION

In the contemporary energy agenda, priority attention is usually given to decarbonization, the development of renewable energy sources, hydrogen energy, and the technological modernization of power systems. However, the energy efficiency of the power generation sector itself, understood as the efficiency of converting primary fuel and energy resources into electrical and thermal energy with due regard to auxiliary consumption and the operating conditions of power plants, is less frequently considered as an independent subject of analysis. At the same time, this aspect largely determines not only the economic efficiency of electricity and heat production but also the stability of power and heat supply. In Kazakhstan, where a sharply continental climate prevails across most of the territory, this issue is of critical importance for life-supporting infrastructure. It also shapes the fuel burden on the industry and influences the further modernization trajectory of the generating complex [1, 2].

For Kazakhstan, this problem is particularly significant due to the sectoral structure of its electric power industry. According to Kazakhstan Electricity Grid Operating Company JSC (KEGOC), electricity generation in the country is carried out by 233 power plants. As of January 1, 2025, their total installed capacity amounted to 25,314.2 MW, while available capacity was 18,890.3 MW [3]. The basis of Kazakhstan's electric power industry is formed by thermal power plants, which account for 19,740.8 MW, or 78% of the total installed capacity. Coal-fired power plants account for 13,592 MW, corresponding to 69% of the capacity of all thermal power plants and 53.7% of the total capacity of all power plants in the country [3]. Kazakhstan's electric power industry therefore remains predominantly coal-based: about 70% of electricity is generated at coal-fired power plants, while combined heat and power plants account for 45% of electricity generation and more than 62% of heat production [2]. Under these conditions, the issue of generation energy efficiency is not a narrow technical problem but a systemic one, since it determines both the fuel economy of power plants and the stability of electricity and heat supply for industrial and social sectors.

In energy statistics, the volumes of energy consumption and conversion are often expressed in tonnes of oil equivalent, a conventional unit that makes it possible to convert different types of fuel and energy into a single comparable basis. According to the internationally accepted conversion, one tonne of oil equivalent corresponds to approximately 41.868 GJ, or about 11.63 MWh of energy. According to the Bureau of National Statistics [1], total primary energy consumption in Kazakhstan in 2024 amounted to 74,304.0 thousand tonnes of oil equivalent, while final energy consumption reached 44,647.3 thousand tonnes of oil equivalent. The structure of total primary energy consumption was dominated by coal at 47.2%, natural gas at 33.1%, and oil and petroleum products at 17.4%. In the structure of final energy consumption, the largest share was accounted for by the residential sector at 36.5% (16.3 million tonnes of oil equivalent), followed by transport at 24.9% (11.1 million tonnes of oil equivalent) and industry at 22.2% (9.9 million tonnes of oil equivalent). Within the industrial sector, the most energy-intensive branches were ferrous metallurgy at 33.6%, mining at 14.6%, and non-ferrous metallurgy at 10.8%. In 2024, the energy intensity of gross domestic product, calculated at 2015 prices, was 0.3 tonnes of oil equivalent per thousand US dollars, while the share of electricity generated from renewable energy sources, excluding large hydroelectric power plants, reached 6.2%. These data show that, despite the gradual movement along the energy transition pathway, the rational use of fuel and energy in the basic generation circuit will remain highly relevant for Kazakhstan over the long term [1].

The strategic priorities of state policy further increase the relevance of this issue. The reference document on best available techniques entitled "Energy Efficiency in the Implementation of Economic and/or Other Activities" emphasizes that Kazakhstan's transition to a low-carbon economy is directly associated with improving energy efficiency [2]. The document sets target benchmarks for reducing the energy intensity of gross domestic product by 30% by 2030 and by 50% by 2050 compared with the 2008 level, achieving a 50% share of alternative energy sources in electricity generation by 2050, and reducing greenhouse gas emissions in electricity production. Therefore, the analysis of energy efficiency in the power generation sector should be considered not only as a technical and economic task but also as a strategic issue linked to the long-term transformation of the national energy system.

Thus, the existing structure of Kazakhstan's electric power industry, the high role of thermal and especially coal-fired generation, and the substantial scale of final energy consumption provide sufficient grounds for identifying this issue as an independent object of research. The purpose of this study is to substantiate the relevance of energy efficiency in Kazakhstan's power generation sector on the basis of fuel and energy balance data, sectoral materials, and scientific publications that reveal the key indicators and factors of thermal generation efficiency.

MATHEMATICAL FORMULATION

The materials of this study include official statistical, sectoral, regulatory, and scientific sources reflecting the current state of the power generation sector in the Republic of Kazakhstan and methodological approaches to assessing its energy efficiency. The empirical basis of the study consists of data from the Bureau of National Statistics of the Agency for Strategic Planning and Reforms of the Republic of Kazakhstan on the 2024 fuel and energy balance, information from the 2024 annual report of Kazakhstan Electricity Grid Operating Company JSC (KEGOC), and provisions of the reference document on best available techniques entitled "Energy Efficiency in the Implementation of Economic and/or Other Activities" [1–3]. The scientific basis of the study comprises publications addressing general approaches to improving energy efficiency in the electric power industry, multi-parameter assessment of power plant efficiency, calculation of specific fuel consumption, combined heat and power generation modes, auxiliary consumption of power plants, the influence of equipment technical condition on the technical and economic indicators of generation, as well as issues of internal plant modernization, utilization of secondary energy resources, and the use of low-grade heat [4–15].

The methodological framework of the article is based on general scientific methods of analysis and synthesis, comparative analysis, structural and logical analysis, and a problem-oriented analytical approach to interpreting statistical, sectoral, and scientific data [1–15]. At the first stage, official materials were analyzed in order to characterize the structure of Kazakhstan's electric power industry, the dynamics of total primary and final energy consumption, and the strategic priorities of state policy in the field of energy efficiency [1–3]. At the second stage, scientific publications were selected, systematized, and comparatively examined to identify the key indicators, factors, and directions for improving the energy efficiency of the power generation sector [4–15]. This approach made it possible to consider generation energy efficiency as a complex object of analysis combining statistical, technical and economic, operational, and technological aspects.

ENERGY CONTEXT OF THE PROBLEM

When considering the energy efficiency of the power generation sector, it is essential to consider not only the sectoral structure of the electric power industry but also the overall dynamics of energy consumption in the country. In this regard, fuel and energy balance data make it possible to determine the scale at which the national energy system operates and to assess the stability of demand for energy resources. In 2015–2024, the Republic of Kazakhstan generally demonstrated growth in both total primary energy consumption and final energy consumption, although certain fluctuations were observed within this period due to changes in economic activity and the overall energy consumption environment [1].

According to the Bureau of National Statistics of the Agency for Strategic Planning and Reforms of the Republic of Kazakhstan [1], total primary energy consumption increased from 54,772.8 thousand tonnes of oil equivalent in 2015 to 74,304.0 thousand tonnes of oil equivalent in 2024, while final energy consumption increased from 38,360.2 to 44,647.3 thousand tonnes of oil equivalent over the same period (Figure 1). The most noticeable increase in total primary energy consumption occurred in 2015–2018. This was followed by a decline in 2020 and subsequent recovery, with the indicator reaching its highest values in 2023–2024. A similar, although smoother, trend can be observed for final energy consumption [1].

As shown in Figure 1, a stable gap between total primary energy consumption and final energy consumption persisted throughout the entire period under review. This circumstance is methodologically important for the present study, since it indicates the presence of a substantial intermediate stage of energy conversion, transmission, and distribution, within which significant parameters of energy system efficiency are formed. In other words, the growth of total energy consumption alone does not explain how rationally fuel and energy resources are used at the stage of their conversion into electrical and thermal energy.

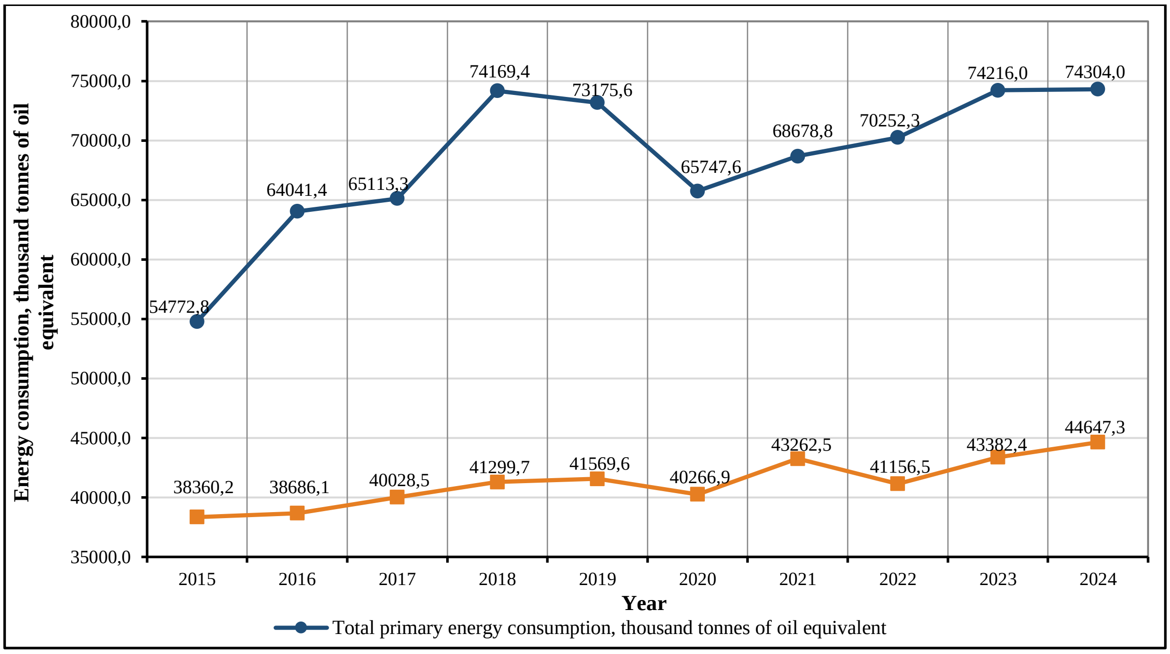

Fig. 1. Dynamics of total primary and final energy consumption in the Republic of Kazakhstan

In this context, the energy background of the problem is determined not only by absolute consumption volumes but also by the fact that the national economy relies on a large-scale and consistently loaded energy system. Therefore, improving energy efficiency should be considered one of the basic conditions for technological modernization and for reducing the energy intensity of the economy. Consequently, under conditions of persistently high energy consumption, the efficiency of the power generation sector acquires practical significance not only for the electric power industry itself but also for broader objectives of economic development and system sustainability [2].

STRUCTURE OF FINAL ENERGY CONSUMPTION AND THE ROLE OF GENERATION EFFICIENCY

In 2024, the largest share in the structure of final energy consumption in the Republic of Kazakhstan was accounted for by the residential sector, which represented 36.5%. It was followed by the transport sector at 24.9% and the industrial sector at 22.2%. Commercial and public services accounted for 11.2%, agriculture, forestry, and fishing for 1.8%, and non-energy use for 3.4% [1]. This distribution shows that final energy demand in Kazakhstan is formed primarily by sectors for which the reliability and economic efficiency of energy supply are of direct socio-economic importance.

Over the period 2015–2024, the structure of final energy consumption changed considerably. The share of the industrial sector decreased from 42.2% to 22.2%, whereas the share of the residential sector increased from 27.9% to 36.5%, and that of the transport sector increased from 14.3% to 24.9% (Figure 2). The share of commercial and public services generally remained within the range of 9.9–12.9%, while the shares of agriculture, forestry, and fishing remained relatively low [1].

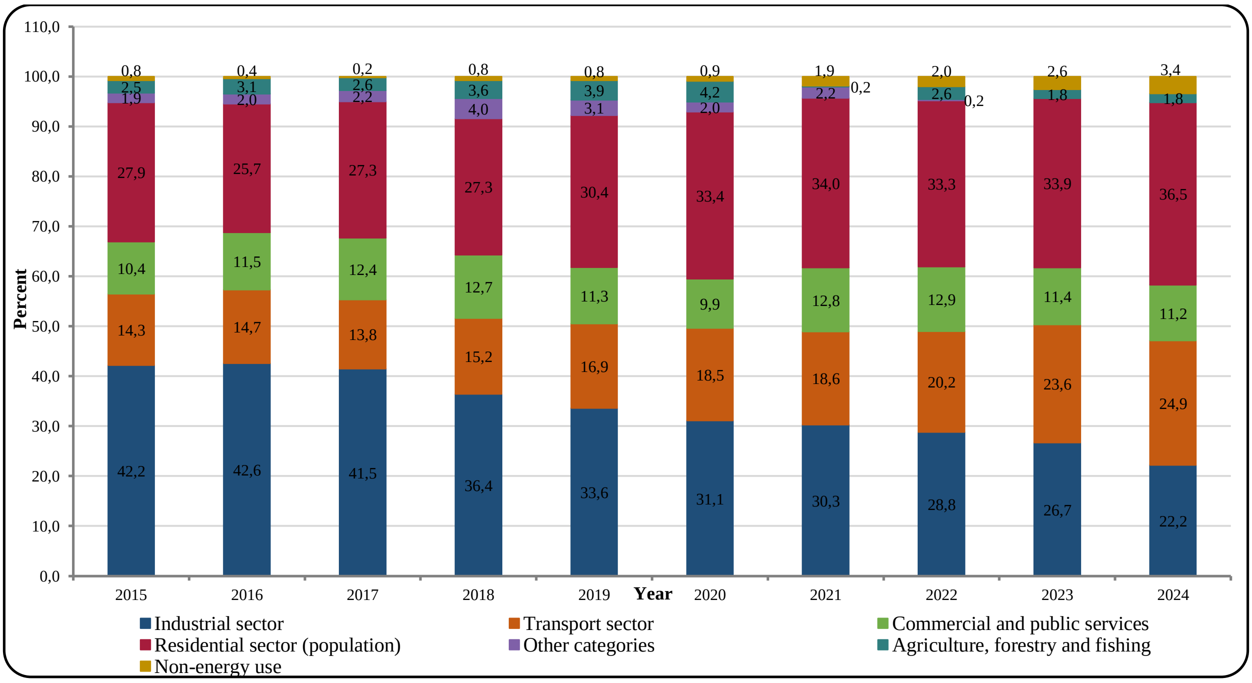

Fig. 2. Final energy consumption by economic sector in the Republic of Kazakhstan

As shown in Figure 2, the role of the residential and transport sectors in final energy consumption increased, while the relative contribution of the industrial sector decreased. This means that generation efficiency should be assessed not only from the standpoint of the fuel economy of power plants but also in terms of ensuring stable energy supply to the population, transport, and municipal infrastructure. In this context, reducing losses, rational use of fuel, and improving the performance of generating equipment acquire broader socio-economic significance [1, 2].

SCIENTIFIC APPROACHES TO ASSESSING AND IMPROVING POWER GENERATION EFFICIENCY

An analysis of the scientific literature shows that, in professional discourse, the energy efficiency of the power generation sector is considered not as a narrow characteristic of fuel consumption but as a complex category reflecting the effectiveness of energy conversion, the quality of equipment operating modes, the level of auxiliary consumption, and the organizational and technical conditions of power plant operation. More general studies emphasize that improving energy efficiency in the electric power industry is associated with a combination of engineering, technological, and managerial measures, including energy audits, improvement of electric drives, heat recovery, enhancement of operating control quality, and optimization of energy flows [4]. At the level of thermal power generation, efficiency improvement is also associated with specific engineering measures aimed at increasing the thermodynamic performance of power units. In study [5], it is shown that increasing the initial steam parameters, applying supercritical and ultra-supercritical operating conditions, using intermediate reheating, and improving regenerative feedwater heating can increase the efficiency of thermal power plants, reduce specific fuel consumption, and decrease harmful emissions. Therefore, generation energy efficiency should be considered not only as a general economic category but also as a set of technically grounded measures implemented within the thermal cycle of a power plant [5]. Taken together, these arguments establish an important initial premise: generation energy efficiency cannot be reduced either to a single local indicator or to an isolated technical measure, since it is shaped by a combination of operational, technological, economic, and system-level factors and therefore requires multi-level analysis.

At the same time, more specific studies show that the systemic nature of energy efficiency is already manifested at the level of the plant thermal scheme and the parameters of individual energy conversion units. In study [6], which analyzes the energy performance indicators of a condensing power plant, it is substantiated that the efficiency of the turbine unit substantially depends on the operation of the condenser and the regenerative system. It is noted that a change in condenser pressure by $1 kPa$ can change the efficiency of a steam turbine unit by approximately 1%, while regenerative heating of condensate and feedwater is regarded as one of the main ways to improve the efficiency of condensing power plants. According to the study, the relative increase in the efficiency of the turbine unit due to regeneration may reach 8–18%. Thus, generation energy efficiency is revealed not only through final fuel consumption but also through the quality of thermal cycle organization, the condition of the condensation mode, and the completeness of using the internal thermal potential of the plant [6].

A related engineering conclusion is presented in study [7], which considers the application of a low-pressure mixing heater in the turbine system of a combined heat and power plant. The study proceeds from the fact that, in surface-type low-pressure heaters, due to thermal resistance to heat transfer, the temperature of the heated water is usually $3-5^{o}C$ lower than the saturation temperature of the heating steam, which leads to additional energy losses. In this regard, it is shown that the partial use of mixing heaters makes it possible to eliminate underheating, improve the thermal economy of the installation, and increase the efficiency of the thermodynamic cycle as a whole. This is important for the present study because it demonstrates the existence of specific internal reserves for improving energy efficiency that are not limited to a general reduction in fuel consumption or to large-scale replacement of main equipment [7].

More specialized studies show that the central methodological issue is the very logic of assessing power plant performance. In study [8], the techno-economic performance of selected power plants is evaluated using actual operational data for hydropower, solar photovoltaic, cogeneration, and thermal power plants. This approach demonstrates that power plant performance cannot be adequately characterized by a single indicator, since the assessment should take into account technical, economic, operational, and environmental parameters, including capacity factor, energy output, levelized cost of electricity, cost of energy, and emissions. Thus, energy efficiency in the power generation sector should be interpreted as a multi-parameter characteristic that combines technical performance with economic and environmental dimensions [8].

This conclusion is further developed in study [9], where the methodological complexity of combined heat and power generation is considered through the allocation of carbon dioxide emissions between electricity and heat produced within a single thermodynamic process. The study emphasizes that, although cogeneration can provide higher overall efficiency than separate heat and power generation, the environmental performance of its products depends on the allocation method used. Since numerous allocation methods exist and may lead to substantially different results, there is no universal consensus on the most appropriate method for all applications. For the present study, this is important because the assessment of combined heat and power plants depends not only on measured energy output but also on the methodological procedure used to distribute resource inputs, emissions, and environmental effects between electrical and thermal energy [9].

The applied dimension of this problem is most clearly revealed in studies based on actual data from operating power plants. In study [10], energy efficiency is considered through a system of specific energy performance indicators, including specific equivalent fuel consumption for electricity supplied from generator terminals, specific fuel consumption for heat output, electricity consumption for auxiliary needs, specific technical water consumption, and other operational indicators. The most important result of this study is that the deterioration of energy efficiency at combined heat and power plants is manifested not in abstract assessments but in measurable deviations of indicators from baseline values. For electricity supplied from generator terminals, an average deterioration in efficiency of 6% is recorded, while significant fluctuations are also identified in electricity consumption for auxiliary needs, associated with the operation of auxiliary equipment. This confirms that the analysis of energy efficiency in the power generation sector should be based on a system of operational indicators and should not be limited to general sectoral characteristics [10].

In turn, study [11] considers the issue at a higher system level and analyzes the flexibility provision of combined heat and power plants from both plant and energy system perspectives. The study shows that the role of such plants is determined not only by their internal technical characteristics but also by their ability to operate flexibly under changing electricity and district heating conditions. In energy systems with increasing shares of variable renewable generation, combined heat and power plants can contribute to variation management through dispatchable electricity supply and interaction with district heating demand. Therefore, the effectiveness of generation is determined not only by the internal parameters of a plant but also by how it is integrated into the overall structure of electricity and heat supply and by its ability to provide operational flexibility at the system level [11].

Another important group of scientific results is related to the influence of equipment technical condition and internal plant consumption on the final efficiency of generation. Study [12] shows that, when forecasting the technical and economic indicators of thermal power plants, it is necessary to take into account not only operating and economic parameters but also the current condition of the main equipment. A wear coefficient is introduced into the forecasting algorithm, thereby confirming that the physical aging of power equipment has a direct quantitative expression in increased fuel consumption and deterioration of the plant's technical and economic characteristics. It is important that, in this approach, equipment wear is considered not as an external background factor but as a variable directly affecting the selection of optimal operating modes [12]. Therefore, the problem of energy efficiency in the power generation sector is inseparable from the problem of technical renewal of generating capacities.

The logic of technical renewal is further developed in study [13], which is devoted to the modernization of a gas turbine power plant. The study considers two options for improving efficiency: the use of a waste heat boiler to generate steam for technological needs and a scheme with a waste heat boiler and a steam turbine for additional electricity generation. Modeling in Aspen HYSYS showed that, in the first case, it is possible to obtain up to 350 t/h of steam, which makes it possible to completely replace the existing boilers at the plant, while in the second case, electricity generation of up to 262.42 MW can be achieved. At the same time, according to the combination of technological, environmental, and economic parameters, the first option is recognized as more preferable [13]. For the present study, this result is important because it shows that improving generation energy efficiency is associated not only with optimizing the operating modes of existing thermal power plants and combined heat and power plants but also with modernizing the configuration of generating units, primarily through more complete use of secondary energy resources.

It is also significant that modern studies point to the importance of utilizing low-grade heat, which is usually dissipated into the environment in traditional schemes. In study [14], devoted to the use of heat pump installations in circulating water supply systems with cooling towers, it is shown that circulating water heated in the turbine condenser can be considered a real source of low-grade heat for heating return network water. The study substantiates the use of R134a refrigerant with a coefficient of performance of 3.8 and shows that the use of a heat pump as part of a combined heat and power plant with a PT-80-130 turbine unit provides fuel savings of 10 tonnes of equivalent fuel per hour, reduces the specific consumption of equivalent fuel for the transformation of 1 Gcal of heat to 74.1 kg of equivalent fuel per Gcal, and gives an estimated payback period of about five years [14]. For the present study, this is particularly important because it broadens the understanding of generation energy efficiency: the emphasis is placed not only on reducing fuel consumption in the main cycle but also on involving secondary thermal resources in useful energy output.

A related but independent aspect is associated with the assessment of useful thermal output and the techno-economic performance of energy conversion technologies. In study [15], the annual thermal performance and techno-economic indicators of a direct absorption solar collector using nanofluids are analyzed. The results show that the use of MWCNT-based nanofluids as heat transfer fluids can improve thermal efficiency compared with water and reduce the cost of useful thermal energy. This is important for the present study because it confirms that energy efficiency assessment should include not only technical performance indicators but also the useful energy output, cost of delivered energy, and payback characteristics of energy conversion solutions [15].

KEY DIRECTIONS FOR IMPROVING ENERGY EFFICIENCY IN THE POWER GENERATION SECTOR

The analysis carried out in this study makes it possible to identify several stable scientific positions concerning the energy efficiency of the power generation sector. First, energy efficiency should be assessed through a system of interrelated indicators, including specific fuel consumption, useful output of electrical and thermal energy, auxiliary consumption, capacity utilization, technical condition of equipment, levelized cost of electricity, and environmental performance [6, 8, 12]. At the same time, the final performance of generation is determined not only by integral technical and economic indicators but also by the parameters of the plant thermal scheme, including the organization of regeneration, the operation of condensing equipment, and the completeness of using the internal thermal potential of the plant [6, 7].

Second, for thermal generation, and especially for combined heat and power generation, the correct methodological treatment of joint electricity and heat production is of fundamental importance. The assessment of combined heat and power plants depends on how resource inputs, emissions, and environmental effects are allocated between electrical and thermal energy, as well as on how flexibly such plants can operate within the wider energy system [9, 11]. Therefore, the efficiency of combined heat and power generation should be considered not only at the level of the plant thermal cycle but also at the level of system integration, district heating demand, and operational flexibility [7, 9, 11, 14].

Third, applied analysis shows that deterioration in energy efficiency at the level of specific power plants is manifested in deviations of measurable operational parameters and therefore should be subject to regular monitoring and managerial intervention [10, 12]. Such analysis should cover not only fuel and electricity consumption characteristics but also specific operating and scheme-related parameters that affect the economic performance of generating equipment [6, 10].

Fourth, technical modernization of generating units and individual elements of the thermal scheme is an essential direction for improving efficiency. This includes both local internal plant solutions, in particular the improvement of regenerative heating, and more complex modernization options associated with the utilization of secondary energy resources, the application of waste heat boilers, the involvement of low-grade heat in useful energy output, and the improvement of heat transfer processes in energy conversion technologies [7, 13–15]. Consequently, the reserves for improving energy efficiency are concentrated not only in operating mode optimization but also in the technical renewal of generating units, the modernization of thermal schemes, and the improvement of heat transfer processes in energy conversion systems [12, 13, 15].

Fifth, auxiliary consumption and the operation of auxiliary equipment remain among the underestimated reserves for improving efficiency, where energy-saving measures may be possible without changing the basic technological scheme [10]. Reducing internal plant consumption should be considered in conjunction with the general technical condition of the plant, the degree of equipment wear, and the possibilities of technological renewal [10, 12].

Thus, the energy efficiency of the power generation sector should be interpreted as a complex characteristic determined by assessment methods, equipment operating modes, the parameters of the plant thermal scheme, auxiliary consumption, the technical condition of generating capacities, the degree of utilization of secondary energy resources, and the organizational and operational conditions of power plant functioning [4–15].

CONCLUSION

The electric power industry of the Republic of Kazakhstan remains largely dependent on thermal generation, with a high share of coal-fired power plants and a significant role of combined heat and power plants in the production of electricity and heat. This structure makes the energy efficiency of the power generation sector a key factor in fuel economy, operational reliability, and the long-term modernization of the national energy system.

The analysis of Kazakhstan's fuel and energy balance for 2024 confirms a persistent gap between total primary energy consumption and final energy consumption. This gap reflects substantial energy conversion processes, auxiliary consumption, and losses within the energy system. Therefore, the efficiency of converting fuel and energy resources into useful electrical and thermal energy remains a critical issue for the country's energy development.

The structure of final energy consumption also demonstrates the broader socio-economic importance of generation efficiency. In 2024, the largest shares of final energy consumption were associated with the residential, transport, and industrial sectors. Consequently, the performance of the power generation sector affects not only the technical and economic indicators of power plants but also the stability of energy supply for the population, transport infrastructure, municipal services, and key sectors of the economy.

The study shows that the energy efficiency of the power generation sector should be assessed as a complex characteristic rather than through a single indicator. It includes specific fuel consumption, useful energy output, auxiliary consumption, equipment operating modes, reliability indicators, the technical condition of generating capacities, and the parameters of the plant thermal scheme. Particular importance should be given to regeneration, condensing mode efficiency, and other thermodynamic parameters that determine the fuel and thermal performance of power plants.

The main directions for improving energy efficiency include the refinement of techno-economic assessment methods, optimization of combined heat and power generation modes, reduction of auxiliary energy consumption, improvement of auxiliary equipment efficiency, and consideration of equipment wear in the management of plant operating parameters. Internal plant modernization, regenerative heating improvement, waste heat boiler application, and the use of secondary energy resources and low-grade heat are also essential. Taken together, these measures form an integrated basis for improving the efficiency, reliability, and sustainability of Kazakhstan's power generation sector.

REFERENCES

[1]. Fuel and energy balance of the Republic of Kazakhstan, 2024 [Electronic resource] // Bureau of National Statistics of the Agency for Strategic Planning and Reforms of the Republic of Kazakhstan: [site]. URL: https://stat.gov.kz/ru/industries/business-statistics/stat-energy/publications/335610/. (Assess date: 20.03.2025)

[2]. Reference document on best available techniques "Energy efficiency in the implementation of economic and/or other activities" [Electronic resource] // Government of the Republic of Kazakhstan: [site]. URL: https://adilet.zan.kz/rus/docs/P2400000024. (Assess date: 20.03.2025)

[3]. Annual Report 2024 [Electronic resource] // Kazakhstan Electricity Grid Operating Company (KEGOC): [site], URL: https://ar2024.kegoc.kz/en. (Assess date: 20.03.2025)

[4]. D. V. Titov. Modern methods and approaches to increasing energy efficiency in electric power industry in the conditions of sustainable development. Science Bulletin, vol. 3, no. 1(82), 2025, pp. 1460–1464.

[5]. C. P. Mammadova, A. P. Abdullayev, I.V. Musazade. Improving the efficiency of thermal power plants research methods. UNEC Journal of Engineering and Applied Sciences, vol. 3, no. 1, 2023, pp. 21–27. DOI: 10.61640/ujeas.2023.0504

[6]. S. K. Abildinova, M. A. Dostemes, S. N. Kamarova. Efficiency of the use of heat pump installations in

water cycle with cooling towers. The Bulletin of KazATC, vol. 4, no. 127, 2023, pp. 471–479. DOI: 10.52167/1609-1817-2023-127-4-471-479

[7] G. A. Manapova, B. B. Bakhtiyar, Zh. Seitova, M. Makhanova. Application of low-pressure mixing type heater in schemes of steam turbine installations of thermal power plants. The Bulletin of KazATC, vol. 3, no. 126, 2023, pp. 435–442. DOI:10.52167/1609-1817-2023-126-3-435-442

[8] B. Akankunda, M. S. Adaramola, S. K. Nkundabanyanga, T. K. Kigongo, N. Mukisa. Techno-economic performance assessment of selected power plants in Uganda. International Journal of Sustainable Energy, vol. 43, no. 1, 2024, 2350980. DOI: 10.1080/14786451.2024.2350980

[9] N. Buchenau, C. Hannen, P. Holzapfel, M. Finkbeiner, J. Hesselbach. Allocation of carbon dioxide emissions to the by-products of combined heat and power plants: A methodological guidance. Renewable and Sustainable Energy Transition, vol. 4, 2023, 100069. DOI: 10.1016/j.rset.2023.100069

[10] O. V. Koftanyuk, A. K. Kinzhibekova. Analysis of the consumption of basic energy resources in the production of electric and thermal energy at the CHP. Bulletin of Shakarim University. Technical Sciences, vol. 1, no. 13, 2024, pp. 324–334. DOI:10.53360/2788-7995-2024-1(13)-40

[11] J. Beiron, L. Göransson, F. Normann, F. Johnsson. Flexibility provision by combined heat and power plants – An evaluation of benefits from a plant and system perspective. Energy Conversion and Management: X, vol. 16, 2022, 100318. DOI: 10.1016/j.ecmx.2022.100318

[12] A.A. Konstantinov, M.M. Sultanov, P.D. Menshikov. Improving the efficiency of generating systems using algorithms for forecasting technical and economic indicators in digital control systems. XII International Scientific and Technical Conference "Electric Power Engineering through the Eyes of Youth". Nizhny Novgorod, Russian Federation, 16–19 September, 2022, pp. 170–173.

[13] D. R. Umyshev, G. A. Akimbek, A. A. Kibarin, M. S. Korobkov, K. S. Olzhabaeva. Conducting technical and economic analysis within the framework of modernization of a gas turbine power plant. The Bulletin of KazATC, vol. 5, no. 128, 2023, pp. 385–398. DOI: 10.52167/1609-1817-2023-128-5-385-398

[14] S. K. Abildinova, M. A. Dostemes, S. N. Kamarova. Efficiency of the use of heat pump installations in water cycle with cooling towers. The Bulletin of KazATC, vol. 4, no. 127, 2023, pp. 471–479. DOI: 10.52167/1609-1817-2023-127-4-471-479

[15] T. I. Juraev, A. S. Halimov, J. S. Akhatov. Investigation of annual thermal performance and techno-economical analyses of direct absorption solar collector by using nanofluids. UNEC Journal of Engineering and Applied Sciences, vol. 3, no. 2, 2023, pp. 39–46. DOI: 10.61640/ujeas.2023.1205

Received: 11.01.2026
Accepted: 25.06.2026

MACHINE SCIENCE
ISSN: 2227-6912
E-ISSN: 2790-0479
web site: msj.aztu.edu.az; e-mail: msj@aztu.edu.az Tel: (+994 12) 538 94 12

SUBMISSION GUIDELINES

General requirements.
Article should not be earlier published in any edition, stated in the short form and edited. The scientific article maintenance should correspond to one of the following scientific directions: Designing of machines; Materials technology; Mechanics; Manufacturing engineering; Economy and management; Automatics and ICT; Technical information.

The documents applied to article.
The conclusion of the corresponding organization (chair, etc.); The expert opinion on expediency of the publication of the article; The covering letter; The Information on the authors (name, patronymic, surname, the exact address, place of work and position, scientific degree, area of scientific activity, contact phones, e-mail address ,etc.).

Preparation rules.
Format - A4; *Margins from each party* - 20 mm; *Program* - Microsoft Office Word; *Font* - Times New Roman, a font size - 12, an interval – 1,15.
The scientific article can be written only in English language, and it is represented in duplicate.
Article volume - 5 … 8 pages.

Sequence of compilation:
1. Article name - on the center;
2. Names and surnames of the authors - on the center;
3. Full addresses of a place of work of authors - on the center;
4. Co-ordinates of authors: e-mail address, phone numbers.
5. The abstract: not less than two-three offers, and no more than 100 words. In the summary: article summary, problem statement, and the information on the received results should be reflected.
6. Keywords: often used 3 ÷ 5 terms under the article.
7. The basic text.
8. The references.

The main text of article should be divided as follows:
For example: "*Introduction*", "*Problem statement*", "*Decision or test methods*", "*Results of the decision or tests and their estimation*".
In introduction: the description of the problem statement, the work purpose and etc.;
In the main part: formation of problem statements; research and methods of the decision, their advantage and difference from existing methods; examples confirming efficiency of the offered method of the decision and the results received.
In the conclusion: evaluation of the results.

Drawings. *Formats* - DOC, JPEG, TIFF and PDF (600 dpi). *The size* – min. 5 × 5, max. 10 × 15. *Arrangement* - ("In the text", in the center). Images of drawings should be accurately visible, and all symbols well are read.
Drawings, paintings, schedules and algorithms should correspond to standard requirements.

Tables are located in the text and are numbered, and the name of each table should be specified in the right top corner.

Formulas should be written down in format *Equation* in the separate line. It is not recommended to use special symbols in the text written on the same line in format *Equation*. Formulas should be written down in certain sequence and are numbered on the right.

The references should correspond to the text and sequence of article. It is recommended to refer to sources published in last 10 years.

The additional information. Edition has the right to spend necessary updating and reductions. Authors bear a scientific article maintenance responsibility. To the publication those articles which have received a positive response are represented only. If article is not published, the edition decision is possible to data of authors, the manuscript and disks do not come back.

MACHINE SCIENCE № 1, 2026

Editorial address:
AZ1073, Azerbaijan, Baku, H.Javid av., 25.
Telephone: (+994 12) 538 94 12

E-mail: msj@aztu.edu.az
Web site: http://msj.aztu.edu.az/

Format: 60×84 1/8.
Number of copies printed: 100.

Publisher: AzTU Publisher